MECHANISMS OF EPITHELIAL PATTERNING AND MORPHOGENESIS

A thesis submitted by

Steven J. Del Signore

In partial fulfillment of the requirements
for the degree of

Doctor of Philosophy

in

Biology

TUFTS UNIVERSITY
Sackler School of Biomedical Sciences

Date
May 2014

Adviser: Victor Hatini

Abstract

Epithelial development requires coordination amongst all constituent cells. Cell fates must be organized in discrete spatial domains by coordinated patterns of gene expression. These patterns of gene expression must then coordinate cell shapes and behaviors to generate morphological diversity. My work has investigated two distinct mechanisms that ensure the robust patterning and morphogenesis of *Drosophila* epithelial tissues. By understanding how these mechanisms ensure high fidelity spatial and temporal control over fundamental cellular processes, we may gain insight into the dysregulation of these same processes in disease.

Patterning of the *Drosophila* notum

During patterning of the *Drosophila* notum, the bone morphogenetic protein (BMP) homolog Dpp acts from the posterior margin to help coordinate a checkerboard-like pattern of gene expression that subdivides the tissue into progressively finer domains. However, it is unclear whether this patterning cue is sufficient to fully pattern the notum. We found that the zinc finger *odd-skipped* family of genes is expressed at the anterior margin of the notum, and is required early in development for notum formation generally, and throughout development for normal anterior programs of gene expression. Further, ectopic pathway activity in the posterior is sufficient to induce an anterior specific program of gene expression across the tissue. These data suggest that the *odd-skipped* genes control an anterior organizer that coordinates with Dpp to robustly pattern the notum.

Morphogenesis of the *Drosophila* pigment epithelium

Cell shape change is considered to be driven by the regulation of E-Cadherin based adhesive forces, and opposing actomyosin based contractile forces. However, most work *in vivo* has focused on the role of actomyosin tension to constrict cell contacts during shape change. We investigated whether alternative pathways might contribute to contact maintenance or expansion. We found that contact length oscillates during cell shape change in the pigment epithelium. These length fluctuations occur at cell contacts under high levels of tension, and phases of contact expansion correlate with pulses of PIP3 and branched F-actin synthesis. Disruption of these pathways alters both cell shape and tissue organization. These studies suggest that branched F-actin dynamics might actively modulate tension in a field of cells undergoing extensive shape changes.

Acknowledgements

First and foremost, I want to thank Victor Hatini, my mentor. Victor has been remarkably invested in and committed to my development as a scientist. He has given me the freedom to explore, and given me guidance to ensure that something actually gets done as a result of (mainly in spite of) these explorations. Over what is inevitably an up and down experience, Victor has remained consistently a source of positive equanimity, urging me always to “go where the light is”.

I have been fortunate also to have an incredibly helpful and positive advisory committee. I want to thank Karina most particularly for her well timed swift kick, which helped bring the Bowl work to completion. I want to thank Jim for (at least trying) to teach me to keep it snappy, and Peter for bringing some very creative (in a good way) ideas for experiments. I want to thank Adam Martin for taking the time to serve as my outside examiner. His careful, quantitative, and exciting work on gastrulation has provided an indispensable model for my work in the eye.

I have been even more fortunate to have been born into a deeply loving, supportive family. It is not necessary or possible to describe everything my parents, brother, and sister have done to help me get to this point, but I will note a few particulars. I want to thank my mom for being so psychotically, irrationally proud of me. I want to thank my dad for always making me feel like I got something productive done, even on days when nothing seemed to work (“How many flies did you kill today?”). I want to thank my brother for always making me feel like a slacker; whether it was living off of like $10 a week and stolen brownies in college, or juggling work, school, and family now, he’s always shown me I can do at least a little more. And I want thank my sister for keeping it real. That’s important. Seriously. Also, I don’t know if says more about

my tenure at Tufts, or that they are part rabbit, but I want to thank both my siblings for the four nephews and niece that were born during (or just before) my time here- Connor, Gray, Brennan, and Harper.

I would be remiss if I failed to acknowledge the important contributions of the Hornets' Nest during my formative years at Tufts, but I would probably more remisserer if I acknowledged them here in writing.

Finally, I want to thank Anna, who has been for some time the single best source of happiness in my life. She's done more than anyone to keep me (somewhat) sane(ish) during what has been an exciting, consuming, maddening, and gratifying experience. But more than anything, she's taught me my true purpose in life: Paaaaaaaaaaaaaaaaahhhhhhhhpiiiiiiiiiiieeeeeeeeeeeees….

Table of Contents

Chapter 1 2

Mechanisms of tissue patterning and morphogenesis 2

Molecular mechanisms of tissue patterning 3

Regulation of intercellular signaling 4

Gene regulatory networks contribute to spatial patterning of gene expression 11

Physical mechanisms of boundary formation 14

Summary 17

Adhesion and Tension Promote Morphogenesis of the *Drosophila* Eye 18

Conceptual framework to investigate epithelial morphogenesis 19

Control of adhesion and tension in epithelial morphogenesis 23

Coupling Adhesion and Contractility 31

Control of actomyosin dynamics by phosphoinositide signaling and RhoGTPases 33

Phosphoinositide signaling could mediate cross talk between adhesion and tension 42

Development of the *Drosophila* Eye 42

Early eye patterning 43

Morphogenesis of the IOC lattice 44

Summary 47

Chapter 2 50

odd-skipped genes and *lines* organize the notum anterior-posterior axis by autonomous and non-autonomous mechanisms 50

Abstract 51

Introduction 51

Materials and Methods 55

Fly strains and clonal analysis 55

Immunofluorescence and microscopy 56

Interaction of Lines with Odd-skipped proteins in S2 cells 56

Analysis of clone shape 57

Thorax measurements 57

Results 58
odd-skipped family members are expressed in distinct patterns in the developing notum 58
odd-skipped genes are required for notum formation at early first instar 60
odd-skipped genes and *lines* regulate Bowl accumulation in the developing notum 61
drm promotes Bowl and Eyg accumulation using cell-autonomous and non-autonomous mechanisms 62
bowl regulates *bar* and *Dl* to pattern the prescutum autonomously 64
odd-skipped genes pattern the eye margin 66
Discussion 68
Epithelia are frequently patterned by signals from opposing field boundaries. 68
odd-skipped genes pattern the notum AP axis using autonomous and non-autonomous mechanisms 69
Redundant versus unique functions of *odd-skipped* genes in notum development 72
Conserved roles for odd-skipped genes and lines to pattern dorsal appendages ... 73
Conclusion 74
Acknowledgements 75
Chapter 3 101

Interplay of contractile and protrusive forces control cell shape in the Drosophila eye 101

Abstract 102
Introduction 103
Experimental Design 106
Immunostaining 106
Fly Stocks 106
Imaging 107
Clone measurements 108
Results 108
Polarized tension within and between cells drives pigment cell shape change. ... 108
Branched F-actin networks promote transient contact expansion 110
Phosphoinositide signaling correlates with contact length dynamics 113
Discussion 115
Autonomous and non-autonomous contractile forces contribute to 2° cell elongation 115

Role of pulsed contractile and protrusive dynamics in eye morphogenesis 118
Hypothetical roles for phosphoinositide signaling in eye morphogenesis 119
Acknowledgements 121
Chapter 4 140

Summary & Future Directions 140

odd-skipped genes pattern the notum AP axis 142
Summary 142
Future Directions 143
Pulses of PIP3 and F-actin mediate shape change in the eye 146
Summary 146
Future Directions 148
Appendix 1 152

References 153

List of Figures

Figure 1.1: Cell intercalation, cell death, and cell shape change form the final crystalline lattice of the *Drosophila* eye epithelium 49

Figure 2.1: Nested expression of Bowl relative to drm and odd along the anterior border of the notum 76

Figure 2.2: Evolution of Bowl accumulation relative to mirr and Eyg 78

Figure 2.3: Roles of lines and bowl in notum specification 79

Figure 2.4: Expression of notum markers in C311>lines discs 81

Figure 2.5: Neither odd nor drm are necessary for the expansion of the Eyg domain 82

Figure 2.6: Regulation of Bowl accumulation by drm, odd, sob and lines in the notum and S2 cells 83

Figure 2.7: Ectopic posterior expression of drm induces ectopic anterior notum and inhibits scutellum formation 85

Figure 2.8: odd-skipped genes promote scutum expansion autonomously and non-autonomously 86

Figure 2.9: Drm induces Bowl, but not Eyg, autonomously and nonautonomously in the wing pouch 87

Figure 2.10: Eyg is maintained independently of Bowl after the early first instar 88

Figure 2.11: bowl specifies the prescutum 89

Figure 2.12: Reduction of Bowl expression and the scope of prescutum in klu>lines nota. 91

Figure 2.13: bowl clones segregate from the bowl domain 92

Figure 2.14: Model of the role odd-skipped genes in notum AP patterning..... 93

Figure 2.15: Bowl is expressed in PE and margin cells of the eye 94

Figure 2.16: Bowl is required for the expansion of the eye field 95

Figure 2.17: Ectopic Bowl accumulation results in cuticle formation, often at the expense of retinal tissue 97

Figure 2.18: *odd-skipped* genes Drm and Bowl regulate the accumulation of Wg at the eye disc margin 99

Figure 3.1: Sqh is required for normal pigment cell morphogenesis 122

Figure 3.3: F-actin pulses correlate with contact expansion 124

Figure 3.4: SCAR colocalizes with F-actin at the apico-lateral surface of cell contacts .. 126

Figure 3.5: Arp3 and F-actin are dynamically enriched at expanding 2°-3° contacts..... 127

Figure 3.6: The Arp3 regulator SCAR is required for normal apical morphogenesis..... 129

Figure 3.7 Dominant negative Rac (RacN17) leads to a disorganized hyper contractile actomyosin network 130

Figure 3.8 PIP3 correlates with contact length..... 131

Figure 3.9: PIP2 does not correlate with contact length 132

Fig 3.10 Expression of $Cdc42^{DN}$ causes expanded PIP3 dynamics 134

Figure 3.11: Manipulation of Pi3k fails to completely abolish PIP3 polarization or cause cell shape defects..... 135

Figure 3.12 Model of pulsed contractile and protrusive dynamics at 2°-3° contacts 137

Table 4.1: List of phosphoinositide binding Rho family interactors 139

List of Abbreviations

APF	after puparium formation
AJ	adherens junction
AP	anterior-posterior
BMP	bone morphogenetic protein
Bowl	Brother of *odd* with entrails limited
CALI	chromophore assisted light inactivation
DAH	differential adhesion hypothesis
Dl	Delta
Dlp	Dally-like
DP	disc proper
Drm	Drumstick
DV	dorsal-ventral
ECM	extracellular matrix
Ed	Echinoid
EGFR	Epidermal Growth Factor Receptor
Fz2	Frizzled 2
GBE	germband extension
Hbs	Hibris
Hh	Hedgehog
HSPGs	heparan sulfate proteoglycans
IOC	interommatidial cell (2° and 3° cells, collectively)
Kirre	Kin of Roughest
MyoII	Myosin II
N	Notch
Odd	Odd-skipped
PE	peripodial epithelium
Pnr	Pannier
PI	phosphoinositide
Ptc	Patched
Rst	Roughest
Sns	Sticks ‘n stones
Sob	Sister of *odd* and *bowl*
TST	tissue surface tension
Ush	U-shaped
Wg	Wingless

Mechanisms of Epithelial Patterning and Morphogenesis

Chapter 1

Mechanisms of tissue patterning and morphogenesis

The normal development of functional tissues, organs, and organisms requires exquisite coordination amongst all constituent cells. Cell fates must be organized and maintained in discrete spatial domains. This patterning process is accomplished by the concerted actions of intercellular signaling and gene regulatory networks. In addition to normal patterning, normal form and function require the coordination of cell shapes, behaviors, and mechanical properties. Coordination at both levels emerges from the dense regulation of a relatively spare set of key effectors by a large number of upstream regulatory mechanisms that work to provide spatial and temporal specificity to pathway activities and interactions. These regulatory interactions help to fulfill two key requirements of development: that developmental mechanisms must be flexible enough to allow for vast functional diversity based on relatively few signaling modules, and that developmental programs must be robust with respect to environmental or genetic variability. In the two sections of this introduction, I will review a number of examples that illustrate key mechanisms by which cells and tissues achieve these goals in the context of tissue patterning (part one), and tissue morphogenesis (part two).

Molecular mechanisms of tissue patterning

Robust tissue patterning requires the precise coordination of gene expression patterns that organize cell fates across potentially wide spatial or temporal ranges. The dominant model by which this coordination is achieved is through tissue organizers, which are special zones within a tissue that signal to neighboring or distant cells to coordinate patterns of gene expression[1]. Integral to this model of development is the idea of iterative pattern elaboration, wherein initial rough patterning cues serve as the platform for progressively finer patterning. A key requirement of this patterning is the creation and maintenance of sharp borders that clearly delineate adjacent domains. Boundaries are crucial for the maintenance of discrete tissue

domains, but they also frequently serve as secondary organizers to promote elaboration of earlier patterning cues. Hence, the robust and accurate formation of boundaries of gene expression is of critical importance to normal development. This is confirmed by a number of diseases and developmental defects that result from improper boundary formation[2–4]. The formation and maintenance of boundaries are controlled at three distinct levels. The first occurs at the level of the signal produced by the organizer. The second occurs at the level of reception of and response to the signal by surrounding cells. The third results from emergent changes that occur as a result of this response. Together, these mechanisms provide an incredible range of flexibility and robustness to pattern formation.

Regulation of intercellular signaling

The proper development of any complex multicellular tissue requires the coordination in space and time of cell fates across the tissue. The first step in this coordination is the communication of positional information and cell fate status between cells. In practice, such communication is generally mediated by special (though not necessarily rare or unique) cells, and these cells most frequently occur at developmental boundaries. The nature of these signals is fundamentally of two kinds, juxtacrine signaling mediated by direct cell-cell interaction, and paracrine, in which a cell or cells communicate with distant cells by means of a secreted signal. Each mode of signaling is capable of producing clearly defined boundaries of gene expression. Below, we will consider the mechanisms that regulate these signals directly to contribute to boundary formation.

Regulation of morphogen gradients

It has been long appreciated by theorists and developmental biologists that a minimal set of rules governing cell communication could, in principle, generate relatively complex

patterns of behavior or identity in a field of cells. The first such model suggested that the reaction and diffusion of opposing signals could simply account for patterns of stripes or spots reminiscent of developmental gene expression patterns [5–7]. An alternative model proposed that a smooth gradient of signal could be interpreted in a concentration dependent manner to organize spatial patterns [8]. Fundamentally, this model has strong explanatory power, in that many diffusible signals have been found that do indeed mediate gene expression patterns in this fashion [9–12].

However, a number of challenges exist *in vivo* that suggest that, in order to robustly achieve normal patterning, a rather more complex set of mechanisms might be required to regulate cell communication [13]. First, the signal to noise ratio of a gradient *in vivo* is likely very low. Noise can come from inherent noise in the gradient, movement of cells during or after gradient formation[4], stochastic response to the signal, and others [15]. The signal resolution, even absent noise, may not in some cases be very high. For a 'simple' long range gradient, neighboring cells might only see a difference of 16% in signal intensity [13,16]. Other factors, such as the timing and duration of signal could have as strong an effect on a cell as the local concentration [17–19]. These challenges reflect the inherent complexity of the task of the morphogen system, which must control multiple cell fates with sharp borders within and across a defined area in a coordinated fashion. Further, it must do so robustly in potentially unpredictable environmental contexts. The fact that these patterning mechanisms are highly conserved suggests that they have been selected not only for these qualities, but also for the ability to be flexible enough to generate morphological and functional diversity between species as a result of evolution [13]. Below I will review selected examples of a variety of mechanisms by which cells regulate the formation of short and long range gradients to contribute to robust boundary formation.

Gradient shaping via ligand modification

Perhaps the most obvious mechanism of shaping a signal gradient is through regulation of the properties of the signal itself. Indeed, ligands undergo a number of modifications prior to secretion, the most common being lipid modification. Wnts, for example, are palmitoylated, though this appears to modulate signal strength, and not gradient formation[20]. By contrast, multiple lipid modifications of Hedgehog (Hh) do not appear to alter signal potency [21], though they do alter gradient formation. In particular, addition of a cholesterol adduct to the N terminus is required for normal signaling range, though the nature of this requirement is somewhat controversial: Some groups report increased range [22–24] following loss of the cholesterol group, while others report decreased range [25–28]. Some of this controversy might stem from different results depending on whether ligand range, signal reception, or target response were assayed. Most direct observations of Hh diffusion suggest that cholesterol modification increases local association with the plasma membrane, and limits the free extracellular diffusion of the ligand [26,28,29]. Interestingly, this association of Hh is only the first step in a complex mode of gradient formation, as will be discussed below [30].

Gradient shaping via ligand interactions

Following secretion, ligand interactions could alter diffusion. Possible interactions could include receptors, secreted inhibitors, or specific and non-specific interactions with components of the extracellular milieu. Heparan sulfate proteoglycans (HSPGs), for instance, interact with a number of ligands with high specificity and low affinity[22]. Despite their low affinity, high levels of HSPGs at the cell surface render these interactions significant. However, the effect of these interactions could be varied, depending on the context. HSPGs could act locally to potentiate pathway activity through the sequestration of ligand. Alternatively, they could facilitate long range signaling, either by generally stabilizing the ligand or by facilitating diffusion [31]. Studies of

signaling by the Wnt homolog Wingless (Wg) provide an interesting example of how the developmental regulation of HSPGs can feed back to modulate the signal gradient [32,33]. Two HSPGs, Dally and Dally-like (Dlp), each fulfill different roles to modulate Wg signaling in the *Drosophila* wing. *dally* mutant clones accumulate lower levels of extracellular Wg, particularly near the Wg source. By contrast, more distant Wg accumulation was inhibited in *dlp* clones [34]. This differential effect on Wg accumulation is consistent with their respective expression patterns. Dally is highly induced near the Wg source, while Dlp is expressed in a complementary pattern, and each is a target of Wg signaling. Together, these data highlight the dynamic interplay between pathway activity and gradient formation, and suggest that the patterning and activity of different populations of HSPGs serves to link the two.

Feedback regulation of gradient signaling

The dynamic interplay between Wg activity and HSPG patterning demonstrates the inherent complexity of gradient formation. This dynamic regulation and maintenance of gradient quality may emerge from a biological requirement for robustness[35]: Successful development requires that the signals and responses that mediate patterning need to be relatively invariant in the face of environmental or genetic fluctuations. Modeling work suggests that 'simple' gradients that decay exponentially cannot simultaneously be robust to fluctuations and mediate long term gradient formation. By contrast, more flexible control of gradient formation over long and short spatial scales could accomplish both goals. The differential patterning and function of Dally and Dlp provide one example.

Interestingly, the Wg pathway may contain another mechanism to promote long range signaling. Binding of Wg to the Fz2 receptor promotes stabilization of the ligand[36]. Conversely, Wg pathway activity inhibited Fz2 expression. It was suggested that this system might allow the

distant diffusion of morphogen by preventing the premature sequestration of ligand near the source, while stabilizing it at a distance. Interestingly, other work suggests that this mechanism may be insufficient to explain the normal Wg pattern. Rather, modeling work suggests that one possible explanation requires unbound Fz2 to interfere with Wg degradation. Hence, close to the source, saturation of Fz2 leads to a higher rate of ligand degradation. At long ranges, occupancy decreases which allows Fz2 to inhibit degradation[35]. Such a mechanism must be more completely tested experimentally, as it is not clear what pathways might be engaged by bound vs unbound Fz2. However, this work highlights the complex requirements for gradient formation and provides a promising mechanism of action to achieve a robust and smooth long range gradient.

The Hh pathway invokes quite a different feedback mechanism to generate a much tighter gradient at the AP boundary of the wing. Receptor feedback contributes to the sharpness of this gradient. In this case, the interaction of ligand and receptor promotes internalization and degradation of the ligand. In contrast to Wg, however, Hh signaling induces expression of its receptor Patched (Ptc)[37]. This maximizes response close to the source, due to high signal flux, and limits signal range by promoting a high rate of ligand degradation[38]. Together, these two examples demonstrate how alternative use of receptor feedback can shape vastly different gradients.

Gradient shaping by regulation of secretion

One of the primary determinants of gradient quality is the quantity of signal released. In the case of EGFR signaling in *Drosophila*, the quantity of ligand secretion primarily determines signal range. Three of the four ligands of the *Drosophila* Epidermal growth factor receptor (EGFR), Spitz, Keren, and Gurken, are produced as inactive transmembrane precursors

sequestered in the ER. Secretion of these ligands requires both trafficking to the secretory compartment, and proteolytic cleavage. The protein Star promotes trafficking of ligand to the secretory compartment[39,40], while the protease Rhomboid acts within the secretory compartment to cleave the ligand[41]. Interestingly, Rhomboid can also cleave Star in the ER, preventing transport to the secretory compartment[42,43]. Together, this restricts the quantity of ligand and hence the range of signaling.

Gradient range can also be influenced by the location of secretion. In *Drosophila*, a number of mechanisms regulate the diffusion of the secreted signal Hh, including interactions with HSPGs and lipid modification of the ligand. The ligand itself is secreted from the apical surface of the cell, where its diffusion is thought to be limited by the HSPG Dally. Surprisingly, another report suggests that under normal conditions, extracellular Hh actually accumulates basolaterally[30]. Following apical secretion, it is suggested that the signaling cell internalizes the Hh ligand and recycles it to the basolateral surface. This is supported by experiments that transiently inhibit endocytosis, which cause apical accumulation of Hh and disrupt both long and short range target gene expression. Basolateral trafficking is similarly required for normal Sonic Hedgehog (Shh) signaling in vertebrates[44], and for the Notch (N) ligand Delta[45]. These data suggest that the subcellular site of secretion can profoundly alter the quality of a gradient, including both its range and its magnitude. It will be particularly interesting to determine whether such mechanisms regulate the site of release to shape gradients in different developmental contexts.

Gradient regulation by control of ligand transport

The frequent presence of lipid modifications on many diffusible ligands raises the question of how potentially membrane bound molecules might act over long distances. Beyond

free diffusion through the extracellular milieu, some data suggest that extracellular lipid particles might facilitate transport. *Drosophila* Hh and Wg each require the apolipoprotein Lipophorin to signal normally. Each co-precipitates *in vitro* and colocalizes *in vivo* with Lipophorin. Depletion of Lipophorin limited the diffusion of each ligand, and resulted in a compression of spatial domains of target gene expression[24]. Further, the association of Wg required cholesterol modification of the ligand. In the case of Hh signaling, the glypican HSPG Dally also interacted with Lipophorin, which enhanced recruitment of lipophorin particles to the tissue. Together, these data suggest that transport on liposomes can regulate both the range of pathway activity[24], and the strength of signaling[22]. It remains to be determined which of these systems are indeed used to control the nature of signal gradients in different developmental contexts.

The above morphogen models require ligand secretion. Alternatively, cells could directly transmit or receive signals via filopodia-like extensions[46,47]. These F-actin based projections, called cytonemes, were first observed converging on the AP compartment boundary in the *Drosophila* wing[48]. These cytonemes target the region of Dpp secretion, and traffic the Dpp receptor Thickveins (Tkv)[49]. This remarkable specificity was also observed for cytonemes directed toward sources of different ligands in both the wing and eye[50]. These extensions also appear to mediate communication between different tissues. Trachea cells oriented cytonemes specifically toward sources of Dpp and FGF in the wing[51]. As in the other cases, these cytonemes exhibited molecular specificity for the target region. Importantly, these cytonemes physically interact with target cells and directly mediate the transport of both ligand and receptor to the receiving cell. Co-expression of GFP-Dpp and Cherry-Tkv receptor specifically in the signaling and receiving cells, respectively, revealed that both were trafficked in a retrograde manner toward the Tkv expressing cells receiving the Dpp signal. Reconstitution of GFP via the GRASP

technique[52] confirms contact between the two cells[53]. Other work suggests that cytonemes could mediate signaling in a variety of developmental contexts. Cytonemes appear to mediate Hh gradient formation[54], and the polarized reception of EGFR signaling during cell fate commitment[55]. Lastly, *Drosophila* cytonemes share many characteristics with similar protrusions observed in vertebrate development[56–58], suggesting such mechanisms may be evolutionarily conserved. Many questions remain regarding the regulation of gradient formation by cytonemes, including mechanisms of recognition, stabilization, and transport of signaling components. It is also not clear precisely how a cytoneme gradient might compare to other models, and how current experimental data might apply. It is important to note that mechanisms such as differential secretion and communication via cytonemes need not be considered apart from one another. Indeed, cytonemes have been shown to localize both basally and apically[49], and could serve to mediate the transport of secreted signals.

Summary

The first challenge in establishing robust domains of gene expression is the distribution of accurate patterning cues over long ranges. It is clear that for each signaling pathway, a number of mechanisms can cooperate to shape the range, slope, and magnitude of morphogen gradients. These qualities in turn regulate the extent and relative domains of expression of various low and high threshold target genes. These programs of gene expression can then act to establish domains of differentiation, or coordinate subsequent patterning through the induction of organizers and signals.

Gene regulatory networks contribute to spatial patterning of gene expression

To understand how a morphogen can coordinate cell fate across a tissue, it is clearly necessary to understand the nature of the response of cells to the signal. Here I will briefly

review two gene regulatory modules that highlight the robust, coordinate regulation of spatial information and boundary formation.

Notum patterning

My own work in the genetic control of tissue patterning focused on the AP patterning of the notum, which serves as an excellent example of how signaling and gene regulatory networks result in functional and morphological diversity in a final developed structure. The *Drosophila* notum, or dorsal mesothorax, is one of the best studied examples of the 'prepattern' model of genetic patterning, where a grid of patterning genes expressed along the AP and DV axes prefigures the placement and specification of specialized cell types and structures[59]. Particularly relevant to the discussion of boundary formation, the intersection of different domains within this checkerboard of gene expression also prefigures morphological landmarks. For example, the prescutal suture, which is an epithelial fold near the anterior notum, occurs at the boundary of Bar gene expression[60]. The notum is particularly advantageous in this regard due to the stereotyped placement of 22 bristles, which provide a clear morphological readout of the genetic prepattern. The placement of these bristles correlates with and requires the highly localized activation of the pro-neural *achaete-scute* complex. A more complete description of the signals and genes that pattern the notum will follow in chapter two; here I will briefly mention one example of how this genetic prepattern controls *achaete-scute* expression to place the bristles.

The primary genes required for activation of *achaete-scute* are the GATA transcription factor *pannier* (*pnr*) and the homeobox *Iroquois* complex of genes (*Iro*-C), which are expressed in complementary medial and lateral domains within the developing notum. Interestingly, though the pattern of *pnr* is well conserved between fly genera, the patterns of bristles are not[61]. This

suggests that indeed the remaining prepatterning genes are important in controlling the scope of *achaete-scute* activation. Two particularly well studied bristles, the dorsocentral bristles, are located within the heart of the *pnr* domain, and are under the control of a specific regulatory element of the *achaete-scute* complex, the dorsocentral enhancer. The enhancer, transcription of *achaete-scute*, and the placement of the dorsocentral bristles all occur at the fringe of expression of the Friend of GATA homolog *u-shaped* (*ush*), which is expressed in a nested dorsal region within the *pnr* domain. This nested expression pattern emerges from the coordination of *pnr* and *ush* gene expression patterns by the morphogen Dpp[62]. Ush interacts directly with Pnr[63], and represses Pnr activity at the dorsocentral enhancer[63,64], preventing *achaete-scute* activity. This provides a clear example where coordinate positive and negative regulation within a gene regulatory network combine to refine the spatial control of target gene activity and ultimately morphology.

Odd skipped genes and lines control cell fate in adjacent domains

The *odd-skipped* family genes are particularly well suited to mediate the formation of distinct cell fate domains within a tissue. The *odd-skipped* (*odd*) genes are a family of four C_2H_2 zinc finger proteins comprised of *odd*, *bowl*, *sob*, and *drumstick* (*drm*). Of note, while *odd*, *sob*, and *drm* are regulated at the transcriptional level, *bowl* is ubiquitously expressed. Accumulation of Bowl protein is instead controlled by the protein Lines, which efficiently leads to the degradation of Bowl protein[65,66]. Relief of this repression is afforded by the expression of other *odd* family members, which can titrate Lines from Bowl.

In a number of developmental contexts, *odd-skipped* genes and Lines accumulate in complementary domains and mediate alternative cell fate decisions. In the hindgut, Lines and Drm/Bowl act in adjacent cell populations to specify small versus large intestine fates[65,67,68].

Similarly, Lines and Drm/Bowl act antagonistically in the dorsal epidermis to specify 4° versus 1°-3° cell fates[66], and in the testis to specify somatic stem cell versus hub cell fates[69]. In the wing, Bowl accumulates in the squamous peripodial epithelium (PE), while Lines accumulates in the complementary columnar disc proper (DP). Expression of Lines in the PE causes adoption of DP fate, while removal of Lines in the DP causes the reciprocal acquisition of PE fate. Of note, these changes also result in sorting of the manipulated cells from the original tissue domain, suggesting that these cell fate choices are required for the sorting of cells into defined domains (see next section). Consistent with a role in defining exclusive tissue domains, *odd-skipped* genes are frequently expressed at tissue boundaries, such as the PE-DP margin[70], in cells flanking embryonic and limb segment boundaries[66,71], and at the foregut-hindgut junction[68].

One mechanism by which *odd-skipped* genes might mediate boundary formation is by the regulation of Notch (N) signaling. In the leg, *odd-skipped* genes are expressed in a zone of N activity proximal to presumptive leg joints[71,72], and N activity is required for *odd-skipped* gene expression. Moreover, *odd-skipped* genes repress the N ligand Delta (Dl), thereby potentiating N activation within the N activated region. Conversely, Lines accumulation in the adjacent domain de-represses Delta expression. Together, this regulatory logic establishes a stable N signaling interface. In the following sections, we will explore mechanisms by which N and other signals can promote the physical separation of tissue domains.

Physical mechanisms of boundary formation

The previous examples have highlighted the need for maintaining sharp borders of gene expression, and suggested several mechanisms by which secreted signals and gene regulatory activities could generate stable boundaries between domains. However, the interaction between cells at an interface is mediated by physical cell-cell contact by junctional proteins and

modulated by the mechanical properties of the cells and tissues (see following section). Hence, ultimately the signals and gene regulatory networks must alter these properties to generate domain boundaries.

Generation of a physical boundary by actomyosin tension

As mentioned, N activity contributes to a stable signaling interface in the leg. At the DV compartment boundary of the wing, N pathway activity is similarly required to prevent domain mixing. The position of the N signaling interface defines the barrier to mixing, and mutations in N at the interface disrupt domain segregation[73,74]. This disruption is unique in that once the barrier is disrupted, both mutant and wild type cells can mix in either direction. This suggests that N establishes a 'fence' to prevent domain mixing at the DV interface. Indeed, both F-actin[75] and MyoII[76] accumulate in a linear cable at N interfaces at the DV compartment border. Manipulation of N activity disrupted or mislocalized cable formation, and direct disruption of the actomyosin cable disrupted barrier formation[75,76]. Similar actomyosin polarization is present at the AP compartment border in the wing[77], and in the *Drosophila* embryonic epithelium[78,79]. In a particularly telling experiment, spatiotemporally specific and direct inactivation of MyoII by CALI at the parasegment border disrupted barrier function and allowed inappropriate domain mixing[78].

Differential affinity mediates cell sorting at tissue boundaries

Holtfreter first suggested that selective homotypic cohesion of cells from different regions of the developing embryo might allow the sorting of germ layers and subsequent tissue lineages [80]. Steinberg subsequently refined this hypothesis to state that the differential adhesion of different germ layers was the primary determinant of sorting [81]. Specifically, the differential adhesion hypothesis (DAH) states that differences in adhesion molecules create differences in

surface tension amongst the different germ layers. I will discuss the assumptions and evolution of this theory of cell sorting and behavior more thoroughly in part two of this introduction. Here, I will focus on the role of differential adhesion to mediate boundary formation during development.

Differential expression of Cadherins correlates with boundaries in the developing brain

The vertebrate brain provides a striking example of the degree of segregation of tissue domains. More than 30 cadherins are expressed in the developing brain, with expression patterns that frequently coincide with segmental boundaries[82]. Within ventricular cells of telencephalon the adjacent compartments of the lateral ganglionic eminence and the presumptive cerebral cortex[83,84] express the cadherins Cad6 and RCad in complementary domains. A smooth boundary of cell contacts delineates the two domains, across which cells do not mix[84,85]. Interestingly, this expression and sorting occurs prior to morphological border formation. The functional requirement for these cadherins, though, remains unclear. While misexpression of cadherins is sufficient to promote sorting, loss of Cad6 does not alter domain formation[84]. It is unclear as yet whether this lack of phenotype suggests some other mechanism of boundary formation, or some level of redundancy between Cadherin family members. It is also possible that the restricted expression of RCad is sufficient to initiate and maintain domain sorting.

Eph/Ephrins

The vertebrate hindbrain is initially patterned by the development of transient segments, called rhombomeres. Rhombomeres form transiently during vertebrate hindbrain development, each representing a compartment with lineage restricted borders[86]. Interestingly, while cells from alternate rhombomeres can aggregate freely, cells from adjacent rhombomeres

sort from one another[87,88]. A number of segmentally expressed genes have been identified that mediate this segregation [89]. Of note, the receptor tyrosine kinase (RTK) type B Ephs and the Type B ephrins are expressed segmentally, and are required for rhombomere segmentation.

The type B Ephs and Ephrins signal bidirectionally[90] to regulate a variety of downstream cell behaviors, including cell migration, proliferation, and differentiation[91]. Of particular note in the context of boundary formation, Ephs and Ephrins are expressed in complementary patterns in the developing hindbrain[92]. Specifically, odd rhombomeres express EphB receptors, and even rhombomeres express Ephrin-B ligands. The ectopic expression of EphrinB2 in odd or EphA4 in even rhombomeres caused sorting to the border between even and odd[93]. Based on the observation that rhombomere boundaries feature an expanded intercellular space, and by analogy to their characterized roles in axon guidance[94], Eph/Ephrin interactions were hypothesized to mediate intercellular repulsion to promote the rhombomere boundary. This is consistent with roles in several systems in which Eph-Ephrin interactions mediate compartmentalization of different cell populations[95–97].

Summary

At each level of pattern formation, from signal reception to cell behavior, a number of mechanisms cooperate to generate consistent domains of gene expression that are delineated by sharp boundaries. This boundary formation is critical for the induction of subsequent patterning cues and is required for the progressive fine patterning of developing tissues. In the next section, we will explore the physical mechanisms by which cells act on these patterning cues to drive morphogenesis.

Adhesion and Tension Promote Morphogenesis of the *Drosophila* Eye

As described in the previous section, intercellular signaling coordinates the activation of gene regulatory networks that create a genetic map of a developing tissue. Subsequently (or concurrently), this genetic map must be acted upon by the constituent cells to drive the morphogenetic process. The repertoire of behaviors with which epithelial cells do so is primarily limited to the control of growth, mitosis, apoptosis, migration, rearrangement, and shape change. Importantly, the interconnected nature of an epithelium entails that the behavior of a single cell both affects and is affected by the behavior of surrounding cells. As such, a complete picture of morphogenesis requires the integrated understanding of the molecular determinants of cell behaviors and cell interactions, the cellular behaviors themselves, and the coordination of these behaviors as a composite network that determines the final form of an epithelium.

A major defining characteristic of an epithelial cell is the adhesive contact it forms with its neighbors. Though the molecular composition and functional roles of these contacts vary between tissues and species, the adherens junction (AJ) is the most critical and conserved[98] in the control of morphogenesis. AJs are highly dynamic adhesive structures that maintain epithelial barrier integrity while simultaneously allowing for the dynamic behaviors mentioned above. In doing so, they play a variety of roles in the control of cell behavior, chief among them regulation of cell-cell signaling [99,100], the regulation of cell adhesion [101], and the communication of mechanical forces within and between cells [102,103]. Though each contributes to morphogenesis, the control of cell adhesion and the communication of mechanical forces exert the most direct control over cell and tissue morphogenesis, and will be the focus of this section of the introduction. In fact, the adhesive and force transduction capacities of the AJ are

inextricably linked at both a molecular and functional level. AJs connect to the cortical actomyosin cytoskeleton, and this association is required for junctional stability. In turn, actomyosin networks generate contractile forces that are communicated directly through the AJ to adjacent cells. In sum, the balance of AJ based adhesion and cortical actomyosin based tension primarily determine many of the morphogenetic behaviors described above[104].

As briefly described earlier, the differential adhesion hypothesis (DAH) of Steinberg states that cells will sort based on their tissue surface tension, much like soap bubbles. This theory provided the first framework to understand how the forces of adhesion and tension ultimately translate into morphology. In the second part of this section, I will review the regulation of these forces in the control of cell-cell contacts during epithelial morphogenesis. Despite the identification of a number of key regulators of adhesion and tension, the mechanisms by which cells balance these forces at particular cell-cell contacts to generate unique and stable cell morphologies and tissue topologies remain poorly understood. My work has attempted to investigate this regulation in the control of cell shape change during *Drosophila* eye morphogenesis. In the final section of this introduction, I will review the development of the eye, with particular emphasis on the contributions of cell adhesion and cortical tension to the morphogenesis of the final structure.

Conceptual framework to investigate epithelial morphogenesis

For more than 30 years, Steinberg's (DAH) served as the most influential intellectual framework for the investigation of epithelial morphogenesis. Though originally formulated to explain the sorting behavior of cells and tissues during gastrulation, the model has been used to explain a host of sorting and morphogenetic processes [105] including compartment boundary formation [73,106], gangliogenesis of the enteric nervous system [107], and cell shape and packing of

the *Drosophila* eye [108–110]. However, as the molecular pathways that regulate the biomechanical properties of cells have evolved, the idea that adhesive forces singularly determine tissue surface tension and cell sorting has expanded to include the generation of cortical tension by the actomyosin cytoskeleton. Indeed, these two forces, and their relative balance, are considered to be the primary determinants of cell and epithelial morphology [104].

Early Conception of DAH

Holtfreter first suggested that selective homotypic cohesion of cells from different regions of the developing embryo might allow the sorting of germ layers and subsequent tissue lineages [80]. Steinberg subsequently refined this hypothesis to state that the differential adhesion of different germ layers was the primary determinant of sorting [81]. Specifically, the DAH states that differences in adhesion molecules create differences in surface tension amongst the different germ layers. This early formulation posits that surface tension is a homogenous property of tissues. Some modeling supports this idea, suggesting that the sorting of embryonic tissues is analogous to the phase sorting of different visco-elastic fluids [111]. Other work supports the claim that differential adhesion mediates the differences in surface tension that drive phase separation. Cells that ectopically express cadherins sort from one another on the basis of the type of cadherin expressed, and sort in explant tissues based on the levels of Cadherin expression within the tissue [112]. A number of *in vivo* experiments further support the idea that differential adhesion mediates cell sorting. As will be discussed in more detail below, differential cadherin expression mediates segregation of cells within a tissue, in *Xenopus* embryos [113,114], or *Drosophila* imaginal discs [106]. Together, these data highlight the importance of adhesion molecules in the sorting of cells during tissue morphogenesis. However, they do not directly test

whether cadherin based adhesion is the primary determinant of tissue surface tension and sorting.

Indeed, several lines of evidence suggest that cell adhesion is insufficient to explain sorting. Cadherin binding specificity does not correlate with adhesion strength or sorting *in vitro* [115,116]. Additionally, despite the finding that E-Cadherin expression is proportional to tissue surface tension [117], it is insufficient to explain the overall magnitude of the tension [118]. Lastly, it is clear that the surface tension of epithelial cell aggregates is not homogenous. Rather, cells sense and respond to external forces or signals, resulting in different levels of tension at cell-cell, cell-ECM, or cell-medium interfaces [119–121]. These data highlight a primary conceptual limitation of the DAH: cells and tissues are not homogenous, passive fluids, but rather are metabolically active agents capable of modifying with spatial specificity a host of biophysical properties [122]. This suggests that additional mechanisms beyond adhesion are required to account for the differential surface tensions that mediate epithelial sorting.

Cortical Tension Contributes to tissue surface tension

An alternative theoretical model, originally coined the differential interfacial tension hypothesis (DITH) posits that tensile force generation is required to fully account for differences in tissue surface tension [122–124]. A key feature of this revision is that it allows for and is supported by experimental evidence that epithelial cells are mechanically polarized during tissue morphogenesis [125], meaning they spatially polarized biomechanical properties such as surface tension or stiffness. This polarity is supported by both biophysical measurements [120,121,126], and the observed polarization of the actomyosin cytoskeleton during both developmental [78,119,127] and experimentally induced [128] cell sorting. These data support the hypothesis that contractile

forces play a key role in morphogenetic processes previously thought to be dominated by cell adhesion[129].

Perhaps the clearest such example is provided by recent work from the Heisenberg lab. In cell pair adhesion assays, the difference in tension between cell-cell interface and the cell-medium interface was the primary determinant of the cell contact size. By contrast, 'adhesion tension', which represents the tendency of adhesion to promote contact expansion, had little effect on contact size. Instead, cadherin complexes served to mechanically couple the cortices of adhering cells [119]. Interestingly, the sorting of these cells in culture is abolished or reversed following inhibition of either MyoII or the upstream regulator Rho kinase [126], supporting the hypothesis that polarized tension mediates not only contact size, but also tissue surface tension and sorting. This is consistent with predictions of the DITH and similar models that suggest that polarized cortical surface tension, and not adhesive differences per se, can account for normal sorting behavior [123,126]. These data are further supported by earlier studies that suggest that polarized acto-myosin activity contributes to expansion of *de novo* cell-cell contacts in cultured epithelial cells (see section below for more detail) [130–134]. These data suggest an interesting elaboration of the original DAH, which proposed that adhesion tension itself was the fundamental source of tissue surface tension. Together, these studies suggest that a key function of cadherin based adhesion is to polarize actomyosin tension, which then provides the driving force for cell sorting.

The primary concepts of the DAH and the DITH generalize to other types of epithelial morphogenetic events. First, the idea that epithelial topology represents an 'energy minimum' in which interfacial energy is minimized across the entire tissue serves as the basis of a number of computational models for morphogenetic processes including *Drosophila* eye cell shape [109,110] and sorting [135], tissue elongation [136–138], and embryonic segmentation [77]. Second, adhesion and

actomyosin based cortical tension are hypothesized to be the primary forces that regulate cell contact dynamics [104] during cell shape change [110] and cell rearrangements [139–142]. The regulation of these forces will be reviewed in the coming sections. The DAH and derivatives provide an outstanding, parsimonious model with which to conceptualize and model cell and tissue behaviors. It remains now to understand how cells regulate so few parameters to generate such morphological diversity.

Control of adhesion and tension in epithelial morphogenesis

Tissue topology emerges from the collective shapes of its constituent cells, while the shapes of cells are fundamentally determined by the number, size, and shape of their contacts with neighbors. These contacts are defined by the local balance of tension and adhesion, while the global integration of these forces determines tissue morphology. Here I will review the best characterized molecular pathways that regulate these forces.

Control of Cell Adhesion

Regulation of contact expansion

Much of our understanding of contact expansion comes from the *in vitro* study of *de novo* contact formation. This work demonstrates that a complex interplay between cadherin based AJs and the underlying cortical cytoskeleton is a critical determinant of cell contact size and strength. In culture, protrusive lamellipodia initiate new cell contacts [132,143]. These contacts lead to the rapid formation of E-Cadherin punctae which then induce a dramatic reorganization of the underlying cortical F-actin cytoskeleton [144]. In primary cultured keratinocytes, nascent contacts generate radially arrayed F-actin cables [143,145] that interdigitate between contacting cells, creating an 'adhesion zipper'. These cables require the recruitment and activity of formin-1[146], which binds to α-Catenin and promotes the synthesis of linear F-actin fibers. As the contact

matures, this interdigitated zipper resolves into a continuous plaque of E-Cadherin and associated junction components [143], though it is unclear whether linear actin pushing forces or actomyosin tension resolve this 'zipper' configuration.

Several mechanisms combine to drive the subsequent expansion of nascent contacts, including both branched F-actin synthesis and actomyosin constriction. The AJ recruits a number of branched F-actin regulators. E-Cadherin interacts with the Arp2/3 complex subunit arpc2 [147], while α-catenin interacts directly with the Arp2/3 activator Cortactin [148]. Both Arp2/3 activity [149] and Cortactin [150] are required for normal contact expansion. Further, the small Rho GTPase Rac1 dynamically localizes to the region just flanking the expanding contact[134,151], where it promotes branched F-actin synthesis. A similar distribution of F-actin promotes apposition of adjacent membranes following cell division within the plane of the *Drosophila* thoracic epithelium [152]. Together, these studies highlight a crucial role for branched F-actin based protrusive force to promote cell contact expansion [134,151].

Protrusive forces are only partly responsible for contact expansion. Additionally, actomyosin contractility plays a crucial role in the expansion, stability, and strengthening of cell contacts. MyoII associates with F-actin at the apico-lateral surface lateral to the expanding nascent contact [132,133,153], and is required for normal formation of the AJ [131,133,143]. This tension correlates with localized Rho1 activity, which is required for the normal expansion of cell contacts. Inhibition of Rho kinase or MyoII stopped or slowed contact expansion, and prevented the formation of E-Cadherin punctae at the expanding contact margin [134]. Together with observations that MyoII accumulation barely accumulates at the cell-cell interface [119,134], these data suggest that contact expansion requires a force imbalance between the contact and the surrounding lateral cortex.

In addition to promoting contact expansion, this polarized tension might contribute to AJ maturation and stability. The net tension, which is oriented away from the contact interface, induces the outward flow of both membrane [154] and E-Cadherin punctae [155] toward the contact margin. This flow is consistent with the observed accumulation of junction components at the margins of cell contacts in other systems [119]. Similar flows occur along the basal-apical axis of the lateral membrane during AJ maturation in culture[156]. Together, these studies paint a picture of a highly dynamic developing cell contact that requires MyoII based tension for proper organization.

E-Cadherin redistribution plays a vital role in the stabilization and strengthening of E-Cadherin based adhesions [133,157,158].The stability of cis interactions between E-Cadherin molecules is quite low, and is insufficient to promote cluster formation [159]. Instead, these transient interactions require stabilization through the interaction of the E-Cadherin cytoplasmic domain with the cortical F-actin cytoskeleton [158,159]. Clustering also requires functional MyoII activity, which could promote clustering by either active clustering or through the re-organization or crosslinking of the underlying F-actin network[160]. Strikingly, similar clusters are observed *in vivo* as intense punctae, and these 'spot' AJ and associated cytoskeletal structures are significantly more stable than surrounding populations[161]. Intriguingly, disruption by cell contacts by either mechanical dissociation or removal of β-catenin can result in the formation of membrane 'tethers' or tubules linking adjacent two cells[126,162,163]. This suggests that under some circumstances, the extracellular binding of E-Cadherin might be stronger than the intracellular link to the cytoskeleton[164], and reinforces the AJ-cytoskeleton interface as a primary determinant of contact stability.

Though our understanding of *de novo* contact formation and expansion is strong, it is clear that the nature of adhesive contacts is highly varied[153,165], raising the question of how

general such mechanisms of contact formation and expansion are. Further, AJs are highly dynamic entities, particularly during morphogenetic processes. It was generally assumed that contact expansion during *in vivo* morphogenesis was the result of a relief of MyoII contractility, though recent work suggests that such a step might be actively regulated[137]. It will be important to determine whether mechanisms similar to those characterized in cultured cells do indeed regulate dynamic contact expansion during morphogenesis. Finally, it will be important to characterize the mechanisms that integrate these cellular processes at the tissue level to control overall tissue morphology.

Control of cortical tension

By contrast to contact expansion, much of our understanding of contact constriction emerges from studies of *in vivo* epithelial morphogenesis. A significant body of work has uncovered many of the molecular pathways that govern biomechanical force generation in developmental processes such as tissue elongation, gastrulation, cell migration, and epithelial folding. As the molecular pathways that regulate biomechanical forces become more completely understood, the emergent challenge is to understand better the spatial and temporal coordination of these forces that allows for the subtle sculpting of epithelial tissues during development. It is becoming increasingly clear that this regulation is highly dynamic. Many instances of cell and junction constriction occur by the pulsed or oscillatory contractions of actomyosin networks. Furthermore, these networks and resulting forces exhibit spatially dynamic flows[166] that drive cell behaviors ranging from cell deformation[142] and cytokinesis[167] to polarization of the *C. elegans* zygote[168,169]. In the following sections, I will review the control of cell and junction constriction during epithelial morphogenesis, focused primarily on the role of oscillations and flows in the spatio-temporal regulation of cell and tissue morphogenesis.

Dynamic MyoII constriction during epithelial morphogenesis

Oscillatory actomyosin flows control planar polarized junction constriction

Perhaps the best studied example of junction constriction driving morphogenesis is germband extension (GBE) of the *Drosophila* embryo. During GBE, cells intercalate along the dorsoventral (DV) axis of the embryo, resulting in a dramatic elongation of the tissue[170]. This cell intercalation is driven by a process of specific cell contact rearrangements. Contacts between anterior and posterior cells ('vertical junctions') preferentially constrict, resulting in the formation of four-fold vertices[171,172] and multicellular rosettes[173]. These unstable conformations then resolve by the formation of new cell contacts orthogonal to the eliminated junction ('horizontal junctions').

A series of live imaging experiments has uncovered some of the mechanisms that regulate these junction dynamics, which occur by oscillatory flows of actomyosin. A medioapical actomyosin network exhibits polarized flow toward vertical junctions, and this flow correlates with pulses of anisotropic junction constriction[142,174]. Interestingly, pulses of junctional actomyosin very frequently followed the polarized apical flows. In contrast to apical flows however, enrichment of F-actin and MyoII at junctions[173,175] did not appear to drive constriction, but rather to stabilize existing constrictions. Together, these data suggest multiple roles for actomyosin tension, both to constrict junctions through an apical contractile network, and to stabilize this constriction by direct association with junctions.

The spatial control of these dynamics emerges from the planar polarization of this tissue, which is established downstream of embryonic AP patterning[173,175]. In particular, E-Cadherin is downregulated at vertical junctions prior to tissue elongation. A number of factors potentially contribute to this asymmetry: the tyrosine kinase Abl is enriched at vertical

junctions, where it phosphorylates β-catenin and increases junction turnover[176]. Similarly, the Rho1 effector Rok is enriched at vertical junctions, where it phosphorylates Bazooka to exclude it from vertical junctions[177]. This polarization of E-Cadherin suggests a paradox, however, whereby actomyosin flows appear directed toward the weakest point of anchorage (where E-Cadherin is lowest). This would contrast with other systems where cortical flows move toward the stronger anchorage[178]. In fact, E-Cadherin levels oscillate at vertical junctions, creating dynamic imbalances between either anterior or posterior vertical junctions within a cell. This imbalance leads to asymmetric anchorage of the contractile network, and subsequent flow. Though horizontal junctions accumulate much higher levels of E-Cadherin, dorsal and ventral contacts appear to exhibit insufficient asymmetries to direct flow. Thus, dynamic asymmetries in E-Cadherin between vertical junctions leads to alternate actomyosin flows within a single cell, which ultimately result in the constriction of both vertical junctions. Adding to the complexity, MyoII itself plays a role in these E-Cad dynamics through the clustering of E-Cadherin and initiation of clathrin mediated endocytosis[141].

These studies illustrate several key principles in the control of polarized contractile cell behaviors. The first is the requirement of a symmetry breaking event or spatial cue. In germband extension, polarized distribution of AJ components and regulators occurs downstream of anterior-posterior patterning [175]. Other such examples include asymmetric reception of a diffusible signal [179], intercellular contact [128], or mechanical disruption[180]. Such symmetry breaking is particularly relevant in the case of actomyosin dynamics, as it can generate actomyosin flows. This leads to a second key principle, which is that of feedback. Actomyosin flows represent one potential source of feedback, where initial imbalances in tension become magnified due to flow, or due to reorganization of the cytoskeleton, which can then potentiate contractility[103,181]. In the case of germband extension, increased MyoII also contributes to E-

Cadherin endocytosis, which serves as a point of negative feedback due to the subsequent decrease in actomyosin engagement. Similar couplings of positive feedback with delayed negative feedback serve as the basis for many biological oscillators.

It will be informative to investigate additional sources of positive and negative feedback in the generation of flow oscillations. Certainly the induction of E-Cadherin endocytosis provides one source of negative feedback. However, MyoII tension has also been shown to enhance junction stability[182–184], and it is possible that MyoII activity could itself potentiate actomyosin contractile forces[185–187]. Each of these mechanisms could serve as sources of positive feedback. In principle, the regulation of these parameters could conceivably alter characteristics such as the threshold for oscillation, or the magnitude or frequency of oscillations. Lastly, convergent extension drives elongation and remodeling of tissues other than the germband[136–138]. It will be interesting to determine whether similar molecular pathways regulate the contact dynamics observed in these varying tissue contexts. Such comparative studies could provide insight into how particular properties of these contractile networks could be tuned to accomplish similar goals in different tissue contexts.

Pulsatile constrictions of actomyosin drive cell constriction

Beyond the junctional remodeling observed during convergent extension, pulsatile constrictions of actomyosin networks drive a host of additional morphogenetic processes. Despite different developmental contexts and cellular behaviors, these processes share several common principles with the constrictions that drive convergent extension. The first is the stepwise progression of morphogenesis, whereby initial transient cell or tissue deformations are stabilized by additional mechanisms. Intriguingly, these two stages are not merely incidental to the process, but can be regulated by distinct transcriptional and mechanical pathways. In

Drosophila gastrulation, apical constriction of ventral midline cells drives mesoderm invagination. Distinct phases of pulsed apical contractility and subsequent stabilization of the resulting apical constriction drive this process. Interestingly, the *snail* and *twist* transcription factors distinctly mediate the pulsed contractile and stabilization phases of apical constriction, respectively [188]. Though it is not clear how Snail promotes constriction, Twist promotes expression of Fog and T48, which together activate Rho1 at the apical surface [189,190]. Additionally, Twist is required to polarize Rho pathway activity at the medioapical surface, and for the formation of stable supracellular MyoII cables that likely stabilize constrictions [191]. These studies provide a striking example of the multiple layers of control the cell exerts over morphogenetic behaviors.

In both germband extension and gastrulation, MyoII contractility completely eliminates by constriction either particular cell-cell contacts or the cells themselves. However, alternative mechanisms drive apical constriction in other contexts to achieve more subtle changes in tissue architecture. These systems can provide key insights into how cells fine tune adhesion and tension to generate morphological variety. In *Drosophila* leg joint formation, zones of apical constriction correlate with the restricted expression of Rho family regulators, which contribute to invagination of presumptive joints [192]. Interestingly, apical constriction in this context appears to cooperate with a number of other mechanisms to promote folding [193–195], suggesting multifactorial control may be a consistent mechanism to control the degree of folding.

A key insight into this question comes from studies of the dorsal folds in the *Drosophila* embryo. The folds are initiated when AJ at the site of fold formation shift basally [196]. Interestingly, of the two folds, the posterior is deeper. In contrast to gastrulation, where all invaginating cells actively constrict their apices, only initiating cells shift AJ positioning. Rather, fold depth is controlled by the number of 'normal' neighboring cells that are brought into the

fold [197], and the extent of incorporation depends on the mobility of adjacent AJ. This mobility requires the modulation of AJ coupling to the underlying cytoskeleton via α-Catenin. During fold progression, the small GTPase Rap1 regulates α-Catenin to control AJ mobility, and the Rap1 regulator Rapgap1 is expressed in cells that will incorporate into the fold. Rap1 also regulates apical constriction during neural tube formation, suggesting the potential for some conserved function of Rap1 in fold regulation [198]. Interestingly, both constitutive Rap1 activation and inhibition each blocked fold invagination, suggesting that Rapgap1 might promote a flux of Rap1 activity to promote dynamic AJ stabilization[197].

Coupling Adhesion and Contractility

Normal morphogenesis requires the integration of the adhesive and force transducing functions of AJs. Together, these roles allow for the coordination of forces across an epithelium. As discussed, a range of mechanisms control the extent of AJ based adhesion and actomyosin contractility to promote morphogenesis. A third layer of control is in the regulation of AJ-actomyosin coupling. Striking evidence of this regulation is provided by C. elegans gastrulation, during which pulsatile constrictions of actomyosin networks precede any cortical deformation[199]. Eventually, however, the pulsed actomyosin dynamics drive apical constriction, as described during *Drosophila* gastrulation[188]. This suggests that the control of contractile dynamics and AJ engagement are separable. Because many AJ components interact with the cytoskeleton in many ways, the control of this engagement serves as an intriguing mechanism to modulate cell or epithelial behaviors.

A comparison of gastrulation and GBE provides an interesting case study in the regulation of actomyosin-AJ coupling. During *Drosophila* GBE, cell constriction and AJ-actomyosin coupling are both much more highly polarized than during gastrulation. Some of this

polarity comes from transient asymmetries in E-Cadherin accumulation, as mentioned [140]. However, additional mechanisms appear to regulate this asymmetric engagement. The afadin homolog Canoe is enriched at vertical junctions, and is specifically required for actomyosin coupling there [200]. By contrast, in ventral furrow cells that undergo apical constriction, Canoe localizes homogenously at AJ, and loss of Canoe results in an isotropic detachment of MyoII from the AJ. Importantly, the localization of Canoe does not depend on the AJ. That core AJ components and canoe are independently localized provides a high degree of flexibility in the regulation of cortical tension engagement. To what degree this modularity is employed in different developmental contexts remains to be determined.

A fascinating aspect of AJ-actomyosin coupling is the degree to which AJ are mechanosensitive. The first description of a mechanosensitive adhesion complex was the focal adhesion [201–203], but it is now clear that several components of the AJ can detect and respond to mechanical strain. In fact, AJ are under constant tension [204,205], which depends upon coupling to the actomyosin network through α-Catenin. Most intriguing are suggestions that AJ respond functionally to increased tension to maintain epithelial integrity. In particular, vinculin may be recruited to AJ in response to tension [206] to enhance AJ stability. This recruitment may be mediated through tension sensitive binding to α-Catenin [184]. These studies relied on cytokine stimulation or Rho-MyoII pathway modulation as proxies for tension. As these pathways can have other direct effects on junction stability, further work will be required to determine precisely how junctions respond to tension.

Some support is provided by the finding that direct repeated mechanical strain across the AJ increases vinculin recruitment, and increases local stiffness in an F-actin and vinculin dependent manner [182]. Furthermore, direct mechanical pulling in another assay was found to increase contact area [207]. However, as MyoII itself could be tension sensitive[208], further

experiments will be required to determine whether the junctions in this system are responding mechosensitively, or whether increased MyoII tension directly causes contact expansion[134]. In either case, these data clearly support the idea that AJ are mechanosensitive, and that the cell can respond adaptively to external tension or mechanical stresses.

Control of actomyosin dynamics by phosphoinositide signaling and RhoGTPases

Morphogenetic cell behaviors require exquisite control over spatial and temporal patterns of force generation. Furthermore, robust behaviors require the coordination of multiple force modalities at different subcellular sites. Cell migration, which proceeds by protrusive behaviors at the front of the cell, and contractile behaviors at the rear, provides a clear example of such coordination. Though a number of mechanisms contribute to this control, the two most direct are the Rho family small GTPases and phosphoinositide signaling. Importantly, these two pathways provide both strong spatial and temporal control with a high degree of coordination. As will be illustrated with several examples, two primary features of both pathways contribute to these properties. The first is the use of both positive and negative regulatory components to enhance spatial and temporal control. The second is the presence of multiple positive and negative feedback loops and cross regulatory interactions that enhance coordination and robustness of pathway activity to ensure normal cell and tissue behavior.

Phosphoinositides are a family of phosphorylated lipids derived from phosphatidylinositol (PtdIns). Phosphorylation at one or more of the 3, 4, or 5 positions of the inositol ring yields at least seven different phosphoinositide species *in vivo*. Specific phosphoinositide species enrich in different subcellular compartments, where they recruit a wide range of effector proteins through via phosphoinositide specific binding domains[209]. Such specificity is fundamental to the core functions of phosphoinositide signaling, which include the

regulation of organelle identity, intracellular trafficking, cell signaling, and cytoskeletal dynamics. Here, we will focus on the control of cytoskeletal dynamics by PI(4,5)P2 and PI(3,4,5)P3 (PIP2 and PIP3, respectively). While PIP2 is present at a low concentration at the plasma membrane, PIP3 is generally produced only in response to a stimulus. Among other features, this renders PIP3 an excellent candidate to mediate morphogenetic cell behaviors with a high degree of spatial and temporal precision.

A prominent target of phosphoinositide pathway activity is the Rho family small GTPases. Rho GTPase activity is generally controlled by the activities of GEFs, GAPs, and GDIs, which respectively activate, inhibit, and sequester to the cytoplasm target GTPases, respectively. Key in this regulation is the incredible degree of cross talk between Rho family members, both at the level of upstream GAPs or GEFs as well as at the level of convergent downstream targets. A complete review of Rho pathway activities is beyond the scope of this introduction[210–213]. Rather, I will review several salient examples that highlight those features that render this pathway indispensable in the regulation of epithelial morphogenesis, with a particular emphasis on epithelial morphogenetic processes.

Phosphoinositides and RhoGTPases regulate cell migration

Phosphoinositide signaling is a well-studied regulator of chemotaxis in a number of cell types, particularly neutrophils and Dictyostelium. During migration, these cells become highly polarized, with a unified protrusive leading edge and a contractile trailing edge[214]. This polarization is striking in that the sharp molecular and cellular polarization can result from very shallow gradients that may vary in concentration by as little as 5%[215]. Phosphoinositide signaling plays a significant role in both aspects of this polarization. At the leading edge, Gi protein coupled receptor stimulation transiently activates Pi3k to produce PIP3[179], and either Pi3k[216] or

PIP3[217] is sufficient to polarize Dictyostelium cells. At the rear and sides of the cell, the PIP3 3' phosphatase PTEN localizes to the membrane and limits the extent of PIP3 accumulation[216,218]. However, PTEN does not localize similarly in neutrophils. Rather, the 5' phosphatase SHIP1 localizes outside of the leading edge, and is required to limit the scope of PIP3[219]. Thus, the localization of PIP3 requires positive regulation by Pi3k and negative regulation by either PTEN or SHIP1. This complementary action can provide high spatial resolution by actively limiting the domain of PIP3, and could provide high temporal resolution by enhancing turnover of PIP3.

In addition to the coordinate regulation of PIP3 localization by Pi3k and PTEN/SHPI1, positive feedback between PIP3 and Rho GTPase signaling further enhances the sharpness of the internal PIP3 gradient. PIP3 signaling recruits the Rac GEF DOCK180 to the leading edge of migrating cells to promote Rac activity there. Normal cell migration requires not only DOCK180 GEF activity, but also normal localization to the leading edge via the PIP3 binding DHR-2 domain[220]. The DOCK180 homolog DOCK2 is similarly required for chemotaxis in neutrophils[221]. Interestingly, loss of DOCK2 not only impairs Rac activation and cell polarization, but also reduces PIP3 accumulation. Further, addition of exogenous PIP3 stimulates endogenous PIP3 production by Pi3k, in a loop that requires Rac actvitiy[222]. This is consistent with reports suggesting that Rac and Cdc42 act both downstream[223,224] and upstream[225] of Pi3k activity. In a particularly interesting experiment, localized photoactivatable Rac activation directed cell migration in a Pi3k dependent manner[226]. It is interesting to note, however, that in these cases, induction of PIP3 at the leading edge is only transient (1-2min), suggesting that positive feedback is not absolute, and that pathway adaptation or additional pathway regulation attenuate PIP3 levels.

Though Pi3k and PIP3 appear sufficient to induce leading edge activity, they are not strictly required for chemotaxis. Studies reveal a range of effects on chemotaxis following

pharmacological or genetic inhibition of Pi3k, ranging from decreased persistence and directionality to decreased speed of migration[216,227]. In particular, deletion of all Pi3k genes as well as PTEN did not abolish chemotaxis, but resulted in decreased directionality of migration in shallow gradients. Other work supports a role for PIP3 in orienting cell polarity in shallow gradients, and also enhancing speed in steep gradients[228]. Notably, in these manipulations cells frequently exhibited bifurcated leading edges or more random pseudopod formation, suggesting that PIP3 might be required for the consolidation of polarized behaviors in these contexts. In addition to gradient strength, the requirement for PIP3 in neutrophils also depends on the cell matrix and the activation status of the cell[229]. These data are interesting in that they suggest that phosphoinositide signaling functions largely to coordinate or modulate the signals or effectors driving migration[230,231]. This might be important *in vivo*, where gradients may be noisy, and additional conflicting biological or mechanical cues might require a robust coordination of pathway activity. Indeed, one group found that normal migration in the intact zebrafish required Pi3k function[226]. This might be highly relevant in an epithelial context, where a particular cell might receive mechanical or signaling inputs from a number of neighbors.

The leading edge, however, is merely half the story. The phosphatases PTEN or SHIP1 enrich at the sides and trailing edge, where Rho mediated contractile networks promote rear edge retraction[214]. In many systems, Rac and Rho antagonize one another[212], suggesting one mechanism by which domains could be established or maintained. However, the relationship in between Rho family members during migration is not purely antagonistic. Rac[232], PIP3, and Cdc42[233] actually potentiate trailing Rho activity and actomyosin based uropod retraction. Of note, inhibition of PIP3 led to multiple uncoordinated uropods, echoing the effect on leading edge lamellipodia. This is consistent with 'local excitation global inhibition' models of chemotaxis, which suggest that PIP3 promotes local F-actin dynamics by positive feedback, but

also triggers some longer range signal to inhibit similar dynamics elsewhere in the cell[234]. Such a signal need not be a diffusible signal, as proposed, but could also be mechanical in nature. MyoII and PTEN both respond to mechanical stimulation[208,235,236], suggesting a biological basis for this mechanism. Though the cues that mediate this coordination remain to be determined, these data suggest that efficient cell migration requires not just the establishment of 'frontness' and 'backness', but the coordination of the two (Appendix 1)[237].

More recent studies suggest that this spatially localized Rho GTPase synergy occurs on much smaller spatial scales during migration. In non-chemotaxing cells, Rho is active in a very narrow zone at the leading edge[238,239]. There, Rho appears to potentiate Rac induced membrane ruffling through the recruitment of the formin mDia. A primary role for Rho in the induction of leading edge dynamics is supported by the finding that Rho activity levels correlate both spatially and temporally with the induction of membrane protrusions, while maximal levels of Rac and Cdc42 lagged by several seconds and several microns[240]. Similar relationships are observed during cell contact expansion[134], wound healing[241,242], and cleavage furrow progression[243]. These data support the canonical model that Rho and Rac/Cdc42 form complementary domains of activity, but further suggest that their respective domains cooperate in an emergent fashion to promote dynamic cell behaviors.

Phosphoinositides in epithelial morphogenesis

As described, polarized phosphoinositide signaling regulates actomyosin dynamics and Rho GTPase activity to promote a range of cell behaviors. Despite clear roles for these pathways in epithelial development, we know very little about direct roles for phosphoinositide dynamics in epithelial morphogenesis. Most work on this question has focused on the role of polarized phosphoinositide accumulation in the elaboration of apico-basal polarity. More recent work,

however, has described planar polarized phosphoinositide signaling in the control of dynamic morphogenetic events. These studies, described below, highlight multiple roles for phosphoinositide signaling in the spatial and temporal control of cellular behaviors that drive morphogenesis.

Phosphoinositide signaling mediates apico-basal polarization in epithelia

Phosphoinositide signaling is a crucial determinant of membrane identity of different cell compartments. Differential phosphoinositide accumulation plays critical roles in the targeting and fusion of vesicle traffic, for instance[209]. Phosphoinositides function similarly in the elaboration of epithelial apico-basal polarity[244]. In MDCK cells, Pi3k and PIP3 accumulate at the basolateral membrane. Exogenous PIP3 caused preferential expansion of the basolateral membrane and ectopic accumulation of basolateral markers at the apical surface. This was associated with an increase in the activity and spread of both Cdc42 and Rac1. Though the mechanism is not definitively clear, this ectopic accumulation is thought to result from the inappropriate recycling of basolateral components to 'apical' membrane[245]. Further supporting a role for PIP3 in basolateral determination, Pi3k inhibition diminished the extent of the basolateral surface[245,246]. Reciprocally, PTEN and PIP2 accumulated at the apical surface. Loss of PTEN eliminated the apico-basal segregation of PIP2 and PIP3, and disrupted cyst formation[247]. Consistent with these experiments, exogenous PTEN was found to localize apically in *Drosophila* embryonic epithelia, where it colocalized with the apicolateral protein Baz/Par3[248]. Specification of apical domain identity by PIP2 required the recruitment of Cdc42 via Annexin2. These data support a consistent role for phosphoinositide signaling in the spatial regulation of Rho GTPase activity. As with cell migration, these data reinforce the importance of a sharp segregation of phosphoinositide species, which is accomplished by the complementary accumulation of Pi3k

and PTEN. It is unclear as yet what causes the localization of either protein however, nor whether there is co- or cross regulation of localization in this process.

A number of questions remain. The mechanisms that promote the initial segregation of phosphoinositide regulators remain unknown, though it is possible that cell-ECM interactions could provide an initial polarizing cue[249]. It is also unclear how consistently PIP3 and PIP2 specify basolateral vs apical membrane domains. In *Drosophila* photoreceptor cells, PIP3 promotes the elaboration of a specialized apical domain, the rhabdomere. As suggested by work in the embryo[248], Baz colocalizes with and is required for normal localization of PTEN to the apicolateral domain. There, PTEN restricts PIP3 accumulation to the apical membrane, where it activates Akt to promote F-actin dynamics[250]. This deployment and mode of action is quite similar to that seen during cell migration[251]. Additional experiments will be required to determine how consistent PTEN and phosphoinositides function in apicobasal polarization. Observed differences, such as between MDCK and *Drosophila* embryonic epithelial cells, could suggest a lack of conservation, or they could reflect differences in the degree of apicobasal elaboration. Or, as with rhabdomere formation, differences could be employed for morphological and functional specialization of particular domains.

Phosphoinositide signaling mediates planar polarized epithelial dynamics

The role of phosphoinositides in the regulation of dynamic epithelial behaviors is largely unknown, though one seems likely given the pleiotropic effects of phosphoinositide signaling on adhesion and actomyosin dynamics. This is supported by two recent studies that have revealed quite different roles for phosphoinositide signaling in epithelial morphogenesis. These differences suggest intriguing and potentially diverse roles for phosphoinositide signaling in morphogenesis, and highlight a clear area for further research.

The first set of studies, performed by the Millard lab, suggests that planar polarized phosphoinositide signaling contributes to the collective migration of the *Drosophila* embryonic epithelium during dorsal closure. A number of cellular dynamics contribute to this process, including constriction of amnioserosa cells[252–254] and actomyosin cable formation in leading edge cells [128,255]. PIP3 accumulates in leading edge cells at the interface with amnioserosa cells. As during apico-basal polarization, the polarized accumulation of PTEN and Baz at cell contacts mediates the polarization of PIP3. In this case, Baz is excluded from the interface with amnioserosa cells, which allows for the enrichment of PIP3. There, PIP3 promotes F-actin dynamics that generate filopodia-like protrusions. Experimental disruption of PIP3 polarization or generation disrupted filopodia formation and hampered dorsal closure, suggesting that this polarization is functional. It does not appear to be strictly required, however, as dorsal closure still proceeded, albeit less efficiently. This is akin to its role in in chemotaxis, where PIP3 appears to enhance polarity rather than define it. While the downstream effectors of PIP3 in this context are not known, both Akt [250] and Rac [256] are likely to contribute. Similarly, the upstream polarizing cue is not known, though some work suggests the nectin homolog Echinoid (Ed) is a likely candidate. Ed is differentially expressed between epidermal and amnioserosa cells, and the interface of Ed and non-Ed expressing cells is required for the formation of the actomyosin cable there. It remains to be determined, however, whether or how this might regulate Baz or PTEN accumulation.

PTEN and phosphoinositide dynamics are also required for the epithelial rearrangements that drive *Drosophila* wing elongation [137]. Several cellular behaviors contribute to wing elongation. Constriction of the hinge generates an anisotropic tension across the proximo-distal axis of the wing, which drives polarized cell shape changes, cell division, and cell intercalation [136]. Similar to embryonic GBE, polarized cell contact constriction and expansion

drive this coordinated cell intercalation. Contact constriction correlates with both MyoII and PIP3 accumulation, suggesting a possible role for PIP3 in the constriction of cell contacts. Supporting this idea, loss of PTEN led to a failure of cells to resolve contact constriction events with the formation of new orthogonal junctions, causing a dramatic increase in contact length heterogeneity and four-fold vertices. This was possibly due to an inappropriate maintenance of MyoII mediated contact tension, as Rok inhibition restored normal cell contact rearrangements. Cumulatively, loss of PTEN led to a subtle decrease in wing elongation. This work convincingly demonstrates that PTEN is required for the normal cell contact dynamics during epithelial elongation, and strongly supports the idea that Rok/MyoII based tension is a critical component of this behavior. However, it is not clear whether this activity is at the level of junction constriction or stabilization. Apical MyoII dynamics were not examined in this work, so it is not clear whether MyoII flows contribute to the constriction observed here. Furthermore, while it is clear that MyoII accumulation precedes contact constriction, the temporal relationships of PIP3/MyoII and PIP3/contact length were not examined, which leaves open the possibility that PIP3 accumulation does not promote constriction, but rather accumulates in response to it.

Together, these studies suggest potentially diverse roles for phosphoinositide signaling that likely depend on the mechanical and signaling tissue context. Beyond these differences, however, both sets of studies reveal striking similarities in the role of phosphoinositide signaling to mediate spatiotemporally specific F-actin or actomyosin dynamics. Both studies also highlight potential difficulties in the investigation of phosphoinositide dynamics in tissue morphogenesis. Manipulation of phosphoinositide signaling in many cases alters only the kinetics of a morphogenetic process, and not the ultimate morphological phenotype. This may explain why such roles for phosphoinositide signaling have long been unexplored, as most research in these areas proceeds from forward genetic screens designed to identify clear morphological

phenotypes. As more examples are uncovered, it will be of paramount importance to understand better how the complex web of potential interactions of downstream phosphoinositide effectors regulate *in vivo* morphogenesis.

Phosphoinositide signaling could mediate cross talk between adhesion and tension

The dense network of potential upstream regulators and downstream effectors of phosphoinositide signaling suggests a potentially high degree of positive and negative feedback between phosphoinositide signaling, adhesion, and actomyosin dynamics. Models of epithelial dynamics such as DITH and DAH reveal the critical nature of the interaction between adhesion and tension, while *in vitro* work has uncovered many of the mechanisms by which these forces operate and interact. Developmental studies of epithelial morphogenesis reveal that these fundamental forces are deployed with incredible spatial and temporal specificity to control a relatively sparse set of cellular dynamics, which nonetheless contribute to incredible morphological diversity across tissues and species. One of the exciting challenges remains to understand better the mechanisms that fine tune the balance of these pathways to generate this broad spectrum of morphology. The subtle nature of PTEN morphogenetic phenotypes [137,257], combined with the ability of phosphoinositide signaling to promote and respond to changes in adhesion and actomyosin activity, support the idea that phosphoinositide signaling could serve as a hub to regulate the balance of adhesion and tension in subtle ways to regulate tissue morphogenesis. My work (Chapter 3) has attempted to address the regulation of this balance to control cell shape in the *Drosophila* eye.

Development of the *Drosophila* Eye

The *Drosophila* compound eye is composed of approximately 800 photoreceptive units, called ommatidia. Each ommatidium consists of eight photoreceptor cells, four lens secreting

cone cells, three sensory bristles, and 11 interommatidial pigment epithelial cells (IOCs). The 11 IOCs plus the three bristle cells organize to form a hexagonal lattice that insulates each ommatidium. This adult structure develops from a relatively undifferentiated epithelium called the eye-antenna imaginal disc. The eye-antenna field is initially specified during embryogenesis[258], and develops into late pupal stages[259]. The overall development of the eye-antenna can be roughly divided into three stages. Initially, the eye field is broadly patterned and grows extensively[260,261]. Next, further differentiation specifies the clusters of photoreceptor cells that prefigure the ommatidia[262]. Lastly, during pupal development the IOCs undergo an elaborate process of morphogenesis and epithelial specialization to generate the unique lattice of the *Drosophila* eye [259]. I will very briefly summarize the first two stages before focusing on the final morphological development of the pigment cell lattice.

Early eye patterning

The initial patterning of the retinal field occurs from mid embryogenesis until the third larval instar. During this time, cells of the eye-antenna disc proliferate extensively to increase the size of the disc from ~70 cells at specification to ~44,000 cells at the end of larval development [261]. Additionally, a highly conserved network of transcription factors promotes retinal identity within the eye field, distinct from the surrounding head capsule and adjacent antenna [260]. Each of the ~700 unit eyes, or ommatidia, is specified within this retinal field. The differentiation of each ommatidium proceeds by the stepwise recruitment of the constituent eight photoreceptor cells and four cone cells. At the third larval instar, a pulse of *hedgehog* (*hh*) signaling at the posterior of the retinal field induces a wave of cell cycle arrest and differentiation that proceeds to the anterior of the eye disc. As cells enter this wave, called the morphogenetic furrow, single R8 photoreceptors are specified at regular intervals. Next, the

remaining photoreceptors are recruited sequentially, starting with the R2/5 pair, followed by the R3/4, the R1/6, and finally the R7 photoreceptor. The signals and transcription factors that specify the fate of each photoreceptor have been well studied [262], and represent some of the earliest descriptions of the structure and function of the Ras, Notch, and EGFR pathways in the specification of cell fate. Following differentiation, the photoreceptor clusters recruit two pairs of cone cells that overlie the photoreceptors and ultimately secrete the lens [263,264]. This group of eight photoreceptors and four cone cells constitutes the core of each ommatidium, around which the remaining pigment IOCs will organize in a similar stepwise fashion.

Morphogenesis of the IOC lattice

By ~10 hours APF, all cells that have not become photoreceptors or cone cells represent a pool of genetically identical interommatidial precursors. Over a period of ~30 hours, these cells will form a hexagonal lattice that surrounds each unit eye and optically insulates it. This lattice is composed of two 1° cells, which enwrap the cone cell core; six rectangular 2° cells, which form the edges of the hexagon; and three each of 3° cells and bristle groups that alternately form the vertices (Fig.1.1). Four main cellular behaviors generate this unique morphology: Protrusion and intercalation of IOCs, preferential adhesion, apoptosis, and cell shape change. The signals that regulate apoptosis in the *Drosophila* eye have been well reviewed, and will not be covered here. Rather, I will focus on the roles of cell intercalation, preferential adhesion, and cell shape change in the morphogenesis of the pigment cell lattice.

Cell Intercalation and preferential adhesion organize the ommatidial lattice

Morphologically undifferentiated IOCs exhibit highly dynamic behavior in which they continuously extend protrusions and regularly exchange neighbors [265]. Organization of the IOC lattice emerges from the selective maintenance of specific cell contacts at the expense of

others. The critical first step in this organization is the recruitment and specification of 1° cells. At ~18 hours APF, two undifferentiated IOC precursors begin to form preferential contacts with anterior and posterior cone cells. These cells, the presumptive 1° cells, gradually expand contacts with the cone cells until the two 1° cells contact one another and fully enwrap the cone cell cluster[259]. This recruitment requires Dl-N signaling from cone cells to presumptive 1° cells[266]. While all cone cells express the N ligand Dl, anterior and posterior cone cells express higher levels of Dl. It is hypothesized that this accumulation of Dl polarizes the recruitment of 1° cells[267] and organizes the 1°-1° cell contacts orthogonal to the AP axis. Functionally, both Dl accumulation in cone cells and N activity in 1° cells are required for normal 1° cell recruitment and specification[266]. The downstream mechanisms by which Dl-N signaling induces the contact remodeling and shape change of presumptive 1° cells are not known.

It is clear, however, that 1° cells are the main determinant in the subsequent sorting of 2° and 3° cells. As the remaining undifferentiated IOCs extend protrusions, they preferentially maintain IOC-1° cell contacts at the expense of IOC-IOC contacts. This causes the sorting of IOCs into single rows between adjacent ommatidia. This behavior requires the differential expression of Neph1 and Nephrin proteins between presumptive 2°/3° cells and 1° cells. Presumptive 2°/3° cells express the Neph1 homologs Roughest (Rst) and Kin of Roughest (Kirre), while 1° cells express the Nephrin homologs Hibris (Hbs) and Sticks 'n Stones (Sns). Interestingly, both Rst[108] and Kirre[268] bind to each of Hbs and Sns, though not to each other. Originally, it was thought that heterophilic binding *in vivo* might stabilize AJs between 1° cells and IOCs, thus providing a mechanism for the preferential adhesion of 2°/3° to 1° cells[108].

The hypothesis that preferential adhesion might mediate the sorting of IOCs is supported by the finding that during sorting, AJ proteins E-Cadherin and β-catenin accumulate at much higher levels along 1°-IOC borders than IOC-IOC borders. Similarly, Rst protein is

completely excluded from IOC-IOC contacts during sorting[108], though it does accumulate at these contacts at earlier and later stages[269]. It is not clear what mechanisms drive the transition from dynamic sorting to the establishment of the final, stable epithelium. Though the time course of Hbs/Sns expression has not been examined, it is possible that transient asymmetries of Hbs/Sns expression mediate these cellular dynamics. It is interesting to speculate whether the induction of Hbs/Sns in presumptive 1° cells mediates the recruitment of these cells to the cone cell cluster. Indeed, disruption of this pathway disrupts the maintenance of 1°-Cone cell contacts and causes dynamic exchange between IOC and 1° cell populations[270].

Despite these data, it remains unclear whether Neph1/Nephrin binding directly regulates junction stability, or by what mechanisms it might do so. Indeed, Rst localization requires the presence of intact AJs[270], suggesting more complex modes of regulation. One possible regulator could be the CIN85 homolog Cindr. Cindr is required for normal IOC sorting, and interacts genetically with Rst and E-Cad[270]. Cindr may directly or indirectly modulate AJ stability and cell sorting via regulation of the F-actin cytoskeleton. Cindr binds to the F-actin capping proteins Cpa and Cpb, and interacts genetically with a host of potential F-actin regulators, including Cpa/Cpb, WASp, SCAR, Chic, Tsr, Rho, and Rac[270]. Furthermore, Cindr binds to the Arf6 GAPs dASAP and dArfGAP3[265]. Arf6 in turn could have direct or indirect roles in the regulation of Rho GTPase activity[271], F-actin dynamics[272], or phosphoinositide signaling[273,274]. Clearly, each of these regulators could have pleotropic effects on F-actin dynamics and cell physiology. The specific contributions of these pathways to normal F-actin dynamics and their contribution to normal ommatidial morphogenesis are not clear.

Summary

Normal epithelial development requires the coordination of cell fate, cell growth, and cell behavior across and between tissue domains. At the levels of signaling, gene regulation, and ultimately morphogenesis, cells and tissues exercise a diverse range of regulatory strategies to achieve both robustness and flexibility. Flexibility is required, because this regulatory complexity belies a surprising simplicity at the effector level. There are only a handful of intercellular signaling pathways, and in the course of development, these transduce rather linearly to downstream effectors [275]. Likewise, the mechanical properties that influence cell behavior are primarily cortical tension, elasticity, and adhesion. However, one needs only to consider the Rho family GTPases and their wide range of regulatory proteins, to appreciate the incredible potential for diversity in the regulation of these forces. Such regulatory diversity allows for an incredible degree of coordinate regulation, pathway cross-talk, and feedback.

Though I investigated two very different questions during my graduate studies, both projects fundamentally concerned mechanisms of coordinate regulation. In chapter two, I describe my findings on the role of *odd-skipped* genes in organizing anterior notum patterning. Previous work in the field focused primarily on the role of *dpp* as a posterior tissue organizer. My work extends this model, demonstrating that the notum anterior posterior axis is coordinately patterned from both anterior and posterior margins. In chapter three, I describe the role of PIP3 and F-actin dynamics in the control of cell shape in the eye. Work in other systems has largely focused on the role of tension to constrict cell contacts during shape change. However, mechanisms of contact maintenance and expansion have been largely unstudied. In chapter three, I show that cell contact length is dynamically regulated by both tension and antagonistic F-actin dynamics. Many of the examples discussed suggest that coordinate regulation is a common mechanism to ensure robust epithelial patterning and morphogenesis.

By understanding how these dense patterns of crosstalk and feedback are deployed in controlled fashion to promote normal morphogenesis, we may be able to provide insight into the dysregulation of phosphoinositide and Rho GTPase signaling pathways that underlie disease states such as cancer and metastasis.

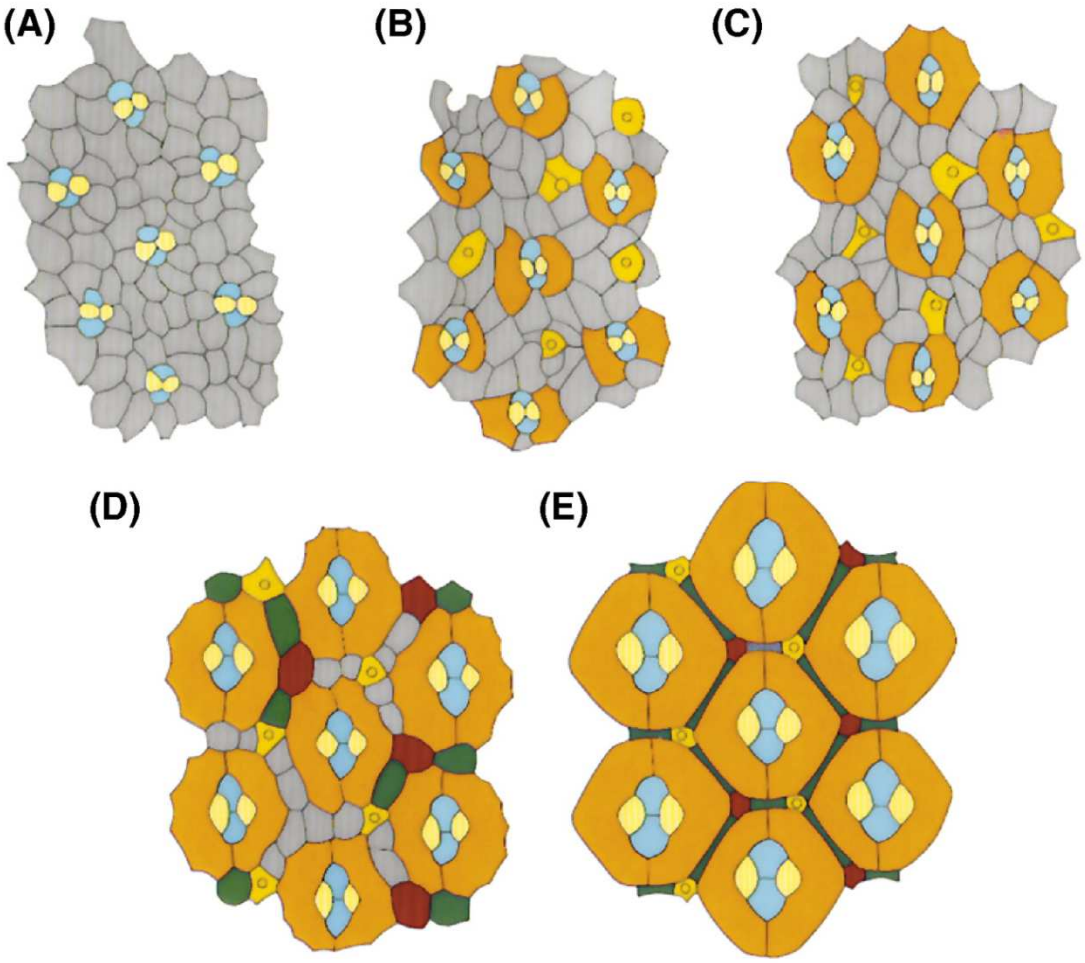

Figure 1.1: Cell intercalation, cell death, and cell shape change form the final crystalline lattice of the *Drosophila* eye epithelium. (A) Initially, the eye epithelium consists of spaced photoreceptor clusters covered by cone cells (yellow and blue) surrounded by morphologically undifferentiated interommatidial precursor cells (IPCs, grey). (B) Delta-Notch signaling from the cone cell cluster induces a pair adjacent IPCs to differentiate into primary pigment cells (yellow), which then enwrap each cluster. (C) Progressive cell intercalation causes IPCs to form single rows between ommatidia. (D) Cell death eliminates extra IPCs, and cell shape changes cause IPCs to adopt a hexagonal arrangement, with tertiary cells (red) contacting three primary cells at each hexagonal vertex, and elongated secondary cells (green) forming the sides of each hexagon. Adapted from [267].

Chapter 2

odd-skipped genes and *lines* organize the notum anterior-posterior axis by autonomous and non-autonomous mechanisms

Abstract

The growth and patterning of *Drosophila* wing and notum primordia depend on their subdivision into progressively smaller domains by secreted signals that emanate from localized sources termed organizers. While the mechanisms that organize the wing primordium have been studied extensively, those that organize the notum are incompletely understood. The genes *odd*-skipped (*odd*), *drumstick* (*drm*), *sob*, and *bowl* comprise the *odd*-skipped family of C2H2 zinc finger genes, which has been implicated in notum growth and patterning. Here we show that *drm*, Bowl, and *eyegone* (*eyg*), a gene required for notum patterning, accumulate in nested domains in the anterior notum. Ectopic *drm* organized the nested expression of these anterior notum genes and downregulated the expression of posterior notum genes. The cell-autonomous induction of Bowl and Eyg required *bowl*, while the non-autonomous effects were independent of *bowl*. The homeodomain protein Bar is expressed along the anterior border of the notum adjacent to cells expressing the Notch (N) ligand Delta (Dl). *bowl* was required to promote Bar and repress Dl expression to pattern the anterior notum in a cell-autonomous manner, while lines acted antagonistically to *bowl* posterior to the Bowl domain. Our data suggest that the *odd*-skipped genes act at the anterior notum border to organize the notum anterior–posterior (AP) axis using both autonomous and non-autonomous mechanisms.

Introduction

The generation of functional tissues and organs requires the precise specification of differentiated cell fates across a field of cells. Early in development, organizers are established within fields of cells to control the expression of transcription factors both autonomously and non-autonomously in patterns that ultimately prefigure the formation of adult structures [1]. The

Drosophila wing imaginal disc gives rise to both the wing blade and the body wall (notum), and serves as an excellent model to study tissue patterning. Most work on organizer function in the wing disc has focused on the coordination of growth and patterning of the wing primordium along its dorsoventral (DV), anteroposterior (AP), and proximodistal (PD) axes. By contrast, the notum lacks an obvious PD axis, suggesting that the mechanisms that coordinate growth and patterning of this structure are distinct from those in the wing. However, such mechanisms have not been well studied.

A gene network specifies the notum territory of the wing disc and progressively subdivides it along the mediolateral and AP axes. The zinc finger protein Spalt major (Salm) is both necessary and sufficient for notum induction and has been proposed to act atop this hierarchy [276]. Subsequently, activation of the *Drosophila* epidermal growth factor receptor pathway (EGFR) in the presumptive notum represses Wg [277] and induces expression of the Iro-C homeodomain proteins to specify notum identity [278–281]. In parallel, the bone morphogenetic protein (BMP)-like signal *decapentaplegic* (*dpp)* emanates from a narrow posterior domain to promote expression of the LIM homeodomain protein Tailup (Tup) and reinforce notum specification [282–284].

Interestingly, several notum specification genes play key roles in subdividing the mediolateral axis. Dpp promotes the expression of the GATA and FoG genes *pannier* (*pnr*) and *u-shaped* (*ush*) in the medial notum, [285–287], where they coordinately promote proper bristle patterning [62,64,288]. Conversely, Dpp restricts expression of *Iro-C* genes to the lateral notum, where they specify the identity of this region. Dpp also acts in concert with the Pax-homeobox protein Eyegone (Eyg) to restrict Hth to the lateral notum to further elaborate the notum mediolateral axis [289].

In contrast to the patterning of the notum mediolateral axis, which is regulated positively by Vn and both positively and negatively by Dpp, the patterning systems that organize the notum AP axis are less well defined. The notum is subdivided morphologically into the anterior prescutum, the central scutum, and the posterior scutellum (see Fig. 2.1F). Each region bears a distinct pattern of sensory bristles comprised of repeated rows of many small bristles called microchaete, and the stereotyped placement of 22 larger macrochaete. Two gene families have been characterized to subdivide the notum AP axis. The homeodomain proteins Bar-h1 and Bar-h2 (hereafter referred to collectively as Bar) are expressed in the presumptive prescutum, where they are required to promote the correct pattern of sensory bristles. *Bar* mutant clones within the prescutum lack microchaete, and result in the elimination of the single prescutal macrochaeta [60]. The Pax-homeobox protein Eyg accumulates more broadly than Bar, both in the prescutum and in the scutum. Loss of Eyg function leads to a severe reduction in size of the scutum, and a complete lack of both micro- and macrochaete. Conversely, overexpression of either Eyg or its homolog Twin of Eyegone (Toy) transforms the scutellum into scutum [289].

Though Bar and Eyg provide mechanistic insight into the AP subdivision of the notum, the cues that elaborate their relative AP expression are not completely understood. It is clear that *Bar* expression in the lateral prescutum requires *wg* function, and that Eyg expression requires both *pnr* and *iro-C* activity. However, these genes are expressed in mediolateral domains, and as such provide no AP patterning cues. Though Dpp secreted from the posterior notum restricts the expression of both *Bar* and *eyg*, the instructive cues that initiate the expression of *Bar* and *eyg* to promote anterior notum patterning remain unknown.

The C_2H_2 zinc finger *odd-skipped* (*odd*) family of genes is comprised of *odd*, *bowl*, *sob*, and *drumstick* (*drm*), and plays key roles in patterning both embryonic and larval tissues. Drm acts atop a relief-of-repression hierarchy in which Drm interacts with the protein Lines to

prevent Bowl degradation [65,66]. In the embryo, this pathway specifies alternative cell fates, depending on whether Bowl is active or repressed. In the hindgut, Lines and Drm/Bowl act in adjacent cell populations to specify small versus large intestine fates [65,67,68]. Similarly, Lines and Drm/Bowl act antagonistically in the dorsal epidermis to specify 4° versus 1°-3° cell fates [66], and in the testis to specify somatic stem cell versus hub cell fates [69].

Though *odd-skipped* genes and *lines* have been studied in a variety of larval tissues, their developmental role appears more complicated than in the embryo. In imaginal discs, *odd-skipped* genes play both essential and redundant patterning roles, depending on context. In the margin of the eye disc, *odd-skipped* genes redundantly promote Bowl accumulation to promote *hedgehog* (*hh)* and trigger firing of the morphogenetic furrow [290]. In the leg, *bowl* is required to specify the distal tarsus [291], while the *odd-skipped* genes act redundantly to promote segmentation [71,72]. In the wing imaginal disc, *lines* represses *bowl* in most of the disc proper to allow normal wing development and PD patterning [292]. Conversely, the *odd-skipped* genes are expressed in and required for the specification of the squamous peripodial epithelium (PE) that overlies the disc proper [70]. Interestingly, we found that in addition to the PE, *odd-skipped* genes were also expressed in the disc proper at the anterior border of the notum, in the presumptive prescutum. Broad expression of *lines* or *bowlRNAi* blocked the specification of the PE, the growth of the entire wing disc, and notably the formation of the notum [70]. This phenotype, together with the expression of *odd-skipped* genes at the anterior border of the notum, suggested a role for these genes in patterning the notum AP axis

Here we investigated the role of the *odd-skipped* genes and *lines* in notum patterning. We find that *drm*, Bowl, and Eyg are expressed in nested domains along the anterior notum.. *drm* was sufficient to promote accumulation of Bowl and Eyg both autonomously and non-autonomously. While the cell-autonomous induction of Eyg strictly required *bowl* function, *drm*

was sufficient to induce Eyg non-autonomously independent of *bowl*. Subsequently, *bowl* was required to promote *Bar* and restrict *Dl* expression to pattern the anterior prescutum cell-autonomously. *lines* acted reciprocally to *bowl* to inhibit expression of anterior genes and promote expression of posterior genes. We propose that the *odd-skipped* genes establish an organizing center along the anterior border of the notum to promote expression of anterior notum genes and repress expression of posterior genes.

Materials and Methods

Fly strains and clonal analysis

FRT42D lines^{G2}, *bowl*^{1} *FRT40A, drm*^{3} *FRT40A,* and *odd*^{rk111}*-lacZ FRT40A* were used to generate mitotic mutant cell clones using the FLP/FRT [293,294] and the MARCM techniques [295] at 48-72, 72-96 and 96-120 hours AEL, which correspond to second, early third and mid third instar. Flies of the genotype *y w hs-FLP; FRT42D Ubi-GFP* (B. Edgar) were used to generated FLP/FRT clones and *y w hs-FLP Tub-GAL4* UAS-*GFP-6Xmyc-NLS; FRT42D Tub-Gal80 hs-CD2, y*$^{+}$ (gift of G. Struhl) to generate MARCM clones. *Ubi-GFP M(2)24F[1] FRT40A* was used to induce mutant clones in a Minute background (gift of E. Moreno). *wg-lacZ* [296], *odd*^{rk111}*-lacZ, bar-lacZ* (gift of T. Kojima)*, mirror*^{DE}*-lacZ,* and *dpp-lacZ* were used to map domains of gene expression. *UAS-Lines9.2* (strong insertion), *UAS-Myc-Lines8* (weak insertion), *UAS-Flag-bowl #21* (strong insertion), *UAS-GFP* (B. Edgar*), UAS-bowlRNAi* #3774 (VDRC) were expressed in clones using *y w hs*-FLP*; act5C>y+>GAL4* UAS-*GFP* [297] or specifically in the anterior notum using *klu-GAL4*, and along the AP compartment border using *ptc-GAL4* and *dpp-GAL4.* Note that *odd* and *sob* are off targets of the *BowlRNAi* due to partial complementarity.

Immunofluorescence and microscopy

Staining protocols have been described elsewhere [66]. Primary antibodies used were: mouse anti-Wg (4D4, DSHB), rabbit anti-Bowl (generated in this study after [291]), rat anti-Al and rat anti-C15 (gifts of G. Campbell), guinea pig anti-Eyg (gift of N. Azpiazu) [289], mouse anti-FLAG M2 (Sigma), mouse anti-β-galactosidase (DSHB), guinea pig anti-Senseless (GP55, gift of H. Bellen) and guinea pig anti-Stripe (gift of T. Volk). Confocal images were acquired using a Zeiss LSM510 in multi-tracking mode. Immuno-*in situ* protocol was based on work described elsewhere [298]. Briefly, Digoxigenin (DIG)-labeled probes were hybridized overnight at 55°C, detected with Peroxidase (POD)-anti-Dig followed by direct Tyramide signal amplification (TSA) Cy3 (Perkin Elmer) to generate a fluorescent signal. Bowl was then detected by indirect immunofluorescence using a standard protocol.

Interaction of Lines with Odd-skipped proteins in S2 cells

HA-Drm and Flag-Bowl constructs were previously described [65,66]. Bowl constructs were generated from cDNA clone RE32660, Odd from clone RE57157, and Sob from clone RE2226. Drm (C28L), Odd (C222L), Sob (C397L) mutant variants were generated by substituting the first cysteine of the first conserved C_2H_2 zinc finger motif with a Leucine. Bowl (R258C) was generated by substituting an arginine in loop 3 of the first zinc finger with a cysteine. Variants of each of the *odd-skipped* family genes were generated by PCR amplification and fused in frame with corresponding tags in pCS2 2X-Flag, pCS2 6X-Myc, or pCS2-2X-HA to generate N-terminally tagged proteins. Primer sequences are available upon request. Three glycine residues separated the tags from the coding region. Following sequencing, tagged cDNA were cloned into either pUAST or pUASp. For analysis of the interaction of Lines with each of the Odd-skipped proteins and their mutant variants, S2 cells were transfected using calcium phosphate in a 6-cm dish with 3 µg of *Ubiquitin-GAL4,* 2.5 µg MT-Lines and 2.5 µg of wild type and corresponding mutant

variant of each Odd-skipped protein. Immunoprecipitation assays were performed as previously described (Hatini et al., 2005; Green et al., 2002) using anti-Flag antibodies for Bowl (M2; Sigma) and anti-HA antibodies for Drm, Odd, and Sob (HA.11, Babco) at 1:40 dilution, followed by immunoblotting with rabbit anti-Myc (A-14; Santa Cruz) at 1:1000 dilution. The amounts of Myc-Lines in unprocessed lysates were used to normalize for variations in transfection efficiency. For competition assays, cells were transfected with 2.5 μg of Ubiquitin-Gal4 and 2 μg of UAS-Myc-Lines, in the presence of increasing amounts of wild type UAS-HA-tagged protein (0, 2 and 8 μg). Immunoprecipitation assays were performed using anti-Flag antibodies followed by immunoblotting with anti-Myc antibodies. For Bowl stabilization assays, cells were transfected with 3 μg of *Ubiquitin-GAL4,* 1 μg of MT-GFP, 2.5 μg MT-Bowl and 2.5 μg of MT-Lines and/or an HA-tagged Odd-skipped protein as indicated. MT-Bowl levels were detected in the lysates and normalized to MT-GFP levels.

Analysis of clone shape

bowl mutant clones were induced from 72-96 hrs AEL and dissected at late third instar. Discs were stained for Bowl and clones analyzed both inside and outside the Bowl domain (n=12 and 21, respectively). Clones were traced manually with ImageJ and analyzed using Shape Descriptors to measure the roundness, circularity and solidity of the clones. Microsoft Excel was used to perform t-tests with a Bonferroni correction for multiple tests to determine differences between groups. Circularity = 4π *(area/perimeter^2*)*. A value of 1.0 indicates a perfect circle; Roundness = 4*area/(π *major axis^2); *Solidity* = area/convex area.

Thorax measurements

Adult flies were photographed using a Fuji FinePix digital camera mounted on a Zeiss Stemi SV11 stereomicroscope and stacks were processed using CombineZP to generate in-focus

composite images (A. Hadley, available: http://www.hadleyweb.pwp.blueyonder.co.uk/). The lengths of thorax subdomains were measured along the dorsal midline from the anterior-most bristle to the anterior limits of the prescutal suture, the scutellar suture, and the posterior limit of the scutellum using ImageJ (NIH, http://rsbweb.nih.gov/ij/). Microsoft Excel was used to perform t-tests with a Bonferroni correction for multiple tests to determine differences between groups.

Results

odd-skipped family members are expressed in distinct patterns in the developing notum

To understand the roles of *odd-skipped* genes in notum development, we followed the pattern of Bowl accumulation throughout notum development and compared it to that of *odd-skipped* family members *odd* and *drm* (Fig. 2.1). By the late second instar Bowl accumulated in the squamous peripodial epithelium (PE), and in a broad anterior region of the notum (Fig. 2.1A). At the third instar, Bowl was limited to the anterior border of the notum in the presumptive prescutum (Fig. 2.1B), and this pattern persisted into pupal development (Fig. 2.1C). We compared the pattern of Bowl protein accumulation to *drm* mRNA expression at late third instar and found that Bowl accumulated more broadly than *drm* (Fig. 2.1D). The nested pattern of Bowl and *drm* expression was most pronounced in the lateral prescutum (Fig. 2.1D, arrowheads indicate the extent of the *drm* domain; arrows point to the limits of the broader Bowl domain). The broader accumulation of Bowl was surprising given that Drm has been considered to stabilize Bowl cell-autonomously by outcompeting the interaction between Lines and Bowl (Green et al., 2002; Hatini et al., 2005). Likewise, the Bowl domain was broader than the *odd* domain, marked by *odd*-GAL4 driving expression of a RFP reporter (Fig. 2.1E). The

relative pattern of *drm*, *odd,* and Bowl expression at the late third instar and in the mature notum is summarized schematically in Figure 1F.

To better understand the dynamics of *odd-skipped* gene expression in the notum, we compared the accumulation of Bowl with both Eyg and *mirror (mirr),* both of which are required for notum specification and patterning (Fig. 2.2). *mirr* is required for notum specification and later patterning of the lateral notum (Cavodeassi et al., 2001), while *eyg* is required to specify the scutum [289]. *mirr* is initially expressed broadly in the notum and becomes restricted to the lateral notum, while *eyg* is expressed broadly within the scutum. At the late first instar, Bowl and a *mirr-lacZ* reporter were expressed in largely complementary domains, with one to three rows of cells expressing both markers (Fig. 2.2A, arrowheads in insets point to overlap in expression). It is plausible that cells that co-express Bowl and *mirr-lacZ* at this stage are recruited to form the anterior border of the notum. Eyg was not expressed at this stage, suggesting that it acts downstream of *bowl* and/or *mirr*. At the late second instar, Bowl accumulated along the anterior border of the notum, while Eyg accumulated in a broader anterior domain. At this stage *mirr-lacZ* was repressed in the medial notum near the disc stalk and in the lateral prescutum (Fig. 2.2B). These relative patterns of gene expression were largely intact at the late third instar. Bowl, Eyg, and *mirr-lacZ* were co-expressed across several cell diameters along the anterior border of the notum, though *mirr-lacZ* was repressed entirely within the medial notum (Fig. 2.2C). The distinct expression patterns of Bowl and *mirr-lacZ* suggested that the two genes act in parallel pathways. In contrast, the broader nested accumulation of Eyg relative to Bowl suggested that the *odd-skipped* genes might promote notum expansion through both the autonomous and non-autonomous induction of Eyg.

odd-skipped genes are required for notum formation at early first instar

We previously showed that broad expression of *bowlRNAi or lines* resulted in a severe reduction of wing growth and in a near complete loss of the notum. Interestingly, *dpp* expression was maintained in these discs suggesting that additional signals whose activities depend on *odd-skipped* genes' function were required to promote notum growth and patterning [70]. To better understand the role of *lines* and *bowl* at early stages of notum development, we expressed *lines* with the peripodial-specific driver *Ubx-GAL4* (Fig. 2.3B, compare to wild type in 3A). In addition, we generated large patches of *lines*-expressing clones at early larval stages (Fig. 2.3C). These manipulations resulted in adult flies lacking either one or both heminota (Fig. 2.3B,C; ΔT indicates missing thorax). This phenotype could arise from a loss of peripodial epithelium required for disc eversion at metamorphosis [299], or from earlier defects in notum specification or growth. To distinguish between these possibilities, we examined the accumulation of Eyg in *Ubx>bowlRNAi* discs (Fig. 2.3E). In wild type discs, Eyg accumulates broadly in the anterior notum, and in restricted patches in the hinge and posterior wing pouch (Fig. 2.3D). Expression of *bowlRNAi* with *Ubx-GAL4* severely downregulated Eyg accumulation in the notum (Fig. 2.3E), but did not affect accumulation in the pouch and hinge (Fig. 2.3E, asterisks). Broad overexpression of *lines* with *C311-GAL4* eliminated expression of the homoedomain proteins C15 and Aristaless (Al), which are normally restricted to the posterior notum. Further, broad ectopic *lines* also eliminated the zinc finger protein Stripe (Sr*)*, which is normally expressed in several anterior patches (Fig. 2.4). We further found that *mirr-lacZ* was still expressed in similar discs generated by induction of *lines* expressing clones at early first instar (Fig. 2.3F). This observation indicates that *lines* does not inhibit the specification of the notum but the elaboration of the notum AP axis. We note that large *bowl, odd,* or *drm* mutant cell clones generated in a *Minute* background failed to recapitulate this phenotype (Fig. 2.3G,

Fig. 2.3), suggesting that two or more *odd-skipped* genes act redundantly to broadly pattern the notum AP axis. However, the identical *lines* gain-of-function and *bowlRNAi* phenotypes supports the hypothesis that an antagonistic relationship exists between *lines* and the *odd-skipped* genes during the early stages of notum patterning, and that the *odd*-skipped genes are required for notum expansion.

odd-skipped genes and *lines* regulate Bowl accumulation in the developing notum

The *bowlRNAi* employed (Fig. 2.3E) is predicted to have off-target effects through partial complementarity with *odd* and *sob* transcripts. Thus, the *bowlRNAi* phenotype is likely to reflect the combined depletion of several *odd-skipped* genes. To test whether the *odd-skipped* genes can act redundantly, we examined the regulatory relationships between *odd-skipped* genes and *lines* in the notum and *in vitro*. As expected, ectopic *drm* expression in FLP-out clones resulted in a cell-autonomous stabilization of Bowl. Consistent with the endogenous pattern of *drm* and Bowl expression, Bowl was also stabilized non-autonomously surrounding the clones (Fig. 2.6A). By contrast, though *sob* and *odd* each promoted Bowl accumulation cell-autonomously, neither gene promoted non-autonomous accumulation of Bowl (Fig. 2.6B,C). Interestingly, we noted that Sob promoted Bowl accumulation to a much greater extent than did Odd. Together, these gain- and loss-of-function analyses suggest that each of the *odd-skipped* genes is sufficient to promote Bowl accumulation, though to varying degrees. Loss-of-function analysis revealed normal Bowl accumulation in *drm* and *odd* mutant clones (Fig. 2.6D,E), also supporting the hypothesis that two or more *odd-skipped* genes act redundantly to stabilize Bowl in the notum.

To explore the molecular mechanism by which the Odd-skipped proteins promote Bowl accumulation, we examined their interaction with Lines by co-immunoprecipitation assays in Schneider 2 (S2) cells. We found that Odd and Sob could each form a complex with Lines that

required an intact N-terminal zinc finger domain (Fig. 2.6F, upper). Increased levels of Odd or Sob outcompeted the binding of Lines to Bowl (Fig. 2.6F, center), and enhanced Bowl accumulation (Fig. 2.6F, lower). Consistent with our overexpression studies, Odd showed a weaker capacity to bind to Lines and outcompete the binding of Lines to Bowl than did either Drm or Sob. In control experiments, we confirmed that Lines binds to Bowl, and that Drm outcompetes this interaction to stabilize Bowl as previously described (Fig. 2.6F) [65,66]. These results suggest that Drm, Odd, and Sob could redundantly stabilize Bowl by inhibiting the interaction of Lines with Bowl. We then examined the regulatory relationship between Lines and Bowl in the notum. We found reduced Bowl accumulation in *lines*-expressing FLP-out clones within the Bowl domain (Fig. 2.6G). Reciprocally, we detected ectopic Bowl accumulation in *lines* FLP/FRT mutant clones outside the Bowl domain (Fig. 2.6H), but no accumulation surrounding the clones. Taken together these data confirm that Drm, Odd, and Sob can each bind and inhibit Lines to promote Bowl accumulation *in vitro* and *in vivo*. The regulatory interactions between Lines and the Odd-skipped proteins are summarized in Fig. 2.6I.

drm promotes Bowl and Eyg accumulation using cell-autonomous and non-autonomous mechanisms

Given the nested domains of expression of *drm*, Bowl, and Eyg, we tested by gain- and loss- of function analysis whether the *odd-skipped* genes are sufficient to mediate notum growth and patterning (Figs. 2.7 & 2.8). First, we asked whether ectopic expression of *drm* could promote anterior notum patterning. Indeed, we found that ectopic *drm* expression along the AP compartment boundary with *dpp-GAL4* generated ectopic anterior notum structures, and led to a reduction of the posterior scutellum (Fig. 2.7B). In discs, this corresponded to a broad expansion of anterior fate marked by Eyg that coincided with the retraction of posterior fate, marked by Tup (Fig. 2.7D compare to wild type pattern in C). Additionally, loss of *lines* in mutant

clones led to the loss of Tup autonomously in the posterior notum (Fig. 2.7E), further supporting the antagonistic relationship between these genes.

Clonal expression of *drm* promoted Eyg accumulation both within and broadly surrounding the clones, and Bowl accumulation both within and just adjacent to the clones (Fig. 2.8A). Thus, ectopic *drm* expression recapitulated the nested expression of these proteins in the notum. To determine whether *bowl* mediated the autonomous and non-autonomous activities of *drm*, we generated *drm*-expressing clones that were mutant for *bowl,* using the MARCM technique. We found that these clones failed to induce Eyg and Bowl accumulation cell-autonomously. However, these clones still induced accumulation of Eyg and Bowl non-autonomously (Fig. 2.8B). To test whether *drm* was sufficient to promote notum patterning outside the notum, we examined *drm* expressing clones in the pouch. As in the notum, *drm* expression induced Bowl both autonomously and non-autonomously (Fig. 2.9A). Also similar to the notum, deletion of *bowl* in *drm* expressing clones abolished the autonomous, but not the periclonal accumulation of Bowl (Fig. 9B). However, in neither experiment did we detect autonomous or non-autonomous induction of Eyg, indicating that the outputs of *drm* activity depend on the tissue context. This observation is consistent with the finding that *drm* does not act to specify the notum, but rather to elaborate the AP pattern within the notum field (Fig. 2.3F).

To determine if *bowl* was sufficient to promote Eyg accumulation in the notum, we generated *bowl* overexpression clones using a strong UAS-*bowl* transgene. We found modest accumulation of Bowl and Eyg in a subset of clones, but none surrounding the clones (Fig. 2.8C). The weaker induction of Eyg in the Bowl expressing clones can be attributed to the lower level of Bowl that accumulated in these clones. Similar to *bowl*-expressing clones, *lines* mutant clones

promoted accumulation of Bowl and Eyg only cell-autonomously (Figs. 2.6H and 2.8D, respectively).

To determine whether *bowl* was required to promote Eyg cell-autonomously, we examined Eyg accumulation in *bowl* mutant cell clones. We found that Eyg was downregulated in clones generated in the first larval instar (Fig. 2.8E). Eyg was also downregulated in *lines* expressing clones generated in the early first instar (Fig. 2.8F). By contrast, Eyg expression remained both in *bowl* mutant and in *lines* expressing clones induced after the first instar, suggesting that the maintenance of Eyg at the anterior border of the notum is independent of *bowl*. Taken together, these results indicate that *bowl* is both necessary and sufficient to promote the cell-autonomous induction of Eyg, and that *odd-skipped* genes can organize notum growth and patterning using both autonomous and non-autonomous mechanisms.

bowl regulates *bar* and *Dl* to pattern the prescutum autonomously

To further characterize the organization of the notum AP axis, we asked whether *odd-skipped* genes were required autonomously to specify the identity of the prescutum. We found that *bowl* mutant clones generated cuticle patterning defects within the *bowl* expressing prescutum (Fig. 2.11B, outlined in red). Expression of *bowl*RNAi or *lines* in the anterior notum with *klumpfuss* (*klu*)-*GAL4* led to a significant reduction in the extent of the prescutum (Fig. 2.11C,D; Fig. 2.12C; $p<.001$). Additionally, microchaete were lost in the ventral prescutum (see arrows in Fig. 2.11C,D). This corresponded to a near total loss of Bowl accumulation in the prescutum (Fig. 2.12A-B). Since *Bar* genes (*BarH1* and *BarH2*) are expressed in the presumptive prescutum and promote the patterning of this region [60], we asked whether the *odd-skipped* genes might promote *Bar* expression to specify the identity of this region. Consistent with the observed adult phenotypes, *Bar-lacZ* reporter expression was lost autonomously in *bowl* mutant

clones (Fig. 2.11E), and similarly in clones of cells expressing either *bowlRNAi* or *lines* (Fig. 2.11F, G). Conversely, Bar accumulated ectopically in *lines* mutant clones (Fig. 2.11H). To further characterize the requirement of the *odd-skipped* genes in prescutum patterning, we examined the accumulation of Dl in the developing notum. Though N signaling has not been previously implicated in notum AP patterning, we noted that Dl accumulated adjacent to the Odd domain, with no accumulation in the presumptive prescutum (Fig. 2.11I). To further characterize whether loss of *bowl* altered the fate of the presumptive prescutum, we examined Dl expression in *bowl* mutant clones. We detected ectopic Dl in clones in the Bowl domain (Fig. 2.11J). Taken together, these results demonstrate that *bowl* is required autonomously to promote *Bar* expression and inhibit Dl accumulation to pattern the prescutum.

During development, cells that adopt a particular cell fate minimize their interaction with cells of alternative fates. Cells that experimentally acquire a new fate frequently extrude from the epithelium or form compact structures to minimize contact with surrounding wild type cells[300,301]. To determine whether the *bowl* mutant clones minimized contact with surrounding wild type cells, we analyzed their circularity, roundness, and solidity compared to wild type twin spots. We found that *bowl* mutant clones that were induced within the Bowl domain adopted a distinctly round and compact morphology in which actin accumulated apically (Fig. 2.13A). Mutant clones inside the Bowl domain were significantly different than clones outside the Bowl domain in all measures ($p<.001$, Fig. 2.13B). This phenotype suggests that the *bowl* mutant clones minimized contact with the surrounding Bowl expressing cells. Additionally, *bowl* mutant clones occasionally sorted from the Bowl domain and formed large composite clones with smooth borders and round morphology (Fig. 2.13C). The morphology and sorting behavior of the *bowl* mutant clones further support the hypothesis that *bowl* promotes cell fate within the prescutum.

odd-skipped genes pattern the eye margin

To determine whether Bowl activity at tissue margins might be a conserved function within dorsal appendages, we investigated the roles of *odd-skipped* genes and *lines* in eye patterning. First, we examined the temporal pattern of *odd*-skipped family expression during eye development. *odd-skipped* genes *drm* (Fig. 2.14A), *odd* (Fig. 2.14B), and Bowl (Fig. 2.14C) accumulate in a pattern similar to the notum, including broad expression in the PE from L2 (Fig. 2.14A-C) throughout larval development at L3 (Fig. 2.14D-E'). Additionally, *drm*, *odd*, and Bowl accumulate at the PE-DP margin, consistent with previous reports[290]. This accumulation is evident by L2, and persists throughout larval development. To extend previous findings and relate these patterns to adult structures, we mapped this domain onto the adult cuticle using a lacZ reporter insertion in *odd* (Fig. 2.14F). In the adult, this domain corresponded to a band of bristled head cuticle that encircled the posterior region of the eye (Fig. 2.14F-F'), suggesting a potential role in the specification of this margin tissue, similar to that of the prescutum.

To determine whether *odd-skipped* genes are required for the early growth of the eye disc, as in the wing, we expressed *lines* with ptc-GAL4. Larvae raised at 25^{o} routinely showed a complete (Fig. 2.15A) or partial (Fig. 2.15B) loss of eye disc derived structures. These defects corresponded to a severe loss of retinal tissue, marked by retinal determination genes Cut (Fig. 2.15C), Nub (Fig. 2.15D) and Senseless (Fig. 2.15E). Consistent with the role of Bowl in the growth of the wing, pharate adults frequently exhibited loss of wing disc derived structures as well (not shown).

We next tested whether *odd-skipped* genes were required at the eye disc margin to pattern this structure, similar its role in the notum. Based on our fate mapping study, we hypothesized that *odd*-skipped genes were required to specify the eye disc margin as bristled cuticle. To test this hypothesis, we generated *lines* mutant clones in the eye. Adult eyes showed

a range of phenotypes including outgrowths of retinal tissue, both increased and decreased retinal field size, and deformation and necrosis of antennae (not shown). The most common phenotypes, however, were the presence of bands of naked cuticle surrounding and/or traversing the retinal field (Fig. 2.16B-C), and an increase in bristles at the anterior ventral portion of the eye field (Fig. 2.16B-C). Occasionally, bristled cuticle was also observed wholly within the retinal field (Fig. 2.16D).

Several genes combine to promote head cuticle specification at the eye disc margin. Wg is required to delineate head capsule and retinal fields[302], while the hox gene Homothorax regulates *dpp* expression to pattern the ventral eye margin[303–305]. To test whether eye defects in *lines* mutant clones were due to a change in the molecular patterning of the disc, we examined the expression of Wg (Fig. 2.16E), *dpp-lacZ* (Fig. 2.16F), and Hth (Fig. 2.16G) in *lines* mutant clones. Consistent with a change to head capsule fate, loss of *lines* induced expression of each reporter. Additionally, *lines* mutant clones near the morphogenetic furrow failed to induce the neuronal specific gene elaV, suggesting a loss of retinal identity. These observations are consistent with the observation that Lines overexpression leads to the formation of unpatterned cuticle at the expense of normal head cuticle (Fig. 2.16B-D). Together, these results suggest that the appropriate pattern of Lines expression and repression is required to specify head cuticle at the boundary of the retinal field.

To characterize the direct contributions of *odd-skipped* genes in margin patterning, we tested whether Drm and Bowl regulate Wg expression at the eye disc margin. Wg is the best characterized determinant of head capsule, and is co-expressed with Bowl along most of the margin (Fig. 2.17A). Wg is expressed at a high level at the posterior margin from where the morphogenetic furrow is triggered, while along the remainder of the posterior margin it accumulates at lower levels. In *bowl* mutant clones, Wg failed to accumulate along the margin

(Fig. 2.17B). Conversely, in *drm* expressing clones, we observed tissue outgrowth similar to those observed in the notum. Drm overexpression induced Odd and Wg to varying degrees within clones (Fig. 2.17C). In some regions of clones, Odd and Wg co-accumulated, while in others one or neither protein was ectopically induced. This suggests that the ability of Drm/Bowl to induce Wg expression depends on the overall tissue context, similar to the capacity of Drm to induce anterior notum. To test whether the effect of Drm required Bowl accumulation, we expressed Drm in a *bowl* mutant clone (Fig. 2.17D). These clones failed to induce tissue outgrowth and failed to induce Wg accumulation, suggesting that Bowl is indeed required downstream of Drm.

These studies suggest that *odd-skipped* genes are required at the eye disc margin for the normal expression of head cuticle patterning genes and for normal head capsule patterning in the adult fly. These data extend previous studies that suggested a more restricted role for *odd-skipped* genes in the regulation of *hh* signaling at the posterior margin. The parallels of expression and function of *odd-skipped* genes between notum and eye margins suggest conserved roles for this gene family in the regulation of patterning at the margin of intersection of the PE and DP in dorsal appendages.

Discussion

Epithelia are frequently patterned by signals from opposing field boundaries.

In many developmental processes, signals that emanate from field borders play a crucial instructive role in patterning morphogenetic fields. The early *Drosophila* embryo is patterned by opposing gradients of Bicoid and Nanos that are generated from localized translation of corresponding mRNAs at the anterior and posterior poles of the embryo [306]. In the embryonic epidermis, the pattern of cell differentiation across each segment is regulated by the secreted

Wg and Hh signals that emanate from localized sources at the anterior and posterior borders of each segment[307]. Similarly, the dorsoventral axis of the vertebrate spinal cord is organized by Shh ventrally, and BMP and Wnt signals that emanate from localized dorsal sources[308,309]. By contrast, current models of notum AP patterning focus mainly on the organizing influence of Dpp, which is secreted from the posterior border of the notum. We previously found that *odd-skipped* genes are expressed along the anterior border of the notum, and that broadly inhibiting their function in early wing discs caused a severe reduction or complete loss of the notum. As this reduction occurred despite the maintenance of *dpp* expression[70], we investigated whether the *odd-skipped* genes might define a second organizing center within the developing notum. Our current findings indeed suggest that signals that emanate from the anterior border of the notum act reciprocally to Dpp to promote expression of anterior notum genes and repress expression of posterior genes (Fig. 2.7-2.8). Through loss- and gain-of-function clonal analyses, we demonstrate that the *odd-skipped* genes pattern the notum AP axis both locally through regulation of Eyg, Bar, and Dl, and broadly through the regulation of Eyg and Tup. Finally, we show that *lines* acts antagonistically to *bowl* in this process (see model of the gene regulatory network in Fig. 2.14).

odd-skipped genes pattern the notum AP axis using autonomous and non-autonomous mechanisms

We found that *drm* overexpression was sufficient to promote Eyg accumulation non-autonomously within the notum. This activity suggests that *drm* controls expression of an unidentified signal that spreads from the *drm* domain to induce Eyg accumulation non-autonomously. Alternatively, *drm* could initiate the propagation of a cascade of local inductive interactions to induce Eyg at a distance. Recent studies have shown that recruitment of cells to the wing field is accomplished by the propagation of a feed forward signal from the DV

compartment boundary[310,311]. In this process signaling at the border between Vestigial (Vg) and non-Vg expressing cells is used to recruit non-Vg expressing cells to the expanding wing field, a process dependent on signaling through the Fat-Dachsous pathway. Though we have yet to characterize a functional relationship between *odd-skipped* genes and Ft-Ds signaling, it is interesting to note that Ds accumulates in a complex graded AP pattern across the notum, consistent with such a role (SD & VH, unpublished observations).

In addition to the broad induction of Eyg accumulation, we were surprised to find that *drm* overexpression also induced Bowl in cells just adjacent to clones. Though the effect was subtle, we note that this pattern of activation recapitulated the endogenous nested pattern of *drm* and Bowl expression in the presumptive prescutum. It is unclear whether the nested expression of *odd-skipped* genes plays a functional role in notum AP patterning. Despite this, the concordance of endogenous and ectopic expression patterns supports the hypothesis that ectopic *drm* induces a physiologically relevant program of anterior gene expression in the notum.

One possible clue as to the relevance of this nested pattern may come from the observation that only *drm* was able to promote Bowl non-autonomously. In contrast, *lines*$^{-/-}$, *odd*$^{+}$, and *sob*$^{+}$ clones each induced only cell-autonomous accumulation of Bowl. Notably, these clones rounded up and segregated from the epithelium, while *drm* expressing clones remained integrated with the surrounding epithelium. One interpretation of these data is that abrupt discontinuities in the level of Odd-skipped proteins may alter epithelial morphology, as previously reported[72]. This interpretation is further supported by the observation that *bowl* mutant clones within the Bowl domain adopt a compact, round morphology relative to clones outside the Bowl domain (Fig. 2.13). We hypothesize that *drm* promotes lower levels of Bowl in

nearby cells to dampen otherwise sharp discontinuities in Bowl activity to regulate local buckling of the epithelium.

Though we have yet to experimentally investigate these discontinuities, it is interesting to speculate as to the underlying mechanism and function of this hypothetical intercellular buffering. As mentioned, Drm could induce a short range signal to stabilize Bowl in adjacent cells. Alternatively, Drm could directly mediate Bowl stabilization in neighboring cells by intercellular diffusion. Drm could diffuse through ring canals, which mediate direct cell-cell communication in *Drosophila* follicle and imaginal epithelia, in addition to their well characterized role in nurse cells[312]. Consistent with such a hypothesis, somatic ring canals allowed the free diffusion and equilibration of proteins among clonal patches of cells. In this way, diffusion of Drm could not just serve to equilibrate, but also to grade discontinuities as discussed.

It is also interesting to speculate whether these sharp discontinuities might underlie the differences in long range signaling between Drm+, Odd+, and *lines* clones. Direct, long range contact by cytonemes contributes, at least in part, to Dpp, FGF, and Notch signaling in the wing disc[48,49,53,313]. These projections are highly sensitive to mechanical disruption[48]. As such, disruption of epithelial integrity in *lines* clones could prevent long range induction of Eyg through the elimination of cytoneme projections to surrounding cells.

This buffering capacity could emerge from differences in the total levels or ratios of Odd family proteins along the anterior border of the notum, which could elicit different transcriptional outcomes. Since Odd and Bowl have been shown to interact with the transcriptional co-repressor Groucho, variation in the levels of the Odd-skipped proteins could titrate Groucho and affect Groucho-dependent transcriptional outputs[292,314]. Alternatively, given their distinct structure outside the zinc finger domain, the Odd-skipped proteins could interact

with distinct sets of target genes to pattern the anterior border of the notum. Though additional experiments will be required to ascertain whether these mechanisms pattern the prescutum, we provide evidence that *bowl* is strictly required for the early autonomous induction of Eyg, the later expression of *Bar* genes, and the repression of *Dl*. These results provide evidence that *odd-skipped* genes act both independently and redundantly to organize the notum AP axis.

Redundant versus unique functions of *odd-skipped* genes in notum development

We show that *bowl* is essential for patterning the prescutum, but not for broadly patterning the notum AP axis. Previous studies have revealed a variety of essential and redundant functions for *odd-skipped* family genes in patterning embryonic and larval tissues. In the embryo, *drm* and *bowl* antagonize *lines* function to pattern the dorsal embryonic epidermis, foregut, and hindgut[65,67,68,315,316], while *odd* functions as a pair rule gene to promote embryonic segmentation[317,318]. In the leg imaginal disc, *bowl* is essential for patterning the tarsal proximodistal axis at early stages, but acts redundantly with other *odd-skipped* genes to control leg segmentation later in development[70,72,291]. In the eye, *bowl* is essential for the initiation of retinogenesis from the eye margin[290], while *odd* and *drm* have been proposed to activate Bowl redundantly.

Our loss-of-function analysis revealed that neither *drm* nor *odd* is necessary to stabilize Bowl. At present we cannot exclude the possibility that *sob* is necessary to promote Bowl accumulation because a null *sob* mutant is not yet available. Our biochemical and genetic analysis demonstrates that not only Drm, but also Odd and Sob can each outcompete the interaction of Lines with Bowl and stabilize the Bowl proteins in S2 cells and *in vivo*. These results suggest that different combinations of Odd-skipped proteins could be used to activate *bowl* depending on context.

Previous work suggested reciprocal roles for *lines* and *odd-skipped* genes in subdividing the early wing disc into disc proper and peripodial epithelium. The loss-of-function analysis described in this study suggests that the *odd-skipped* genes act redundantly to control the early specification of the PE and the subsequent expansion of the notum, while revealing an essential role for *bowl* in specification of the anterior prescutum. Redundancy can increase the robustness of essential developmental processes and provide a buffer against fluctuations in activity of single genes. The redundant role of the *odd-skipped* genes in PE specification and notum expansion could therefore serve to ensure the optimal growth of the wing disc at early stages and that of the notum at later stages and protect these critical processes from perturbations.

Conserved roles for odd-skipped genes and lines to pattern dorsal appendages

We further found that *odd-skipped* genes pattern the eye disc margin to promote head capsule formation, in a manner similar to their roles in notum AP patterning. *odd-skipped* genes are expressed at the posterior margin, in cells fated to become marginal head cuticle (Fig. 2.15). Ectopic accumulation of *bowl* in *lines* mutant clones resulted in ectopic head capsule formation, particularly along the ventral eye margin, and occasionally within the retinal field, corresponding to induction of marginal genes *dpp*, *wg*, and *hth* with no effect on genes typical of retinal fate, such as dac (Fig. 2.16). We found that Drm overexpression partially phenocopied lines loss of function. Interestingly, we found that Drm induced Wg in a Bowl dependent manner (Fig 2.18). Together, these suggest that *odd*-skipped genes regulate a pattern of gene expression that promotes normal head cuticle formation. This extends prior work that posited more restricted roles for Bowl to suppress ectopic retinal field formation[319], and to promote hh signaling to

trigger retinogenesis[290]. Together, these findings suggest that *odd-skipped* gene activity at the PE-DP interface is functionally relevant in both wing and eye discs.

The homology between eye and wing is not obvious at the both the morphological and molecular level. However, a number of threads of evidence suggest they are indeed serial homologs. The mutation Opthalmoptera[320] transforms the eye to a wing. This transformation is supported by transdetermination studies in culture, which showed that cultured eye discs generated allotypic wing structures[321]. Interestingly, notum tissue was the most common, though allotypic notum, hinge, and pouch tissues were found. At a molecular level, DV signaling in the wing pouch and eye contributes to the growth of each structure. However, with some exceptions (*iro-c*, *pnr*), the expression of key DV patterning genes appears dissimilar between eye and notum. By contrast, the parallel complementary accumulation of *odd*-skipped genes and lines between PE and DP in both eye and wing, and the consistent requirement for *odd-skipped* genes to pattern the PE-DP margin suggests that wing and eye discs share common mechanisms of molecular patterning. These results suggest that Lines and Bowl may have controlled both eye and wing development prior to the diversification of these structures by the activity of homeotic genes such as *omb* and field selector genes such as *eyeless* in eye and *vg* in the wing.

Conclusion

The growth and patterning of the wing field are coordinated with the elaboration of the wing PD axis. The developing notum lacks an obvious PD axis, and instead is subdivided into a series of AP and mediolateral domains[59]. The establishment of organizers that act antagonistically from opposing field borders is a robust strategy to subdivide the notum AP axis. Our work demonstrates that the *odd-skipped* genes act autonomously at the anterior border of

the notum to specify the prescutum, and non-autonomously at short and long range to control the expression of transcription factors that prefigure the differentiation of the notum AP axis. Though further experiments will be required to characterize the mechanism by which this putative organizer acts, our studies provide evidence that the anterior border of the notum exhibits the functional attributes of an organizer.

Acknowledgements

We thank S. Bray, G. Campbell, K. Irvine, T. Kojima, R. Mann, E. Moreno, P. Mitchell, C. Rauskolb, G. Struhl, B. Edgar, T. Volk, N. Azpiazu, U. Walldorf, H. Bellen, the Bloomington Stock Center, the Vienna *Drosophila* Research Center (VDRC), and the Developmental Studies Hybridoma Bank for generous gifts of fly stocks and antibodies. We also thank D. Nusinow, K. Wharton, and members of the lab for comments on the manuscript. This work was supported by a grant from the NIH to V.H. (R01GM06806).

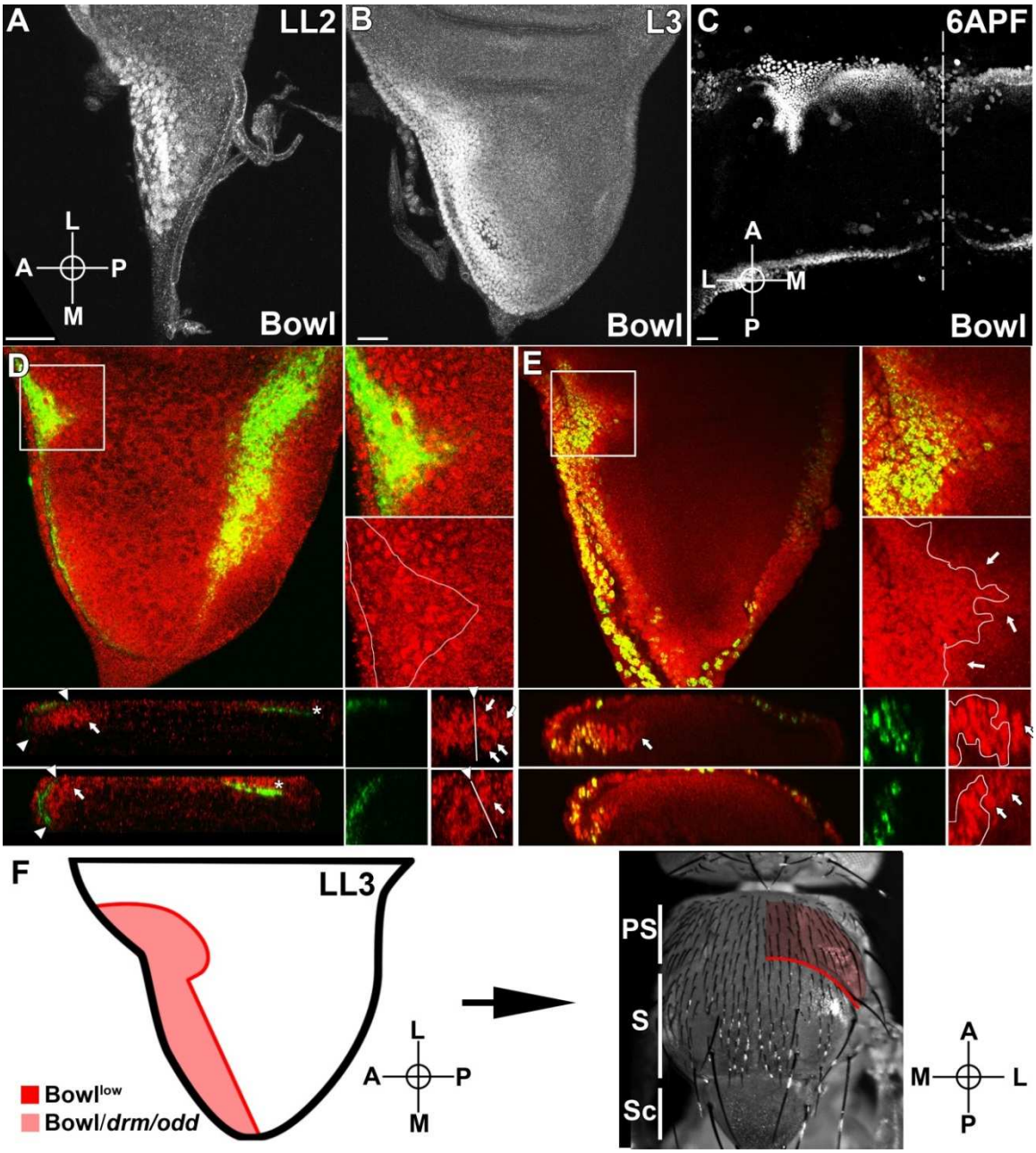

Figure 2.1: Nested expression of Bowl relative to drm and odd along the anterior border of the notum. (A-C) Pattern of Bowl accumulation during notum development. (A) Late second instar; Bowl accumulates in a broad anterior domain. (B) Third instar; the Bowl domain is limited to the anterior border of the notum. (C) 6hr APF; this pattern of Bowl accumulation persists into pupal stages. (D-E) Third instar; the Bowl domain (red) is slightly broader than the *drm* domain (green,

D), and *odd*>RFP domain (green, E) Broader Bowl accumulation marked by arrowheads in insets. Note that the tissue curvature obscures much of the *drm* in situ signal, which accumulates apically (see Z sections inset; extent of *drm* signal marked by broad arrowheads). Note also that posterior expression of *drm* is in the overlying cuboidal epithelium, not the disc proper. (F) Schematics depicting the Bowl, *drm*, and *odd* domains in the notum at third instar (left) and pupal (right) stages. In this and all subsequent images, boxes indicate magnified regions shown in insets, arrows along the left side of an image indicate plane of Z section shown in corresponding insets. Scale bar indicates 20 μm in all panels.

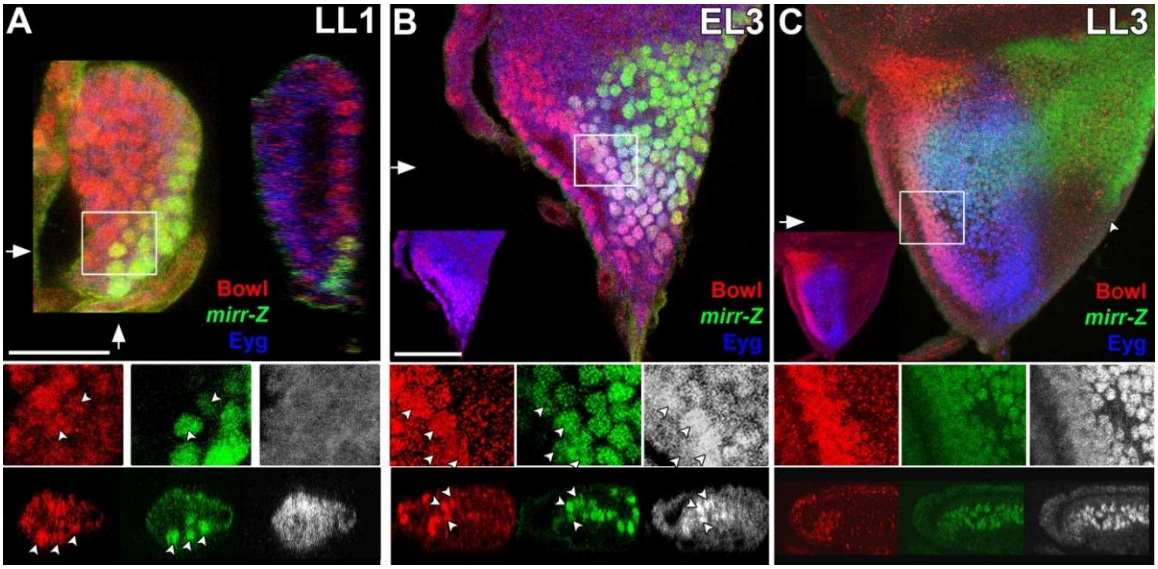

Figure 2.2: Evolution of Bowl accumulation relative to mirr and Eyg. (A) 36-48 hr wing disc; Bowl (red) and *mirr-lacZ* (green) are detected in the notum prior to Eyg (blue/white). Bowl and *mirr-lacZ* expression overlap across 1-3 cell diameters (see arrowheads). (B) 72-84 hr notum; Bowl, *mirr-lacZ*, and Eyg are all expressed at this stage (arrowheads note nuclei expressing all markers in B and C). Bowl is largely restricted to the anterior margin, though it accumulates in a slightly broader domain across the medial notum (see inset). Eyg accumulates more broadly in the presumptive prescutum. *mirr*-lacZ is expressed broadly throughout the notum, except in the medial and antero-lateral regions. (C) These relationships are maintained at the third instar, though Bowl is more highly restricted to the prescutum, and *mirr*-lacZ is completely excluded from the medial notum (arrowhead marks medial boundary of expression). In this and all subsequent panels, all stains marked blue in merged images are shown as white in corresponding insets for clarity.

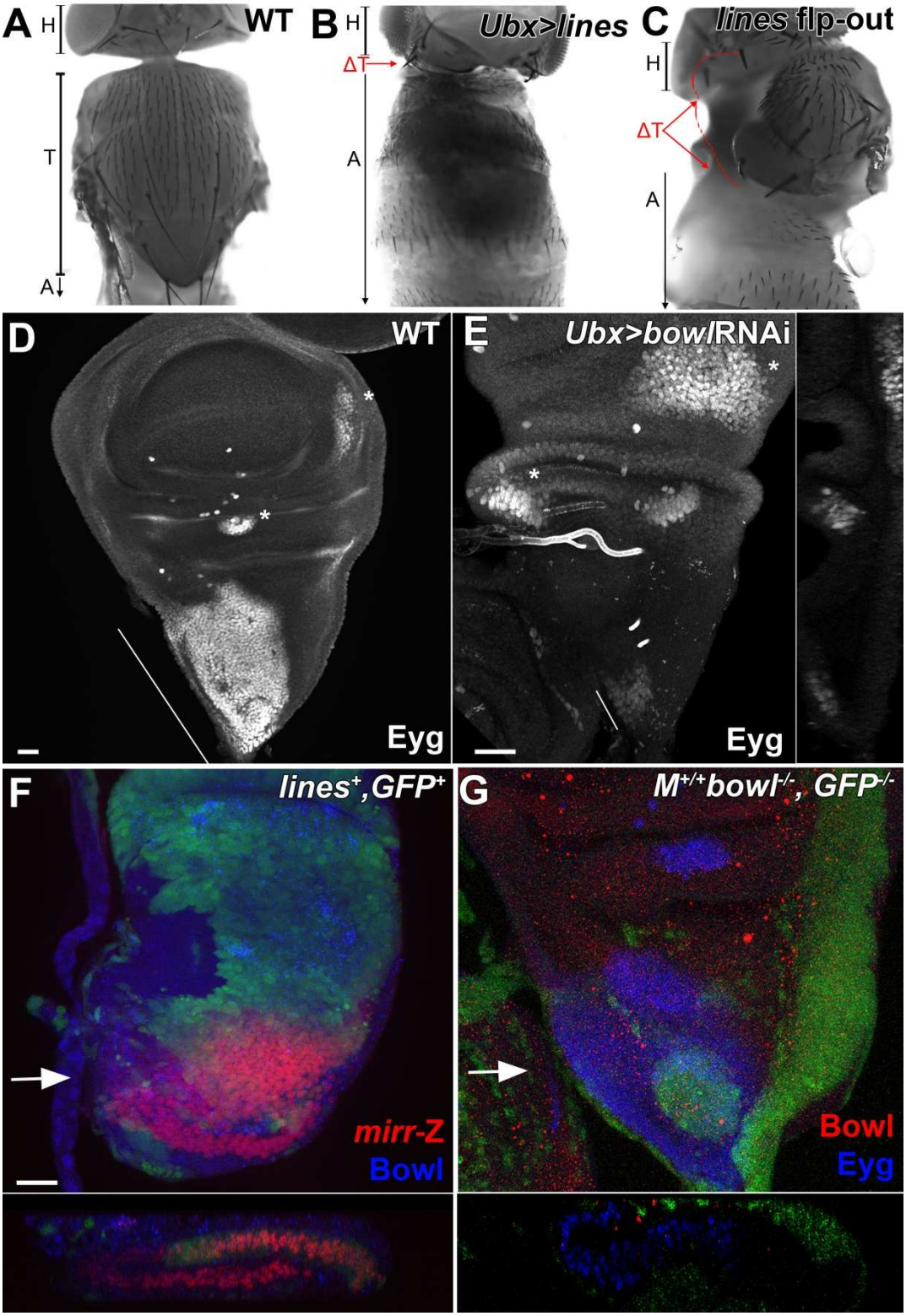

Figure 2.3: Roles of lines and bowl in notum specification. (A-C) Dorsal views of adult head [H], thorax [T], and anterior abdomen [A]. (A) Wild type. (B-C) Expression of *lines* with *Ubx-GAL4* (B)

or in early first instar clones (C) disrupted the formation of the adult notum or heminotum, respectively. (D, E) Expression of *bowl*RNAi with *Ubx*-GAL4 resulted in a loss or severe elimination of AP notum gene expression. (D) Wild type; Eyg accumulates in a broad anterior domain in the wild type notum. (E) *Ubx>bowl*RNAi; Accumulation of Eyg in the notum was severely reduced. Only a small region expressed Eyg at low level near the disc stalk (compare bar to wild type). By contrast, Eyg accumulation in the pouch and hinge (marked with asterisks) was not affected. (F) In a disc bearing large patches of *lines* expressing FLP-out clones, *mirr*-lacZ expression was largely retained. (G) Early large Minute *bowl* clones did not adversely affect notum development, nor did large Minute *odd* or *drm* mutant clones (see Fig. 2.9).

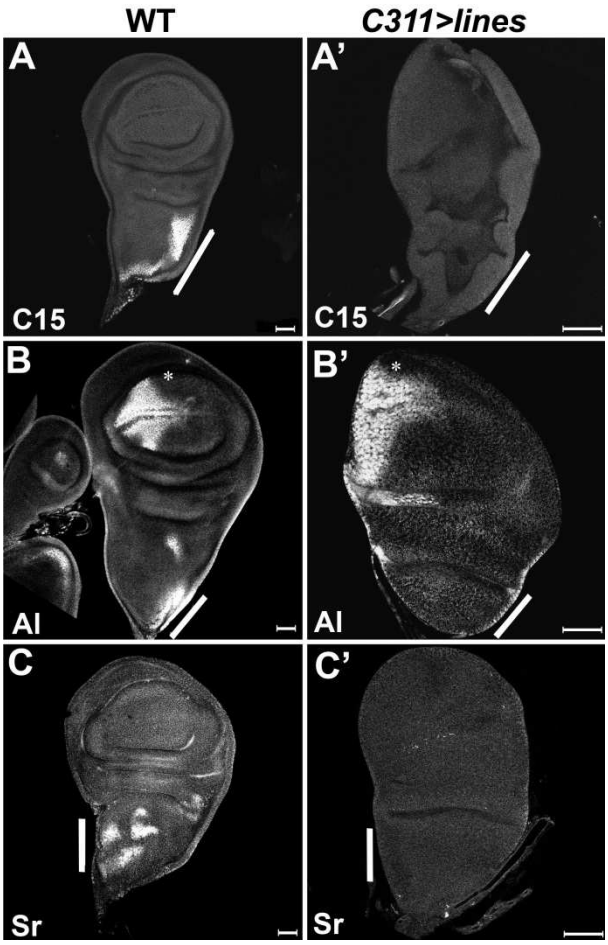

Figure 2.4: Expression of notum markers in C311>lines discs. (A-C) wild type; (A'-C') *C311>lines* third instar wing discs; Broad expression of *lines* resulted in loss of notum markers C15 (A'), Al (B') and Sr (C'). Expression of Al (B) persisted in the pouch (asterisk in B') suggesting that lines expression preferentially disrupts notum patterning. Likewise, expression of other hinge and pouch markers persisted in these discs as described previously [70].

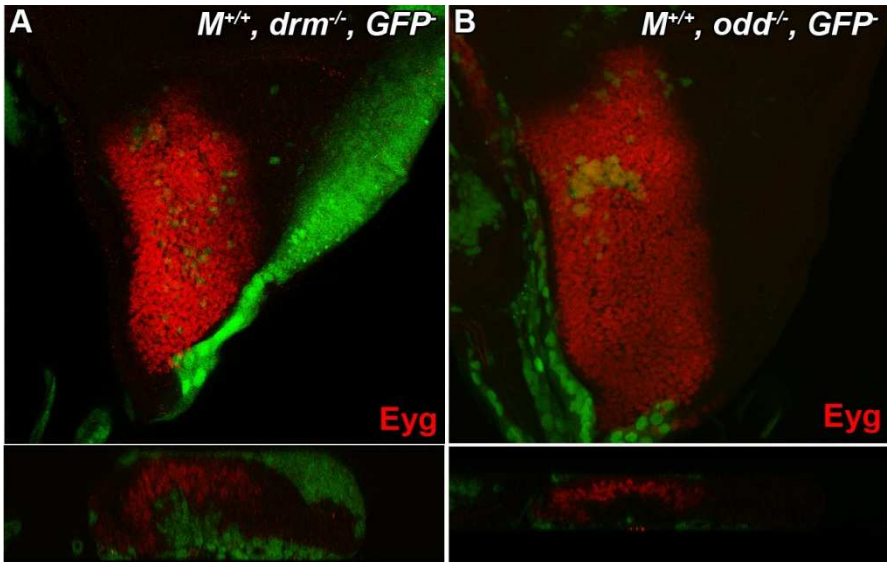

Figure 2.5: Neither odd nor drm are necessary for the expansion of the Eyg domain. Large negatively marked *drm* (A) or *odd* (B) mutant clones induced in a *Minute* background show largely normal expansion of Eyg (red).

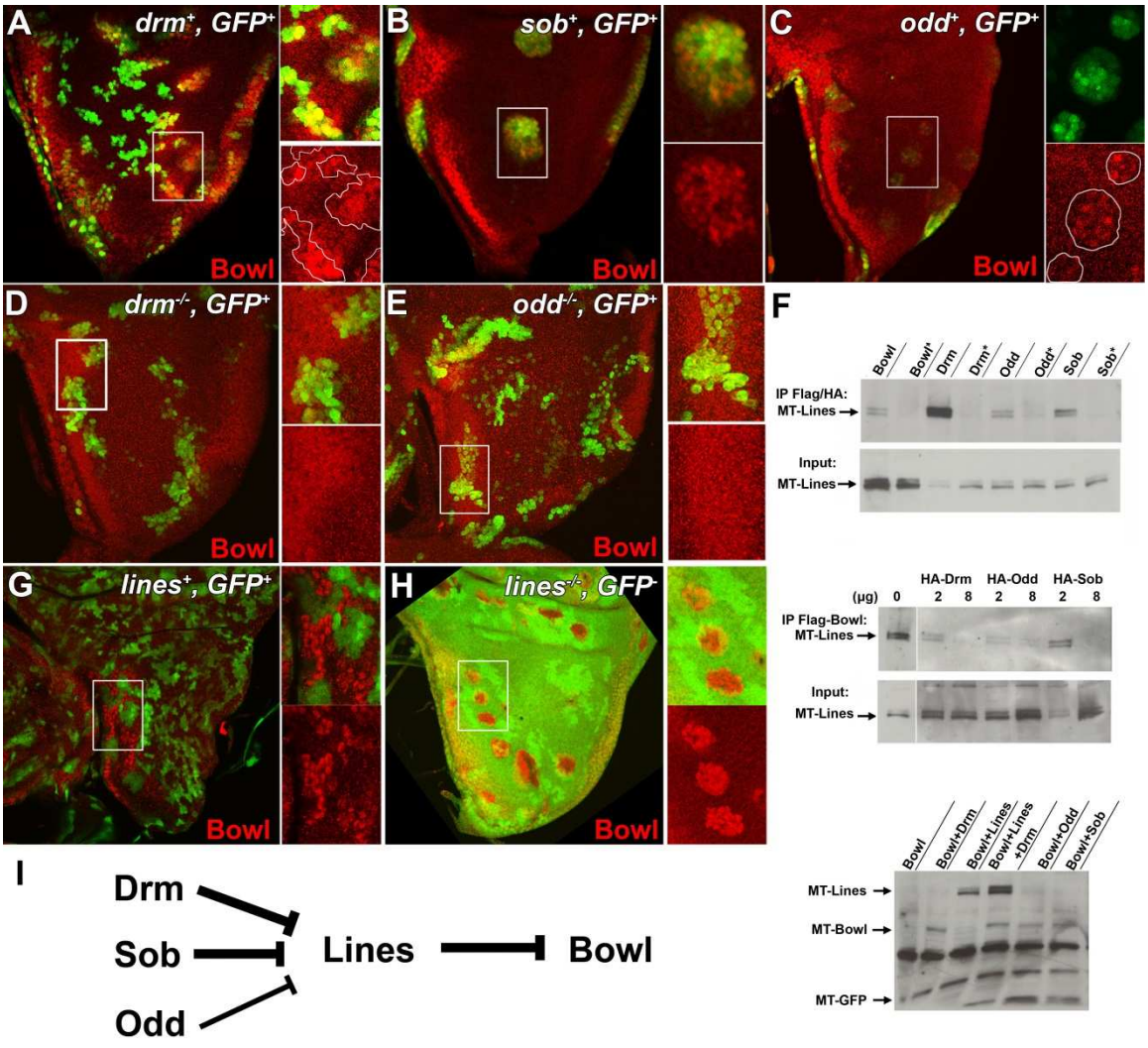

Figure 2.6: Regulation of Bowl accumulation by drm, odd, sob and lines in the notum and S2 cells. All clones are positively marked with GFP (green), except in G where clones are negatively marked by loss of GFP. (A) Ectopic *drm* resulted in both autonomous and periclonal (arrowheads) induction of Bowl (red in all panels in figure). (B-C) Ectopic *sob* (B) or *odd* (C) led to autonomous, but not periclonal, Bowl accumulation. (D-E) Neither *drm* (D) nor *odd* (E) mutant clones resulted in loss of Bowl accumulation. (F) Upper panel: Co-immunoprecipitation between FT-Bowl, HA-Drm, HA-Odd or HA-Sob and MT-Lines. Asterisks indicate mutant variants with a disrupted N-terminal zinc finger. MT-Lines formed a complex with each Odd family member containing a functional N-terminal zinc finger. Middle panel: Increasing levels of HA tagged Drm,

Odd, or Sob outcompeted the interaction of MT-Lines with FT-Bowl. Lower panel: FT-Bowl accumulated at low levels in S2 cells (lane 1). Co-transfection with Myc-Lines further suppressed Bowl levels (lane 3), while co-transfection of Drm with Lines reversed this effect (lane 4). Co-transfection of Bowl with Drm (lane 2), Odd (lane 5) or Sob (lane 6) increased Bowl levels. (G) Bowl was lost along the presumptive prescutum in *lines* expressing clones, while it accumulated ectopically in *lines* mutant clones posterior the prescutum (H). (I) Schematic of functional interactions between Odd-skipped proteins and Lines. Thickness of arrows schematically suggests relative strength of interactions.

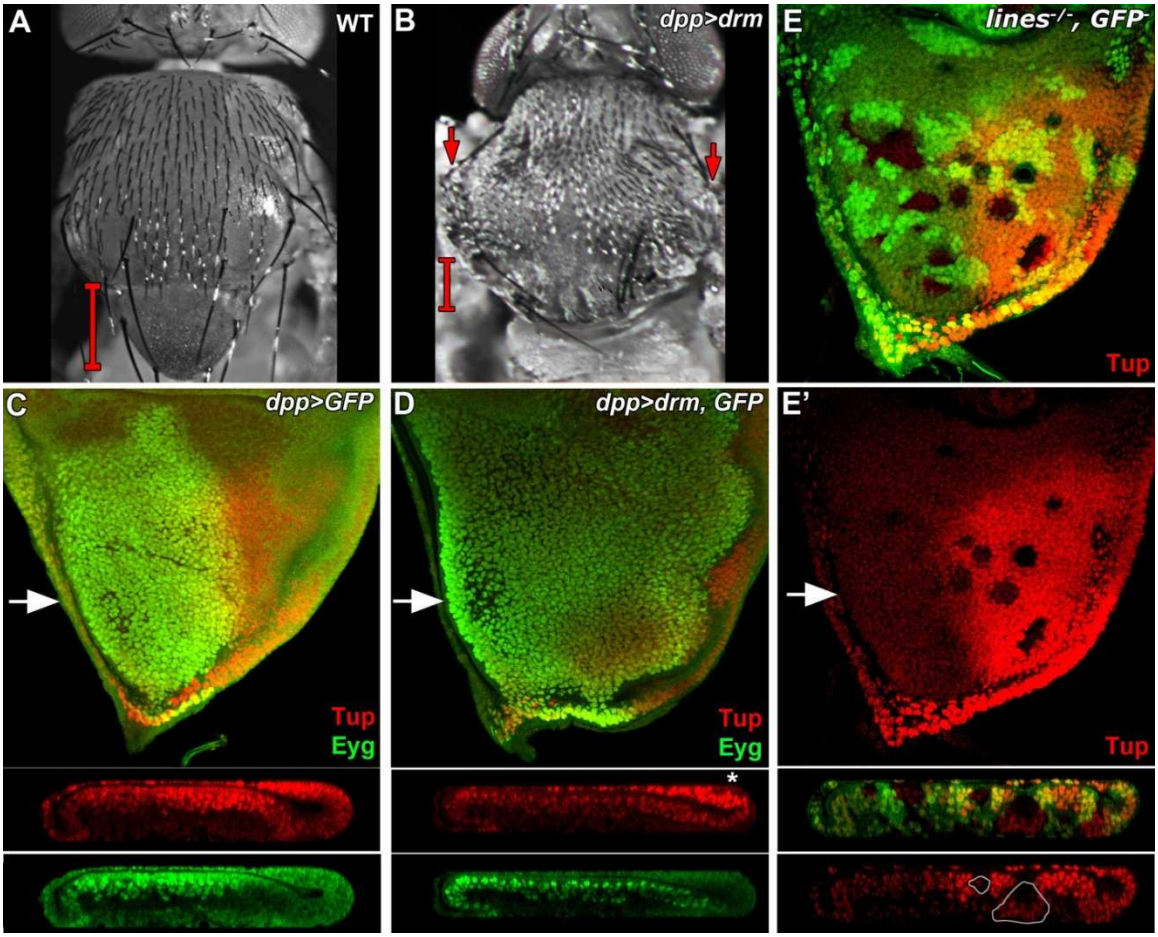

Figure 2.7: Ectopic posterior expression of drm induces ectopic anterior notum and inhibits scutellum formation. (A-B) Dorsal views of adult nota. Expression of *drm* with *dpp-GAL4* resulted in the generation of ectopic anterior notum structures (red arrows) and a reduction of the posterior scutellum (red bracket, compare to wild type in A). (C) Third instar *dpp>GFP* notum; Eyg (green) and Tup (red) mark broad anterior and posterior domains, respectively, with a small overlap in central notum. (D) Third instar *dpp>drm* notum*;* Eyg was expanded ectopically into the posterior notum, while Tup expression was strongly diminished (expression remained in the overlying cuboidal epithelium, marked with an asterisk). (E-E') Tup (red) was downregulated in *lines* mutant clones (negatively marked) within the Tup domain.

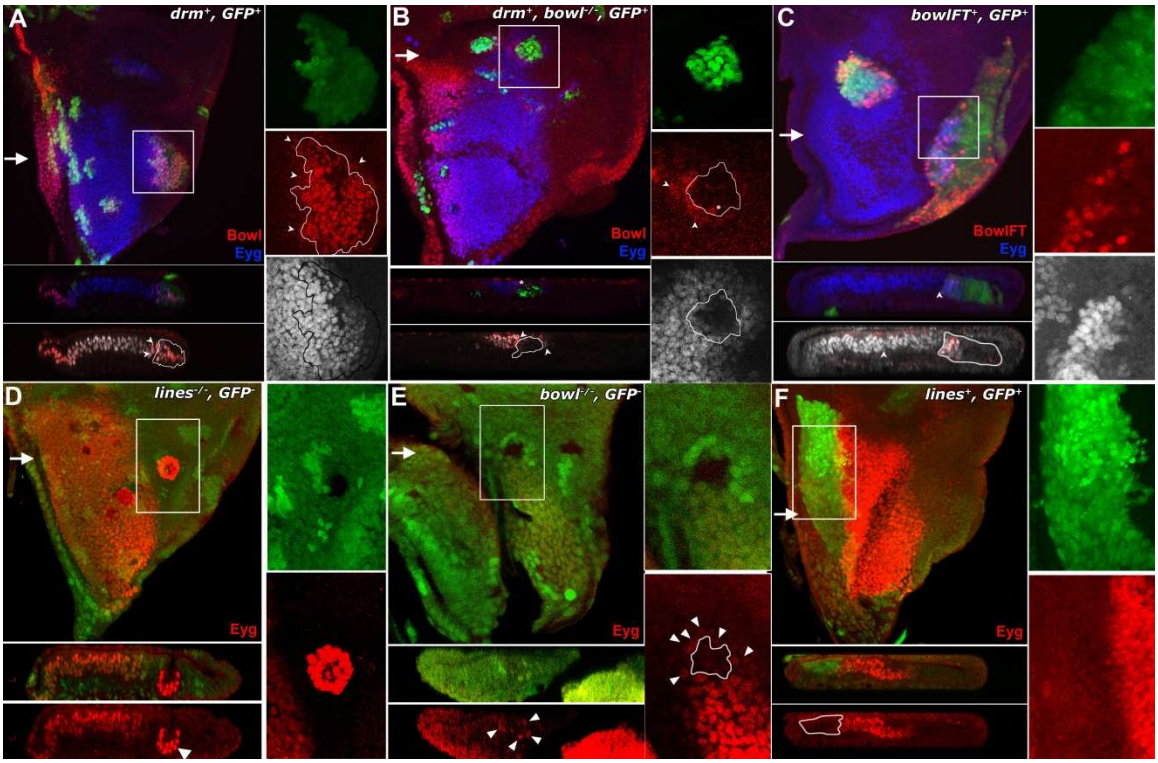

Figure 2.8: odd-skipped genes promote scutum expansion autonomously and non-autonomously. (A) *drm* overexpression in clones (green) posterior to the Eyg domain (blue/white) led to the autonomous and broad non-autonomous induction of Eyg (extent of non-autonomous induction outlined in white on main panel). (B) The autonomous, but not the non-autonomous, induction of Eyg was lost in *drm* expressing clones mutant for *bowl*. Apparent overlap in GFP and Eyg is due to projection (note lack of overlap in Z-sections). (C) In cases where clonal *bowl*-FLAG overexpression led to ectopic Bowl accumulation (anti-FLAG, red), it promoted autonomous expansion of Eyg accumulation. (D) Eyg (red) was induced autonomously in *lines* mutant clones posterior to the Eyg domain. (E-F) Eyg (red) was lost autonomously in early first instar *bowl* mutant clones (E) and in *lines* expressing clones (F, green). Arrowheads in E indicate Eyg positive nuclei surrounding the clone.

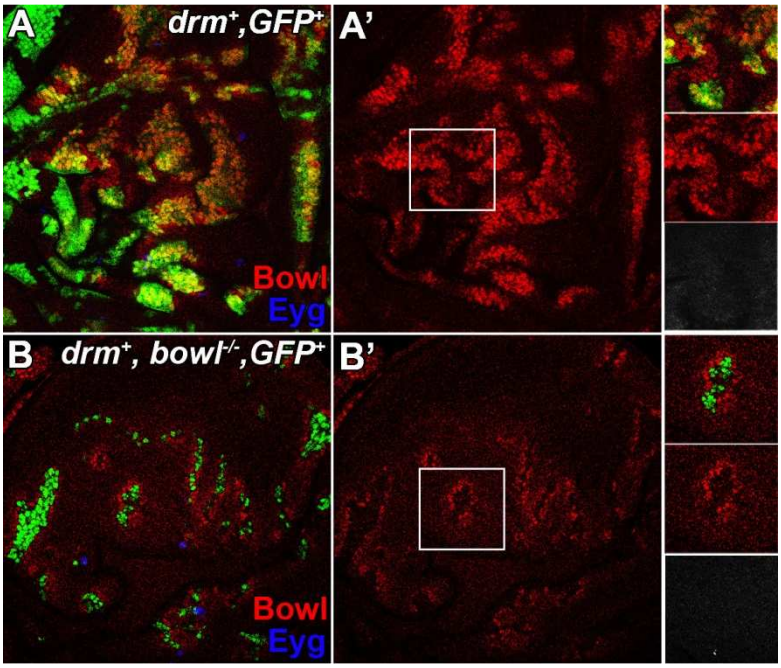

Figure 2.9: Drm induces Bowl, but not Eyg, autonomously and nonautonomously in the wing pouch. A. Third instar wing pouch bearing *drm* expressing clones (green). As in the notum, Bowl (red) is induced within and surrounding the clone, though Eyg is not induced. (B) Third instar wing pouch bearing MARCM drm^{+}, $bowl^{-/-}$ clones induced at late second instar. Ectopic *drm* expression (green) induces Bowl accumulation (red) immediately surrounding the clones, despite the loss of *bowl* within the clone (note lack of accumulation within clone). Similar to (A), these clones fail to induce Eyg expression.

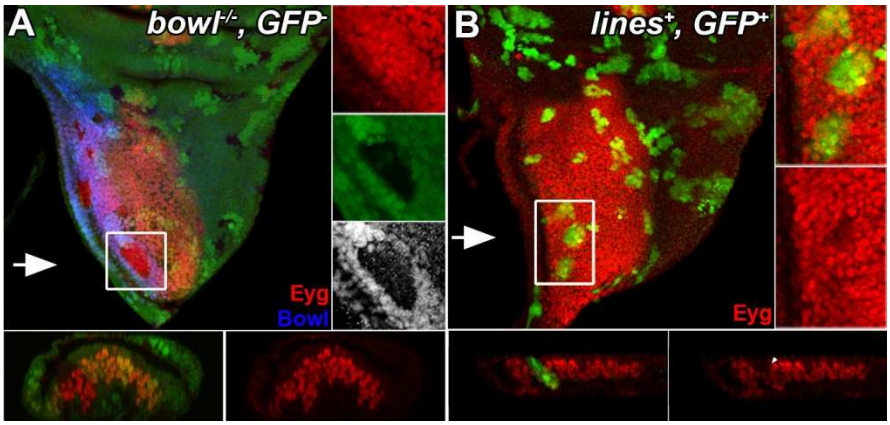

Figure 2.10: Eyg is maintained independently of Bowl after the early first instar. Eyg expression (red) was retained in *bowl* mutant (A) or *lines* expressing (B) clones induced after the first instar (clones shown were induced at early third instar).

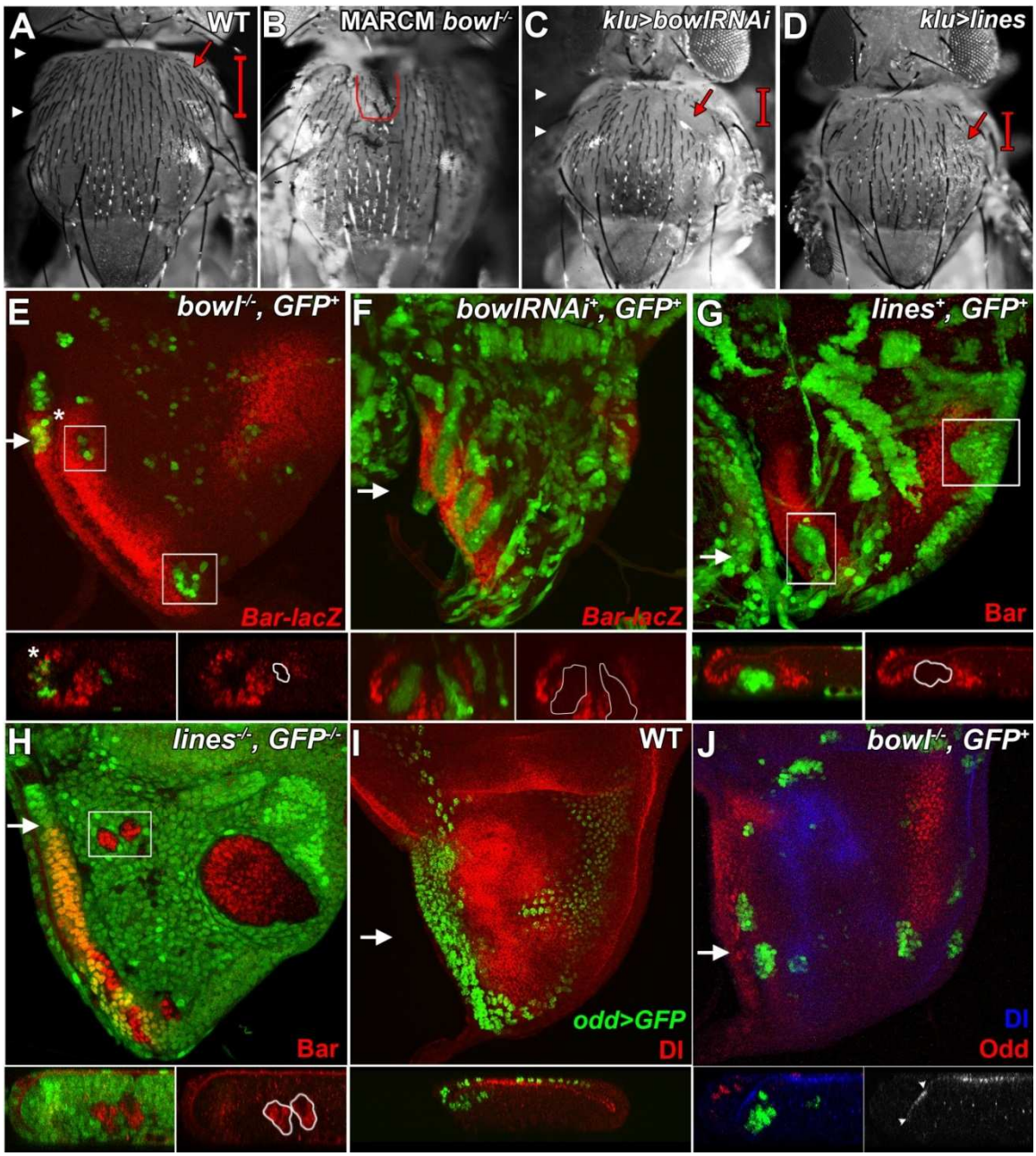

Figure 2.11: bowl specifies the prescutum. (A-D) Dorsal views of adult nota. (A) Wild type; red bracket demarcates prescutum. (B) Anomalies in cuticle differentiation (red outline) were observed in the prescutum of flies bearing *bowl* mutant clones. (C, D) Broad expression of *bowl*RNAi (C) or *lines* (D) with *klu-GAL4* reduced the extent of the prescutum and eliminated lateral microchaete (red arrows). (E-G) *Bar* (shown by *Bar*-lacZ reporter) expression in the

prescutum was lost in *bowl* mutant clones (positively marked, E), in *bowl*RNAi (F), and in *lines* (G) expressing clones. (H) Bar accumulated ectopically in *lines* mutant clones. (I) In control discs, Dl (red) accumulated adjacent to the *odd* domain (green, shown by *odd>GFP*). (J) Dl (blue/white) accumulated ectopically in the prescutum in *bowl* mutant clones (arrowheads delimit ectopic Dl accumulation).

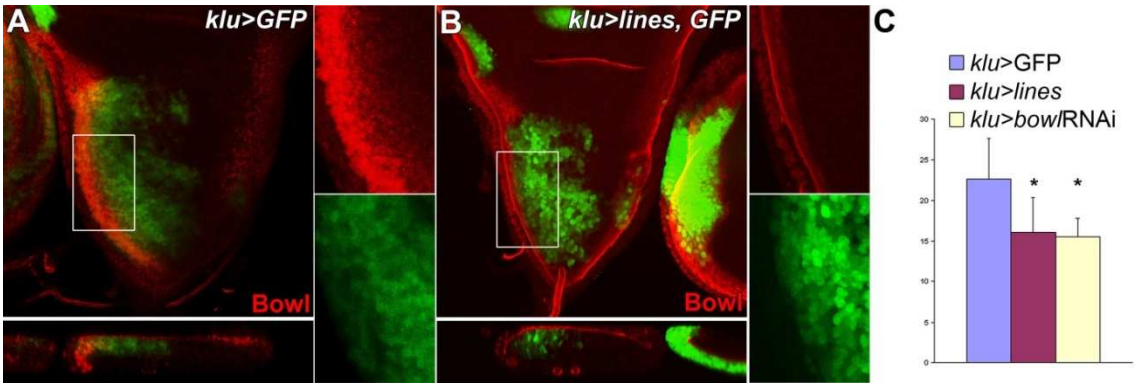

Figure 2.12: Reduction of Bowl expression and the scope of prescutum in klu>lines nota. (A) Quantification of presutum reduction in *klu>lines* and *klu>bowl*RNAi nota compared to wild type. Asterisks indicate significant (p<.001) differences between experimental and control *klu>gfp* nota. (B) Bowl and *klu*-GAL4 (marked by *klu>GFP*) expression overlap in the prescutum. (C) Expression of *lines* with *klu*-GAL4 eliminated Bowl in the prescutum where expression of Bowl and *klu*-GAL4 overlaps.

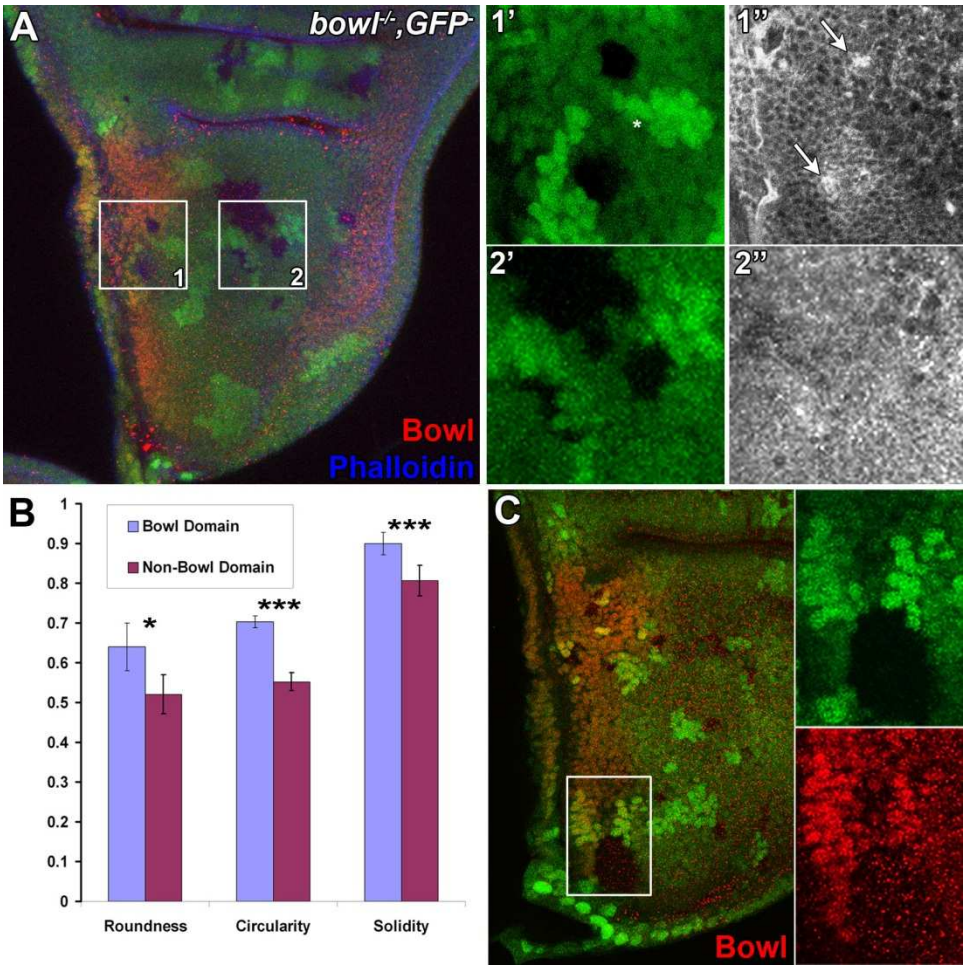

Figure 2.13: bowl clones segregate from the bowl domain. (A-B) *bowl* mutant clones induced at third instar in a wild type background adopted a rounder morphology and tended to segregate from the Bowl domain. (A) Boxed regions show clones inside (box 1) and outside (box 2) the Bowl domain (red). As quantified (B), *bowl* mutant clones within the Bowl domain were significantly rounder ($p<.05$), more circular ($p<.001$), and more compact ($p<.01$) than clones outside the Bowl domain (see section 4.4 for details). Asterisk marks twin spot clone within Bowl domain, which possesses normal morphology. (C) An example of a large composite clone at the edge of the Bowl domain.

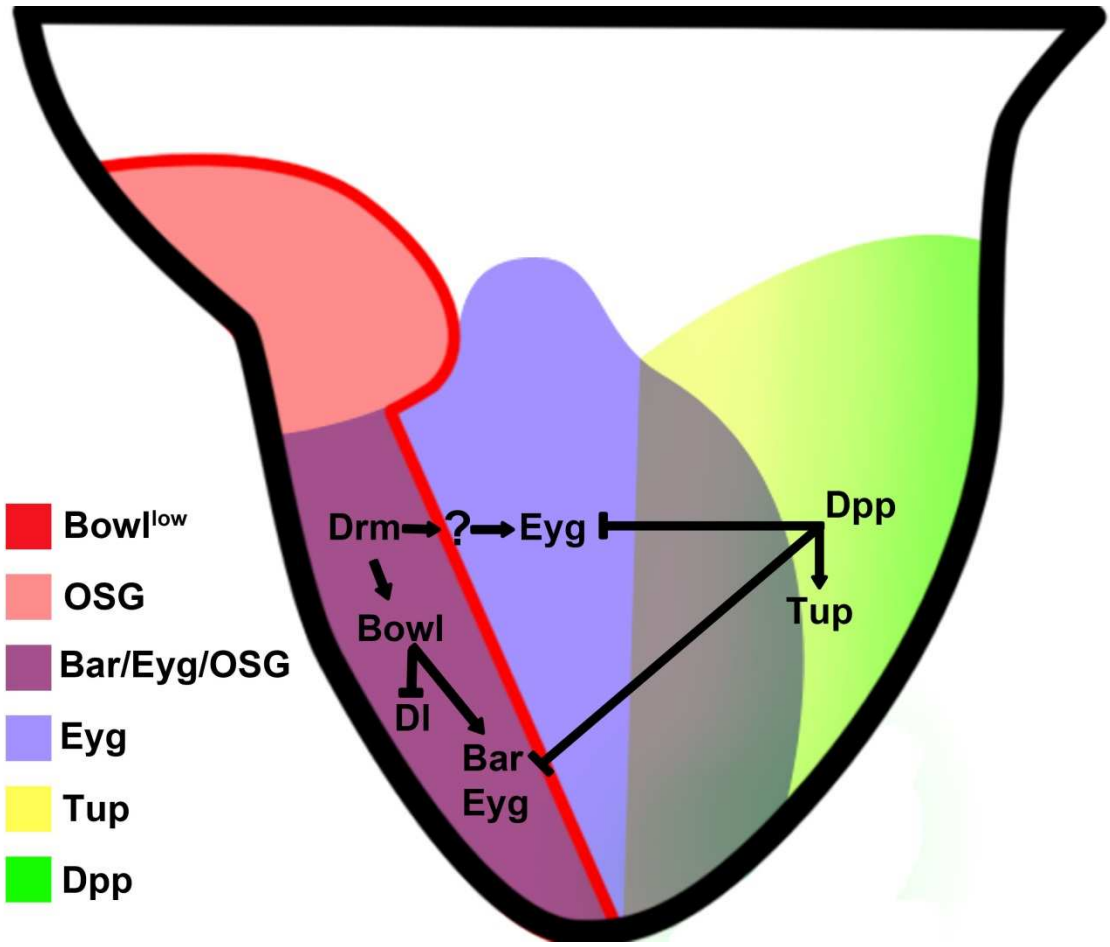

Figure 2.14: Model of the role odd-skipped genes in notum AP patterning. Schematic of notum AP gene expression patterns and regulatory relationships. *odd-skipped* genes are abbreviated OSG. Note that Bar, OSG, and Eyg overlap in the prescutum, and that Dpp and Tup overlap in the posterior notum. Bowl accumulates in a slightly broader domain than *drm* and *odd* in the prescutum. There, Bowl is required autonomously for Eyg accumulation at the first instar, while *drm* acts redundantly with other *odd-skipped* family members to induce Eyg non-autonomously by unknown mechanisms. Further, *odd-skipped* genes autonomously stabilize Bowl in the prescutum to promote Bar and inhibit Dl expression to pattern this region. Dpp diffuses from the posterior to inhibit anterior genes Eyg and Bar [60,289].

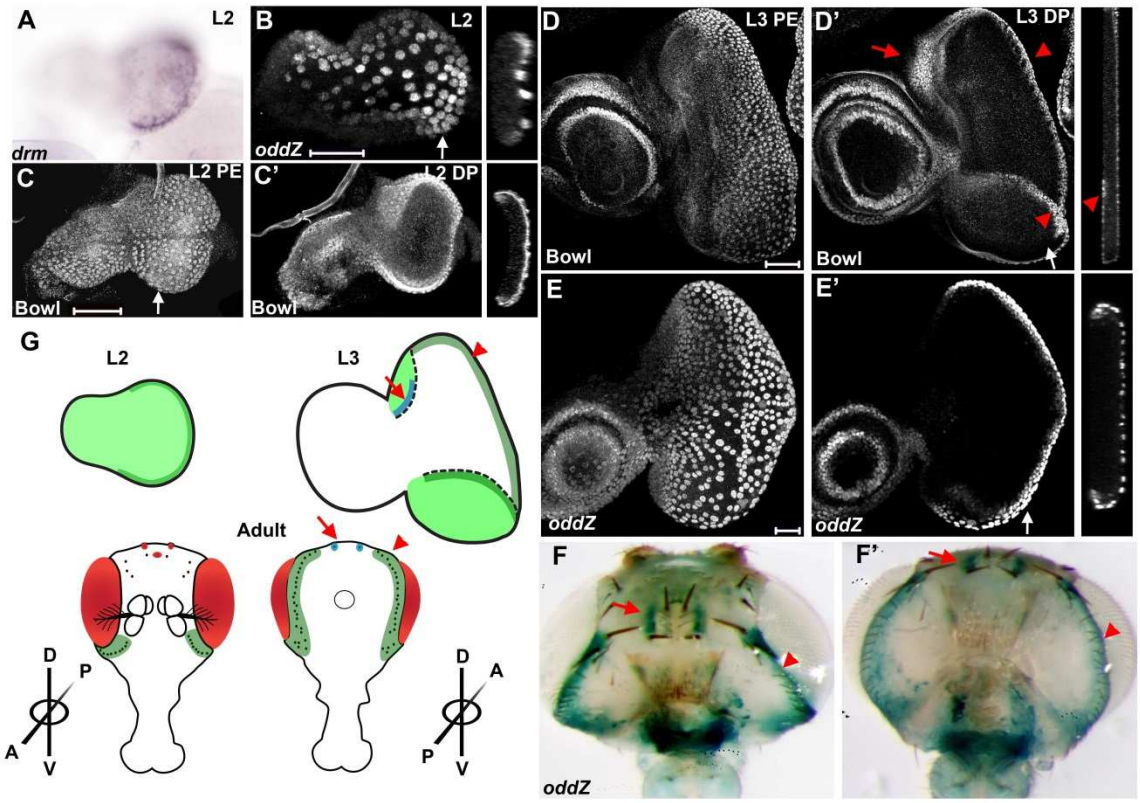

Figure 2.15: Bowl is expressed in PE and margin cells of the eye. (A-C') L2 eye discs (D-D') L3 eye discs. In situ hybridization with probe against *drm* (A), enhancer trap line in *odd* (B) and antibody to Bowl (C-C') reveal early expression of *odd-skipped* family members in the PE (C) and DP margin (C'). (D-D') Bowl continues to accumulate in L3 eye disc PE (D) and margin cells (D', arrowheads) as well as in a patch of ventral cells (D', arrow). (E-F') *odd-lacZ* enhancer trap demonstrates that *odd* expression coincides with Bowl accumulation. (F-F') Activity stain of *odd* enhancer trap in pharate adult head cuticle. Enhancer trap is active in bristled head cuticle (arrowheads) that borders the retinal field, as well as two stripes on the dorsal head that are closely associated with bristles (arrows). (G) Simplified schematic highlighting summarizing *odd-skipped* gene accumulation. Shown are PE (pale green) and margin (dark green) in L2 and L3 discs, and corresponding areas on the adult head cuticle. Detail in the antenna has been published [319], and is omitted for clarity.

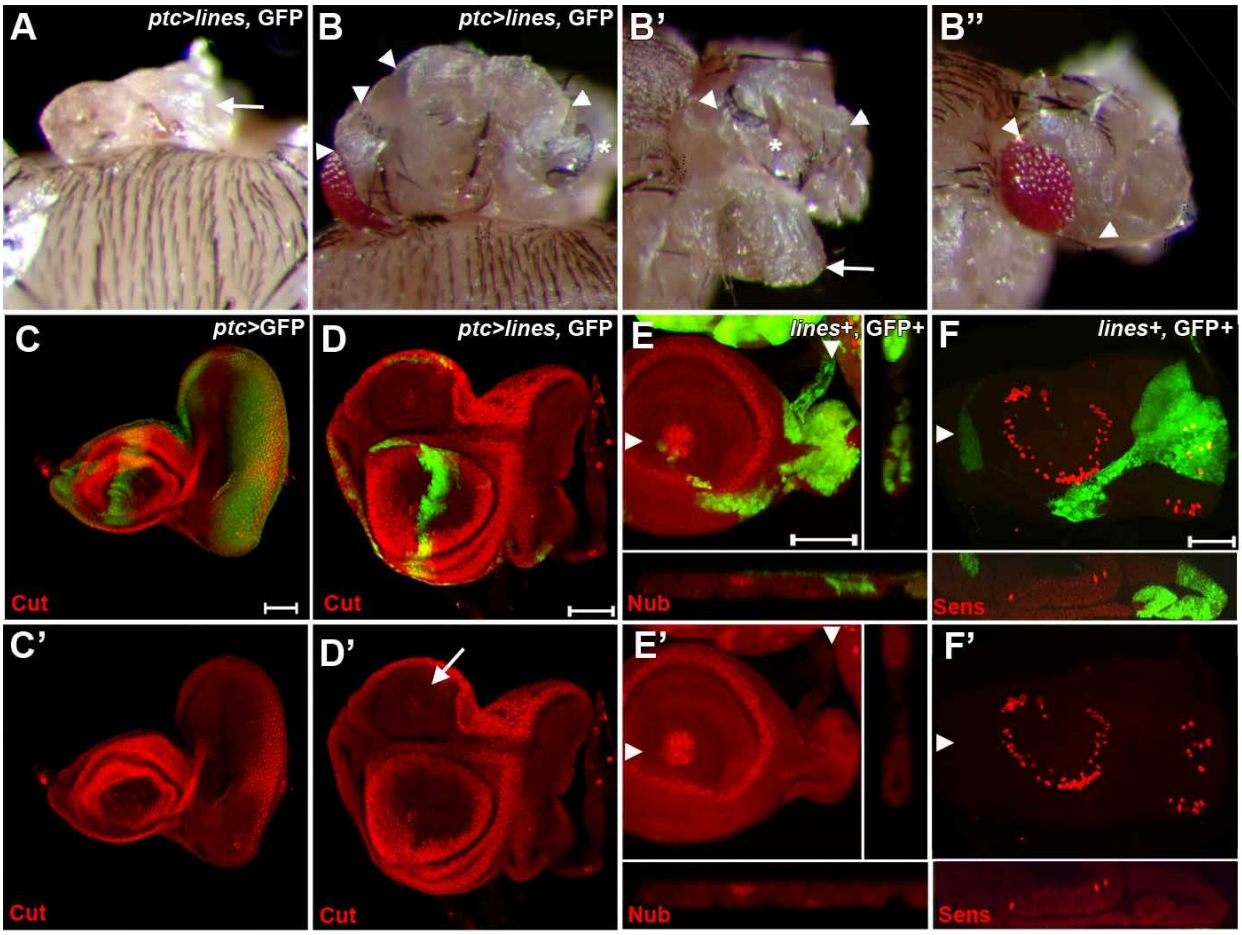

Figure 2.16: Bowl is required for the expansion of the eye field. A-B'' Dorsal (A-B) and lateral (B'-B'') views of pharate *ptc>lin* adults. Larvae were raised at 18^{o} for 7-10 days, and generated a range of phenotypes from a complete loss of eye disc derived structures (A) to a reduction or loss of retinal tissue and antenna (B-B''). Unpatterned cuticle replaced retinal tissue (between arrowheads in B-B''). Arrows mark mouthparts in (A-B'), asterisks mark malformed antenna in (B-B'). (C-D') Third instar larval eye-antenna discs, stained with Cut antibody. In control *ptc>GFP* discs (C-C'), Cut accumulates in a ring pattern in the presumptive antenna, and in retinal cells in the eye field. Expression of *lines* reduced retinal field, and occasionally resulted in the transformation of PE to DP and the induction of an ectopic antenna field (arrow). (E-F')

Expression of *lines* in FLP-out clones transformed the PE into DP and prevented the expansion of the retinal field. Nubbin (F-F') and Sens (G-G') highlight preservation of antennal disc.

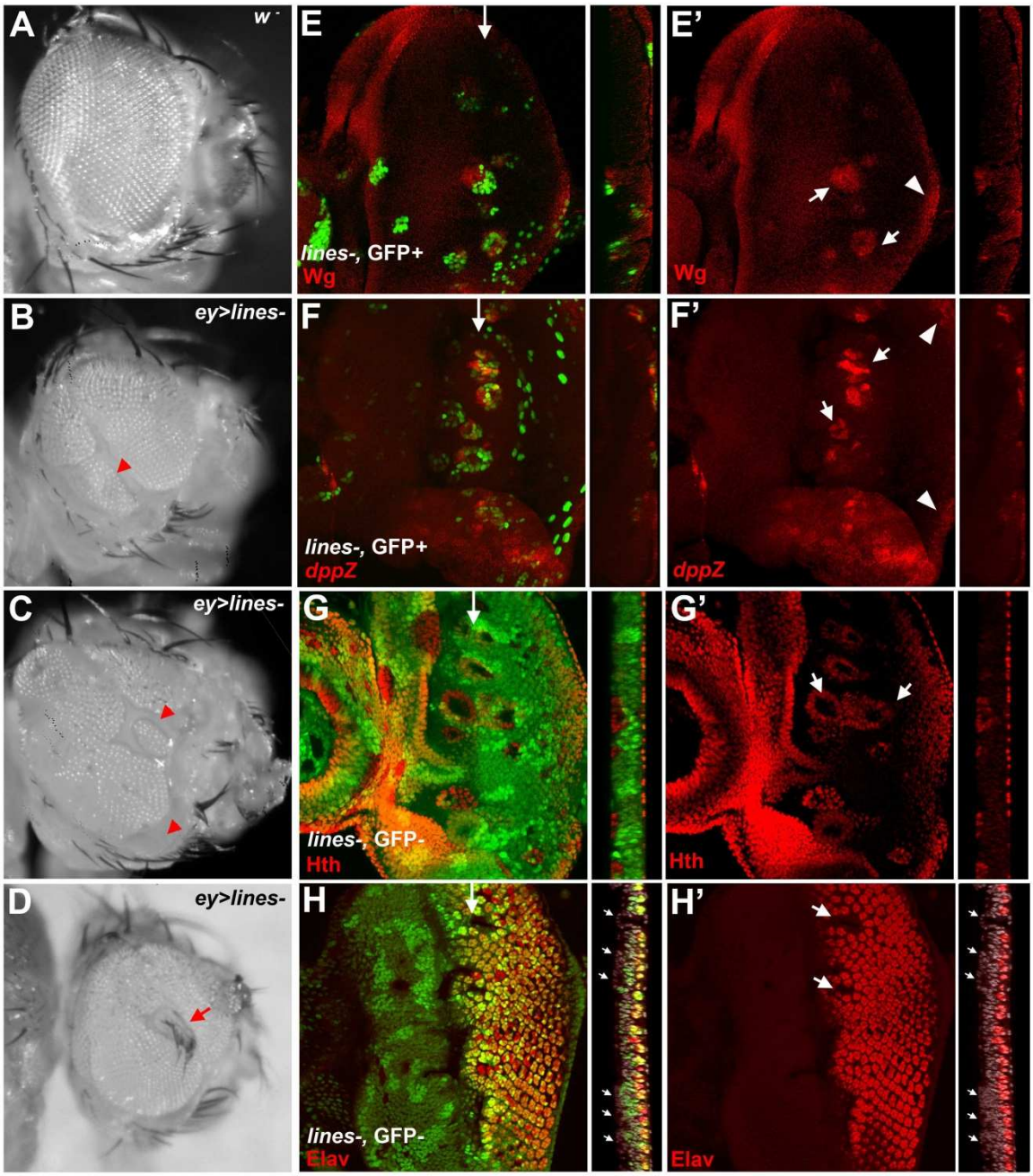

Figure 2.17: Ectopic Bowl accumulation results in cuticle formation, often at the expense of retinal tissue. (A-D) Lateral views of adult heads. (A) Control *w-* eyes consist of an uninterrupted retinal field surrounded by bristled cuticle. (B-D) Eyes bearing unmarked *lines* mutant clones formed ectopic bare cuticle (arrowheads) within (B,C) and around (C) the retinal field.

Additionally, clones resulted in expansion of bristles at the ventral portion of the eye/head cuticle margin (B,C) and ectopic islands of bristled cuticle within the retinal field (D). (E-H') Molecular characterization of L3 eye discs bearing *lines* mutant clones induced from 72-96 hrs. Loss of *lines* in clones (arrows) induced expression of genes required for head cuticle specification, including Wg and Hth (E-E', G-G'). Loss of *lines* also induced a *dpp-lacZ* reporter that normally accumulates in the eye margin (arrowheads, F-F'). (H-H') Loss of *lines* suppressed expression of the retinal differentiation marker elaV in clones anterior to the morphogenetic furrow (arrows).

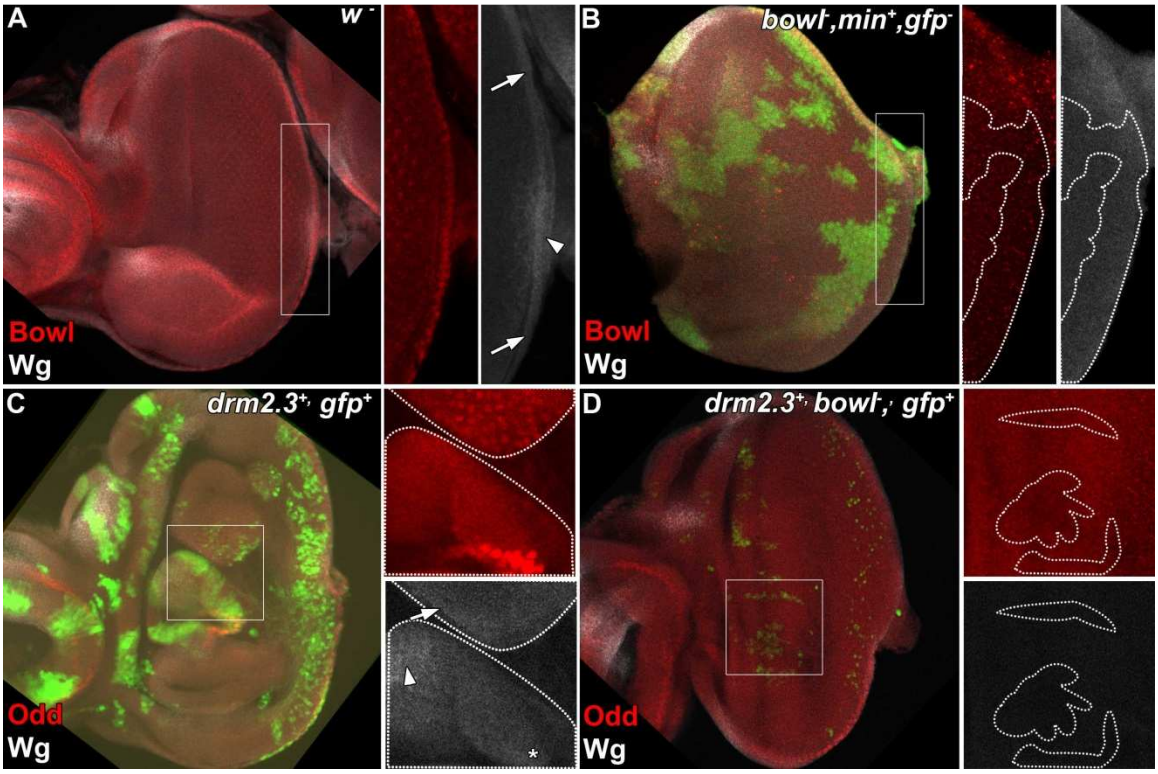

Figure 2.18: *odd-skipped* genes Drm and Bowl regulate the accumulation of Wg at the eye disc margin. (A) Third instar control *w-* eye disc. Bowl (red) and Wg (white) accumulate along the eye disc margin (arrows, inset). Wg accumulates most intensely at the posterior margin, where it accumulates more extensively than Bowl (arrowhead). (B) Loss of Bowl, in *bowl* clones induced in a *minute* background, result in loss of Wg along the disc margin, though not directly adjacent to the posterior margin from where the morphogenetic furrow initiates. (C) Overexpression of Drm in FLP-out clones leads to large clones composed of both Drm overexpressing (green) and non-expressing tissue. Drm expression had a variable effect on Odd and Wg accumulation, with some areas exhibiting ectopic Bowl and Wg accumulation (arrow, inset), while others showed Odd independent Wg accumulation (arrowhead) or Wg independent Odd accumulation (asterisk). (D) Drm overexpressing *bowl* MARCM clones. Both the Drm induced tissue overgrowth and ectopic Odd and Wg induction do not occur in *bowl* mutant clones (green).

Chapter 3

Interplay of contractile and protrusive forces control cell shape in the Drosophila eye

Abstract

Coordinated cell shape changes promote the morphogenesis of many epithelial tissues during development. During processes such as germ-band extension or gastrulation, actomyosin based contractile forces drive cell shape changes through the constriction of cell-cell contacts. The molecular pathways that control the spatial and temporal dynamics of these contractile forces are becoming well understood. By contrast, mechanisms that antagonize such forces to allow for contact maintenance or expansion during morphogenesis are not known. To investigate such mechanisms, we analyzed shape changes of secondary (2°) pigment cells during *Drosophila* eye morphogenesis. As development proceeds, 2° cells dramatically narrow and elongate to adopt a rectangular shape. Normal contact narrowing required localized, pulsed Rho kinase- and MyosinII- associated contractile forces. In contrast to other developmental models, these forces did not eliminate constricting cell contacts. Notably, complementary pulses of branched F-actin appeared to generate protrusive forces that transiently expanded constricting cell contacts. Further, normal contact maintenance and cell shape required the branched F-actin regulators Rac and SCAR. Together, these data suggest that both contractile and protrusive forces regulate cell contact dynamics during shape change. Furthermore, branched F-actin dynamics correlate with levels of phosphatidylinositol 3,4,5-trisphosphate, suggesting that this signal might coordinate contractile and protrusive forces. These data identify a previously unappreciated role for protrusive F-actin dynamics in control of contact length, and suggest that cross-talk between contractile and protrusive force generating pathways regulates cell shape during epithelial morphogenesis.

Introduction

Cell shape changes drive the morphogenesis of many epithelial tissues during development[322,323]. These shape changes emerge from the constriction or expansion of particular cell-cell contacts, and require a high degree of spatiotemporal control over the distribution and dynamics of the force-generating actomyosin cytoskeleton. Studies of *Drosophila* gastrulation and germ-band extension have provided significant insights into the mechanisms by which actomyosin based contractile forces constrict cell-cell contacts. However, in these systems contractility completely eliminates cell-cell contacts[139,173,208], and it remains unclear what molecular pathways and biomechanical forces might oppose actomyosin contractility to maintain or expand cell-cell contacts during cell shape changes.

The Rho family small GTPases are the best characterized regulators of cytoskeletal dynamics. The Rho family member Rho1 plays multiple roles to control contractile actomyosin forces. During cell migration, Rho1 promotes linear F-actin organization and contractile stress fiber formation. Rho activates the downstream Rho kinase (Rock), which in turn phosphorylates the MyoII regulatory light chain to generate contractile forces[324,325]. In epithelial tissues, polarized Rho pathway activation promotes pulsed actomyosin dynamics that drive shape changes during germ-band extension[142,175] and gastrulation[191].

In addition to actomyosin based contractile forces, Rho family GTPases also promote protrusive forces through the synthesis of linear[257,326] and branched[327] F-actin networks. Branched F-actin based networks have been particularly well studied in the context of cell migration, in which they promote protrusive lamellipodia formation to drive motility[327]. These protrusive networks are regulated primarily by the Rho family members Cdc42 and Rac, which

control the downstream effectors WASP and SCAR, respectively[327–330]. These regulators in turn control the activation of the Arp2/3 complex, which directly nucleates F-actin network branching[331]. Interestingly, during polarized cell migration, protrusive branched F-actin networks at the leading edge coordinate with contractile actomyosin arrays at the trailing edge. While similar coordination of contractile and protrusive forces could control contact length during epithelial cell shape changes, such a role has not as yet been studied.

Phosphoinositide signaling provides one potential mechanism to coordinate Rho GTPase family activity levels. The phosphoinositides phospatidylinositol 4,5-bisphosphate (PIP2) or phospatidylinositol 3,4,5-triphosphate (PIP3) can control the localization and activation of a number of Rho family regulatory proteins[210,211]. PIP2 appears to act upstream of the Rho effector Rho kinase (Rock) to stimulate contractile stress fiber formation in cultured cells[332], while PIP3 promotes localized Rac activity during cell migration[220,222]. Conversely, Rho and Rac can both act upstream of PIP2 or PIP3 synthesis, respectively, suggesting multiple levels of interaction between these pathways[221,222,226,333,334].

Phosphoinositide signaling could also coordinate contractile and protrusive cytoskeletal dynamics directly, as PIP2 and PIP3 regulate a number of actin regulatory proteins[335]. In many systems, spatially restricted phosphoinositide signaling regulates cytoskeletal dynamics to promote specific cell behaviors[250,257,336]. Importantly, distinct phosphoinositide species can segregate into distinct membrane domains[137,257,337,338], which could afford a high degree of spatial specificity to cytoskeletal regulation. Taken together, we hypothesized that phosphoinositide signaling might coordinate contractile and protrusive forces by controlling the engagement or disengagement of opposing RhoGTPase and/or cytoskeletal modalities. Further, we hypothesize that the balance of this engagement could serve to tune tension levels with spatial and temporal specificity to control cell shape in a developing epithelium.

To determine whether contractile and protrusive cytoskeletal dynamics coordinately regulate cell contact length during shape change, we have investigated the cell shape changes that drive morphogenesis of the *Drosophila* eye (see detailed description, Chapter 1). In particular, we examined shape changes of secondary cells (2° cells), which dramatically narrow and elongate during development. Elongation occurs by expansion of contacts between 2° cells and primary (1°) cells, and by constriction of contacts between 2° and tertiary (3°) cells. Several studies suggest some degree of coordination of Rho family member activities in the control of apical tension and surface area during pigment cell morphogenesis. Rho1 is required to maintain pigment cell apical tension[339], while Cdc42 inhibits Rho1 pathway activity to limit this tension[340]. Reciprocally, Cdc42 is required to promote endocytosis of AJs, while Rho1 is required to inhibit endocytosis and thereby maintain the integrity of the AJs. This is consistent with a number of systems in which the activity of these family members is mutually antagonistic[241,243,341,342]. Based on the requirement for both pathways to control apical tension, we hypothesized that antagonistic Rho family member activities must coordinate to control contact length and cell shape change.

To test the hypothesis that contractile and protrusive cytoskeletal dynamics coordinate to control cell contact length, we focused on the 2°-3° cell contact, which constricts but is not eliminated during 2° cell elongation. We found that Rho kinase and MyoII enriched at this contact, and were required for normal constriction. Importantly, 2°-3° contact length did not constrict linearly. Rather, contact constriction was interrupted by pulses of contact expansion, which strongly correlated with pulses of PIP3 and branched F-actin. The branched F-actin regulator SCAR accumulated with F-actin at these contacts, and was required for normal pigment cell morphogenesis. Similarly, normal Rac activity was required for protrusive branched dynamics, normal cell shape change, and maintenance of epithelial integrity. Together, we

propose that dynamic PIP3 signaling controls protrusive F-actin dynamics to maintain 2°-3° contact integrity and promote normal pigment cell shape change.

Experimental Design

Immunostaining

Discs were stained as described previously in chapter 2. Antibodies used were rat anti-DCAD2 (DSHB, 1:100), anti-SCAR (DSHB #P1C1 1:5). Phalloidin was stained with rhodamine-phalloidin (Cytoskeleton, Inc #PHDR1 1:150). Secondary antibodies were Jackson ImmunoResearch Alexa647 conjugated anti-rat or Alexa488 conjugated anti-mouse used at 1:100.

Fly Stocks

Fly Lines

The following fly stocks were acquired from the Bloomington Drosophila Stock Center: PH^{GRP1}::GFP (#8163), PH^{PLCD1}::GFP (#39693), UAS-lifeact::ruby (#35545), sqh^{AX3},sqh::GFP (#42234), UAS-Arp3::GFP (#39723),sqh-GFP-rok (#52289), UAS-$Pi3k^{CA}$ (#8294), UAS-$Pi3k^{DN}$ (#8289), GMR-GAL4 (#8121), $SCAR^{\Delta 37}$ FRT40A (#8754),UAS-Rac.N17 (#6292), UAS-Cdc42.N17 (#6288), sqh^{AX3} FRT19A (#25712), $arp3^{83F}$ FRT40A, $arp3^{515FC}$FRT40A. Additional stocks used were: sqh:cherry[188] (Adam Martin), pten[117] FRT40A[25] (Ernst Hafen).

Genetic analyses

Transgenes were expressed broadly in the eye with GMR-GAL4 (Bloomington #8121). FLP-out clones were generated using AyGAL4, UAS-GFP (Bloomington #4411). The FLP/FRT[294] and MARCM[295] techniques were used to generate genetically marked recombinant clones. The stock ubi-RFP, w*, hsFLP122, FRT19A (Bloomington #31418) was used to generate *sqh* mutant clones by FLP/FRT recombination. The stock *yw*hsFLP, UAS-GFP^{nls}, tub-GAL4; tub-GAL80 FRT40A (Gary

Struhl) was used to generate *SCAR* and *arp3* mutant clones by the MARCM technique. In all cases, clones were induced by a one hour heat shock at 37° during late third instar (120-144 hours).

Imaging

Image Acquisition

All data were collected on a Zeiss LSM510 confocal microscope. Live imaging of pupae was conducted according to protocols developed by the Cagan lab[343]. Briefly, pupae were staged from 0APF as white prepupae at 25° in humidified chambers. The head was exposed by removal of the pupal case, and eyes were directly apposed to a coverslip for imaging. Pupae were held in an agarose pad, and imaged inside a humidified chamber. Time series data were typically acquired at two frames/minute in ~6 2uM optical sections.

Image Processing

All image processing was performed using ImageJ. Time series data were registered in the Z dimension by a custom ImageJ macro. Following registration, images were projected by summing the three planes surrounding the level of AJ, marked generally by F-actin or MyoII. Projected images were then registered in the XY plane by the StackReg plugin, and bleach corrected (settings:linear, background determined empirically by measuring in ImageJ).

Image Analysis

Contact dynamics were analyzed by a custom ImageJ macro as follows: Users selected individual cell contacts with a line selection. A membrane mask was then generated: multiple image channels were summed, then smoothed by a Gaussian filter (sigma=2), and segmented by thresholding (settings: Default auto threshold). This mask was used as the basis for contact length measurements as well as to capture mean pixel intensity data. Pixel intensity for each

channel at each time point was normalized to the overall fluorescence intensity of the entire image. Additionally, kymographs were generated by copying the region surrounding the membrane mask (generally 70x20pixels) for each channel and time point. Subsequent analyses were performed using Python, along with packages NumPy and ScipPy. Data were analyzed by Pearson cross correlation (time windows from +/-20 to 30 minutes). Data presented are the average Pearson cross correlations pooled from 6-8 junctions within a single eye, and are presented as the mean R +/- SD. The macro was validated by manual measurement of contact pixel intensities and lengths for a subset of contacts, and compared with automated measurements.

Clone measurements

Clone areas (for *SCAR*$^{\Delta 37}$ and *sqh*^{AX3} clones) and cell contact lengths (for *sqh* ^{AX3} clones) were measured manually in ImageJ. For *SCAR*$^{\Delta 37}$ clones, data are presented as the ratio of the apical area of a mutant cell to its adjacent 1° cell neighbor. Controls were random pairs of wild type cells from within the same field of cells. Both sets of data were compared with two tailed t-tests.

Results

Polarized tension within and between cells drives pigment cell shape change.

Actomyosin based apical tension controls apical cell area in pigment epithelial cells of the *Drosophila* eye[339,340]. However, the contribution of this tension to the dramatic elongation of 2° cells has not been investigated. Polarized tension could contribute to 2° cell elongation by two distinct mechanisms: constriction of the 2°-3° contact could narrow the cell autonomously, while constriction of the 3°-1° contact could promote 2° cell elongation non-autonomously. To test these possibilities, we examined contact lengths in 2° and 3° cells mutant for the Myosin II regulatory light chain, *spaghetti squash* (*sqh*). Loss of *sqh* in 2° cells (see Fig 3.1B,E) caused a

marked increase in the length of 2°-3° contacts (n=12 cells; 247% relative to control cells, $p<.01$), but only a modest increase in length of 2°-1° contacts (n=12 cells; 30.1%, $p<.01$). This suggests that, in 2° cells, tension is higher at the 2°-3° contact than the 2°-1° contact, and is required to narrow the 2° cell.

By contrast, loss of *sqh* in 3° clones yielded a pattern of contact expansion complementary to that seen in 2° cell clones (Fig 3.1C,F). 3°-1° contacts expanded dramatically (n=12 cells; 351%, $p<.01$), while 3°-2° contacts expanded only modestly (n=12 cells; 64.2%, $p<.01$). Thus, the loss of *sqh* in 2° cells resulted in a greater increase in 2°-3° contact length than did loss of *sqh* in the 3° cell ($p<.05$). Interestingly, loss of *sqh* in 3° cells impaired 2° cell elongation, as wild type 2° cells adjacent to mutant 3° cells adopted an isometric shape (Fig 3.1C). These data suggest that tensile forces are differentially polarized within 2° and 3° cells, with each playing a distinct role in 2° cell elongation. High tension within 2° cells at the 3° cell contact is required to narrow 2° cells, while high tension within 3° cells at the 1° cell contact is required for normal elongation of the neighboring 2° cell (Fig 3.1C).

The *sqh* clonal phenotypes suggest that contractile actomyosin networks are activated preferentially along certain cell contacts. To test this idea, we examined accumulation of Rok and MyoII during pigment morphogenesis by live imaging of Rok::GFP and Sqh::Cherry contstructs. Rok and MyoII enriched at constricted 2°-3° contacts, consistent with the polarized constriction of these contacts, as revealed by the analysis of *sqh* mutant clones. Qualitatively, Rok levels correlated with contact constriction (Fig 3.2), while MyoII levels appeared to correlate more variably, depending on the cell contact analyzed (not shown). This suggests that increased Rok and MyoII at the 2°-3° contact may promote and/or stabilize constriction of the 2°-3° contact. Further analyses with higher temporal resolution will be required to determine precisely the relationship between Rok, Sqh, and contact length. However, these studies are

consistent with the hypothesis that polarized actomyosin networks generate anisometric tensile forces that contribute to 2° cell narrowing. Similar anisotropic contractile forces drive shape changes in systems such as germband extension and gastrulation[142,191]. In these cases, however, constricting cell contacts are completely eliminated. During pigment cell morphogenesis, these contacts are maintained in a stably constricted conformation that results in the narrow, elongated morphology of 2° cells.

Branched F-actin networks promote transient contact expansion

As the molecular mechanisms that oppose actomyosin contractility to maintain contact integrity are very poorly understood, we focused our subsequent analyses on pathways that might balance tension at the 2°-3° contact to prevent contact elimination. To begin to characterize the mechanisms that prevent elimination of contractile 2°-3° contacts, we imaged F-actin and MyoII dynamics in developing eyes at 32 hours APF (Fig. 3.3A). As noted, MyoII appeared enriched at the 2°-3° contact, and we observed clear instances where MyoII levels increased at constricting junctions (Fig. 3.2). However, we were unable to detect a consistent relationship between MyoII levels and contact length by Pearson cross correlation analysis (Fig. 3.3B, see discussion). By contrast, F-actin consistently correlated with contact expansion (Fig. 3.3B). This suggests that dynamic F-actin networks, distinct from contractile actomyosin networks, might antagonize MyoII based tension to prevent elimination of 2°-3° contacts.

We hypothesized that these F-actin dynamics represented protrusive branched networks. In motile cells, similar branched networks drive protrusion of leading edge lamellipodia. These dynamics are controlled by localized activation of the small Rho GTPase Rac1, which promotes branched F-actin synthesis through activation of SCAR and the Arp2/3 complex[344]. To test whether the observed F-actin dynamics indeed are composed of branched

networks, we examined the localization and function of SCAR and Arp3, two regulators of branched F-actin synthesis that act downstream of Rac[345]. SCAR co-localized with F-actin at the apico-lateral membrane (Fig. 3.4). SCAR localized to all cell contacts, but was particularly enriched at 2°-3° contacts that exhibited high levels of F-actin accumulation. By contrast, the related protein WASP was more homogenously distributed across the apical surface (not shown). To examine the dynamic regulation of branched F-actin synthesis, we assessed the localization of Arp3, a core component of the Arp2/3 complex, by live imaging of a GFP tagged construct (Fig. 3.5). Similar to SCAR, Arp3 accumulated at most cell contacts (Fig 3.5A). Furthermore, Arp3 levels at 2°-3° cell contacts correlated with both F-actin intensity and contact expansion (Fig. 3.5B). This supports the hypothesis that branched F-actin dynamics correlate with contact expansion.

To determine whether this branched network was required for normal shape change, we examined cells mutant for branched F-actin regulators SCAR and Arp3. As we were unable to recover *arp3* mutant clones in the eye, we focused our analysis on *SCAR* mutant clones. *SCAR* mutant cells exhibited a constricted morphology (Fig. 3.6). Additionally, medioapical F-actin networks organized into more intense foci (Fig. 3.6), which could result from an increase in actomyosin contractility. Apical constriction of *SCAR* mutant cells is seen most clearly in 1° cells, which constricted significantly more than wild type neighbors (Fig 3.6A,D). 2° cell clones preferentially constricted along the 1°-2° contact, causing elongation of the neighboring 3° cell (Fig. 3.6B) or displacement of the adjacent bristle (not shown). We were unable to identify any unambiguous 3° clones (n=3 eyes, 46 1° clones, 20 2° clones, 0 3° clones). Loss of 3° cell clones could be consistent with a preferential requirement for SCAR in 3° cells to maintain 2°-3° contacts, complementary to the role of MyoII in 2° cells to constrict this contact. However, one class of apparent 2° cell clones exhibited an elongated morphology that formed inappropriate

2°-2° cell contacts (Fig. 3.6C). As yet we cannot rule out the possibility that these cells are in fact mutant 3° cells that have stretched to fill both the 3° and the missing 2° niche. Live imaging of *SCAR* mutant cells will be required to resolve this ambiguity. Together, these data are consistent with the hypothesis that SCAR and branched F-actin are required to promote branched F-actin dynamics to balance actomyosin based apical tension.

To further characterize the requirement for branched F-actin dynamics to antagonize contractile forces during shape change, we disrupted normal Rac signaling by overexpression of a dominant negative form of Rac (Rac^{DN}) broadly in the eye, and analyzed cell contact dynamics in relation to F-actin and MyoII dynamics (Fig. 3.7). Rac^{DN} caused a frequent loss of 2°-3° contacts, which resulted in aberrant contact between 1° cells from neighboring ommatidia. At the molecular level, Rac^{DN} caused a dramatic increase in F-actin and MyoII colocalization, and disrupted the normal correlation between pulsed F-actin and contact expansion (shown qualitatively in Fig. 3.8). In contrast to normal eyes, in which pulses of F-actin coincide with phases of contact expansion, we identified numerous instances in which F-actin associated instead with MyoII in intense, localized foci that constricted and completely eliminated the 2°-3° contact (see insets, Fig. 3.7). These observations suggest that Rac activity is required to promote normal protrusive dynamics to control the balance of contractile and protrusive forces required to maintain 2°-3° contacts during constriction.

In addition to defects in contact maintenance, Rac^{DN} also caused a defect in contact constriction. 2°-3° contacts frequently adopted an expanded morphology with low levels of F-actin and MyoII across the contact. Contact constriction proceeded only when actomyosin intensity increased along the contact (see kymograph, Fig 3.7). This could reflect a requirement for Rac in controlling the coupling of contractile networks to AJs, or could suggest that contractile forces must be balanced to prevent excessive tension from spontaneously

disassembling contractile networks[346] (see Discussion). These observations suggest that Rac may be further required to control physiological levels of contractile force generation.

Phosphoinositide signaling correlates with contact length dynamics

The complementary requirements of contractile and protrusive networks at the 2°-3° contact suggest the existence of some mechanism to coordinate these opposing molecular dynamics. In a host of morphogenetic processes, spatially restricted phosphoinositide signaling directly or indirectly regulates polarized and dynamic F-actin behaviors [137,179,257]. We hypothesized that dynamic phosphoinositide signaling might balance the relative contribution of contractile and protrusive networks to control 2°-3° contact length. To begin to test this hypothesis, we analyzed the abundance of key phosphoinositide species PIP3 and PIP2 at the plasma membrane by live imaging of fluorescently tagged PH domains specific to each phosphoinositide. Both species appeared enriched at 2°-3° cell contacts relative to 1°-2° contacts (Figs. 3.8,3.9). PIP3 levels oscillated at 2°-3° contacts, and correlated strongly with contact expansion. Qualitatively, PIP3 pulses were observed at single contacts within a cell as well as multiple contacts simultaneously, though it is yet to be determined whether these pulses coordinate spatially or temporally. Though pulses were largely restricted to 2°-3° contacts, occasionally a PIP3 pulse would 'spread' to adjacent 1°-2° or 1°-3° contacts (not shown). Importantly, PIP3 levels correlated strongly with contact length and F-actin (Fig. 3.8B,C), suggesting a possible role for PIP3 in detecting and balancing tension by promoting expansion of 2°-3° contacts. Though PIP2 also appeared to be enriched at 2°-3° contacts (Fig. 3.9A), PIP2 levels remained relatively constant and did not correlate with contact length (Fig. 3.9B).

The dynamics of PIP3 and F-actin accumulation and contact expansion suggest that contractile forces might engage PIP3 signaling and F-actin dynamics to promote contact

expansion. The Rho GTPase Cdc42 inhibits Rho1 pathway activity to limit apical tension in pigment epithelial cells[340]. To test the hypothesis that tension induces PIP3 signaling as a form of negative feedback, we overexpressed a dominant negative Cdc42 ($Cdc42^{DN}$) in the eye to increase Rho mediated actomyosin tension. In $Cdc42^{DN}$ discs, PIP3 and F-actin pulses were observed more broadly than in controls, at both 2°-3° and 2°-1° contacts (Fig. 3.10). This observation is consistent with the hypothesis that tension can promote PIP3 activity and F-actin dynamics. Additional studies will be required to assess the magnitude and frequency of this activation, and to determine more rigorously whether and how tension activates PIP3 and F-actin dynamics.

To investigate whether phosphoinositide signaling is required for normal pigment cell morphogenesis, we utilized constitutively active or dominant negative forms of the key enzyme that mediates the synthesis of PIP3 from PIP2, Pi3k. We expressed Pi3k variants either broadly (Fig 3.11A,B) or in patches of cells (Fig 3.11C,D) to enhance or inhibit PIP3 production, respectively, and examined cell morphology at 40hr APF. In both experiments, the shape of experimental cells was not noticeably altered. However, PIP3 levels still appeared polarized (Fig 3.11A,B), suggesting that these manipulations may not be sufficient to abolish normal PIP3 signaling. As an alternative approach to elevate PIP3 levels, we also examined cell shape in 40hr APF eyes bearing *pten* mutant clones. Large patches of *pten* clones were associated with a variety of defects in ommatidial morphology, including missing cells, misplaced cells, and extra cells. However, single isolated clones appeared normal (Fig 3.11C), as was the case for $Pi3k^{CA}$ (not shown) and $Pi3k^{DN}$ clones (Fig. 3.11D). Further experiments will be required to determine whether PIP3 signaling is indeed required for normal shape or shape change dynamics.

Discussion

The shape changes that drive the morphogenesis of many epithelial tissues require a remarkable degree of control over biophysical force generation. At the level of a single cell, actomyosin tension must be regulated with spatial and temporal specificity to control polarized behaviors such as contact length change, cell intercalation, and migration[171,177,191]. While many of the molecular pathways that drive contractile actomyosin dynamics are known, the mechanisms that antagonize these pathways to fine tune tension remained unstudied.

We investigated this question in the developing *Drosophila* eye, which undergoes an elaborate series of shape changes to generate a remarkably regular hexagonal lattice composed of pigment epithelial cells[267]. Here, we showed that tension is polarized in the developing eye, and is required for normal cell shape (Figs 3.1-3.2). Importantly, this polarized tension is opposed by dynamic pulses of branched F-actin (Figs 3.3, 3.4, 3.5), and disruption of branched F-actin networks by inhibition of Rac (Fig 3.7) or *SCAR* (Fig 3.6) disrupted normal cell shape and contact maintenance during constriction. Finally, we showed that PIP3 strongly correlates with these protrusive F-actin dynamics (Figs 3.8-3.11). These data establish that protrusive branched F-actin networks antagonize contractile actomyosin forces to control contact length during pigment cell shape change, and suggest one mechanism to fine tune biomechanical force generation during epithelial morphogenesis.

Autonomous and non-autonomous contractile forces contribute to 2° cell elongation

Our data indicate cell-type specific roles for actomyosin contractile forces in shaping the pigment epithelium. Previous modeling[109,347] and experimental work[339,340] suggest that tensile forces are required generally for normal morphology, but did not specifically characterize how these forces determine the specific cell shapes found in the *Drosophila* eye. Our work identifies

cell type specific, subcellular patterns of contractile force generation. Our analysis of *sqh* mutant clones (Fig. 3.1) suggest that an unexpected combination of autonomous and non-autonomous force generation by 2° and 3° cells, respectively, contribute to 2° cell elongation and ommatidial patterning. Other modeling work suggests that expansion of 1° cells plays a role in ommatidial morphology[135]. However, our data are not consistent with such a role for 1° cells. Though loss of *SCAR* caused constriction of 1° cells (Fig. 3.6), it did not alter the shape of neighboring 2° or 3° cells. By contrast, expansion of *sqh* 2° cell clones caused a dramatic compression of adjacent 1° cells. Together, these data suggest that polarized actomyosin tension in both 2° and 3° cells primarily determines ommatidial morphology, and that 1° cells more passively respond to this tension.

The observed tension polarity suggests a far more specific role of actomyosin contractility in the control of pigment cell shape than previously described. The Longmore lab reported that a balance of Rho and Cdc42 signaling is required generally to control apical tension and surface area, but did not examine any spatially or temporally specific roles for these pathways in the control of shape changes such as 2° cell elongation. Specifically, the Longmore lab proposed that a Cdc42/Par-6/aPKC complex inhibits Rho pathway activity generally in the pigment epithelium. We found that expression of $Cdc42^{DN}$ disrupted the molecular polarization of pigment epithelial cells (Fig 3.10). To integrate our findings with the Cdc42/Par-6/aPKC model, we hypothesize that the activity of the Cdc42/Par-6/aPKC complex is polarized to 1°-2° contacts, to reduce tension and promote expansion of these contacts. The absence of this complex would then allow high levels of Rho activity and actomyosin tension to drive 2°-3° contact constriction. While it remains to be tested whether Cdc42, Par-6, or aPKC are polarized, this model could enhance our understanding of the molecular basis for biomechanical force polarization during cell shape change.

In addition to being spatially polarized, actomyosin contractility was temporally dynamic. 2°-3° contact constriction occurred by transient pulses of constriction and contact expansion. This is consistent with shape changes in other systems, in which pulsed cell behaviors drive tissue level behaviors such as germ-band extension and gastrulation[142,188,200]. We qualitatively observed pulses of MyoII and Rok at 2°-3°, and these pulses appeared to correspond to pulses of contact constriction. In contrast to other systems[142,188,200], constriction of 2°-3° contacts does not eliminate these contacts, but results in the acquisition of a stably constricted 2°-3° morphology. As such, pigment epithelial morphogenesis could serve as a novel model to understand the role of cytoskeletal forces in the acquisition of stable cell morphologies. This is an intriguing question, as contractile forces must be polarized, as during transient shape changes, but they must be modulated to prevent the inappropriate elimination of cell contacts.

Here we describe the first instance of regulated, pulsed contact expansion. Whereas previous models suggested that contact expansion is a passive process that results from relief of contractility, here we show that pulses of PIP3 and branched F-actin dynamics correlated with pulses of contact expansion during constriction. This is the first description of protrusive F-actin dynamics acting antagonistically to contractile forces during pulsed constrictions. We propose that these antagonistic dynamics fine tune tension and allow for the controlled constriction of 2°-3° contacts while maintaining contact integrity (see summary Fig 3.12).

Branched F-actin dynamics could promote expansion by a number of mechanisms. Branched F-actin could provide a mechanical pushing force to promote expansion of the contact, similar to that observed *in vitro* during *de novo* formation of AJ[134]. Additionally, it is possible that such networks could antagonize local actomyosin tension, either by altering engagement of the contractile apparatus to AJ[199] or by disrupting the contractile apparatus

itself. The timescale of contact dynamics in most cases is consistent with a viscous response of the underlying actomyosin network, and it is possible that network remodeling alters the stiffness or viscosity of the apical domain to modulate morphological responses to changes in cortical tension[168].

Role of pulsed contractile and protrusive dynamics in eye morphogenesis

It will be important to determine whether and how contractile forces coordinate with protrusive forces during shape change (See summary, Fig 3.12C). Several mechanisms could control pathway oscillations to fine tune the biomechanical forces exerted on cell contacts: Positive feedback within the contractile pathway, between PIP2 and Rho pathway activity[177,348], or between tension and MyoII[208], could ensure robust contractile forces. Likewise, positive feedback in the protrusive pathway between Rac and Pi3k[333,336,349] could ensure robust protrusive force generation. Several mechanisms could then mediate interplay between these pathways. High levels of tension could induce PIP3, as suggested by the finding that $Cdc42^{DN}$ leads to broad PIP3 accumulation (Fig. 3.10). Reciprocally, PIP3 could recruit or activate Rok at a high threshold[137] to link protrusion to contractile force generation. Additional studies will be required to test these pathway interactions, but in principle such a model could provide novel insights into the coordination both of antagonistic Rho family member activities and of biomechanical forces.

It will also be important to determine whether and how these oscillations contribute to normal eye morphogenesis at the tissue level. Contact length oscillations could allow cells to coordinate shapes amongst groups of cells. This coordination could ensure that the cells of an epithelium experience similar mechanical forces to achieve an overall energy minimum. Though prevailing models of epithelial topology suggest that final morphology represents a minimal

interfacial energy state[77,136,347], the acquisition of that morphology must pass through energetically unfavorable states[172]. Contact oscillations could allow individual cell contacts to sense and respond to the overall tension landscape of the epithelium and achieve an energy minimum that is consistent with the molecular patterning of the tissue, particularly with respect to the distribution of adhesion molecules[108]. It is clear that both adherens junctions[165,182,204,350,351] and MyoII[208,352] are responsive to tension, supporting a mechanism for such coordination. Mechanical coordination of cell shapes could provide an intriguing mechanism by which epithelia robustly acquire a consistent morphology, such as that seen in the crystalline lattice of the *Drosophila* eye.

Hypothetical roles for phosphoinositide signaling in eye morphogenesis

As yet, the functional contribution of PIP3 dynamics at the 2°-3° contact remains unclear. A recent study determined that PIP3 correlates with Rok/MyoII accumulation and junction constriction[137]. By contrast, our work suggests that PIP3 correlates with branched F-actin synthesis and contact expansion. In both cases, the precise mechanism by which PIP3 mediates the downstream cytoskeletal dynamics is yet to be determined. There are a number of important differences between these two systems that could account for the presumed different roles of phosphoinositide signaling. While AJ are relatively homogenous in the wing, they are sharply polarized in the eye. The Neph1/Nephrin homologues Hibris and Roughest are differentially expressed between 1° and 2°/3° cells[108]. Interactions between these molecules could independently recruit phosphoinositide or cytoskeletal regulators that could alter the functional output of dynamic phosphoinositide signaling. The potentially contrasting roles of PIP3 between the wing and the eye could help to determine precisely how phosphoinositide dynamics are coupled to cytoskeletal dynamics during epithelial morphogenesis.

Though I was unable to detect phenotypes following manipulation of phosphoinositide signaling, I examined only terminal phenotypes, and the manipulations used may not have sufficiently abrogated phosphoinositide signaling (Fig. 3.10). Loss of PTEN could hypothetically be overcome through engagement of an alternative phosphatase. During cell migration in Dictyostelium, PTEN is the primary phosphatase that mediates PIP3 polarization, while in mammalian cells, the 5' phosphatase SHIP1 fulfills this function[218,354]. *Drosophila* possesses a 5' phosphatase Synaptojanin, though thus far described roles for this protein are limited to the synapse[355,356]. Generally speaking, these molecules could function in one of several ways. They could act at 1°-2° contacts to restrict PIP3 accumulation to the 2°-3° contact to enhance spatial resolution of phosphoinositide signaling. Additionally, they could act generally as a ligand sink, to improve temporal resolution of PIP3 signaling. Alternatively, they could more specifically be recruited to the 2°-3° contact, either as negative feedback to PI3k activity or to potentiate Rho activity.

Another possibility is that phosphoinositide signaling provides a spatial cue to coordinate downstream Rho family or cytoskeletal dynamics (Table 3.1). This is consistent with the strong correlation between PIP3 and F-actin during contact expansion. It is important to note, however, that phosphoinositide signaling correlates strongly with a number of dynamic processes for which it is required only for normal efficiency. Though PIP3 is sufficient to induce polarized migration in neutrophils, it is not strictly required for migration. Nor is PIP3 required for epithelial sheet movement in *Drosophila* dorsal closure, despite the fact that it localizes to the leading edge and directs F-actin dynamics there[257]. In each case, however, alterations in phosphoinositide levels altered the speed or persistence of the behavior in question. These data suggest a facilitative role for PIP3 or phosphoinositide dynamics in polarized cell behaviors. Such a role is supported by its rich network of interactions with an immense range of cytoskeletal and

Rho GTPase pathway regulators, though it is perhaps surprising that this dense network does not contribute to more severe morphological defects following inhibition or activation of pathway activity. It is worth noting that some downstream components, particularly the RhoGTPases, exhibit their own cross regulatory interactions, and can feed back directly to phosphoinositide signaling. Further studies will be required to determine whether these or other qualities contribute to the robust nature of these morphogenetic processes.

Acknowledgements

We thank Ernst Hafen, Ross Cagan, and Tom Millard, the Bloomington Stock Center, and the Developmental Studies Hybridoma bank for stocks and reagents, and Rodrigo Cilla-Ugarte for assistance at various points in the analysis of imaging data.

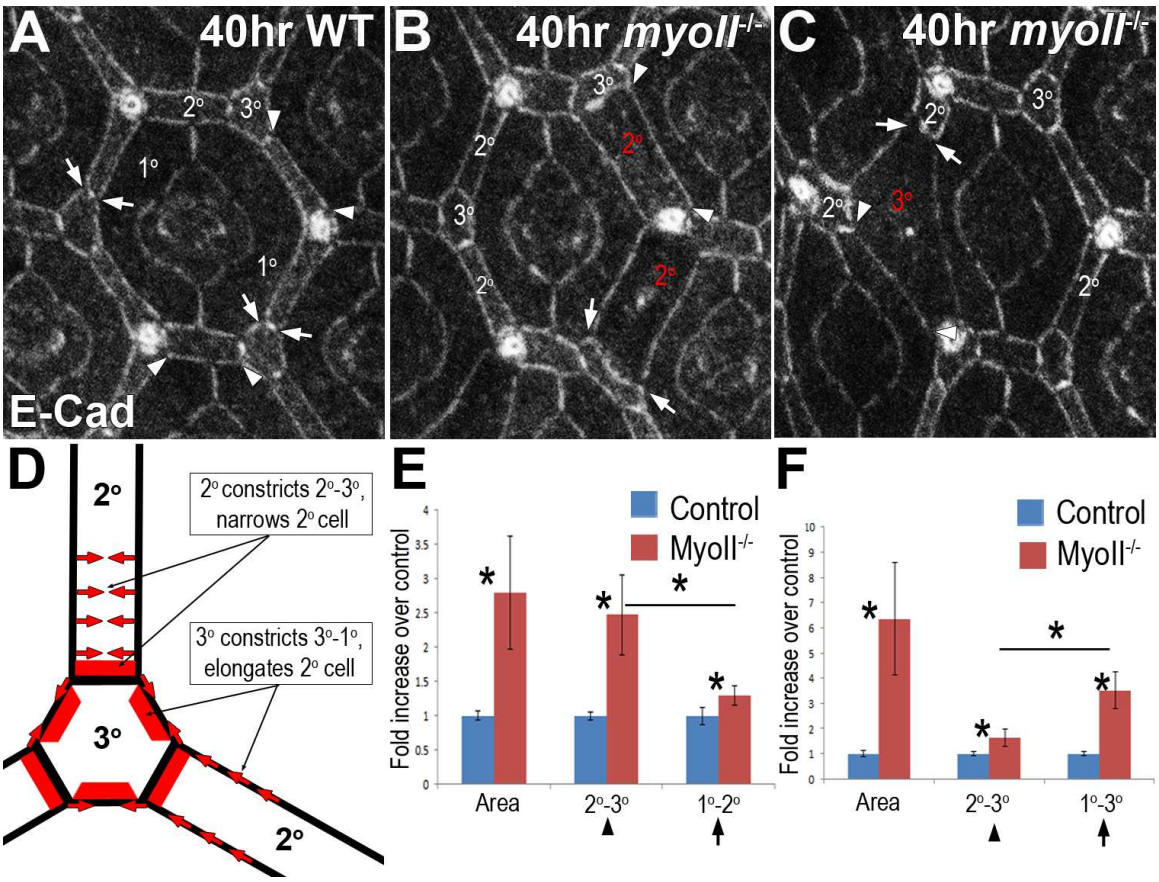

Figure 3.1: Sqh is required for normal pigment cell morphogenesis. (A) 40hr APF eye disc showing normal cell shapes. 2° cells are elongated, with expanded 2°-1° contacts (demarcated by arrowheads) and constricted 2°-3° contacts (demarcated by arrows). (B-C) 40hr eye bearing *sqh* mutant clones (marked by red text). (B) 2° sqh mutant cells, preferentially expanded 2°-3° contacts (quantified in E). (C) 3° *sqh* mutant cells preferentially expanded 1°-3° cell contacts (quantified in F). (D) Summary of contractile forces suggested by *sqh* mutant analysis. Red bars indicate polarized tension; arrows indicate apparent cell shape deformation. Tension is high in 2° cells at the 2°-3° contact, and causes constriction there to narrow the 2° cell (upper left). Tension is high in 3° cells at the 3°-1° contact to constrict this contact and cause non-autonomous expansion of the 2°-1° contact (lower right).

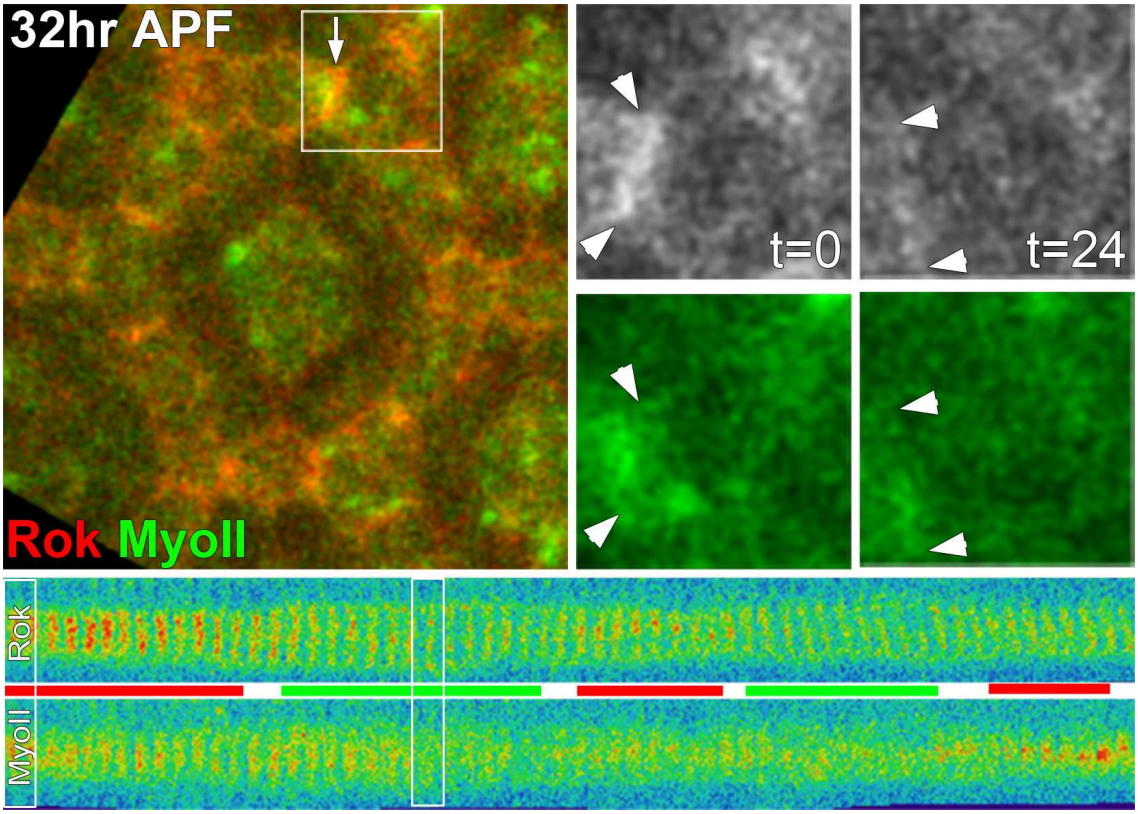

Figure 3.2: Rok levels appear to dynamically enrich in constricting contacts. 32hr APF eye expressing Rok::GFP (red, white inset) and Sqh::mCherry (green). Both Rok and Sqh appear enriched at constricted 2°-3° cell contacts. Inset shows two contacts at frame 0, when contacts are constricted, and frame 24, when contacts are expanded. Arrowhead demarcates length of contact shown in kymograph. Kymograph reveals apparent dynamic enrichment of both Rok and Sqh at constricting junctions. In this and all subsequent kymographs, phases of constriction are marked with red bars, phases of expansion are marked with green bars, and frames shown in inset are shown in boxed region.

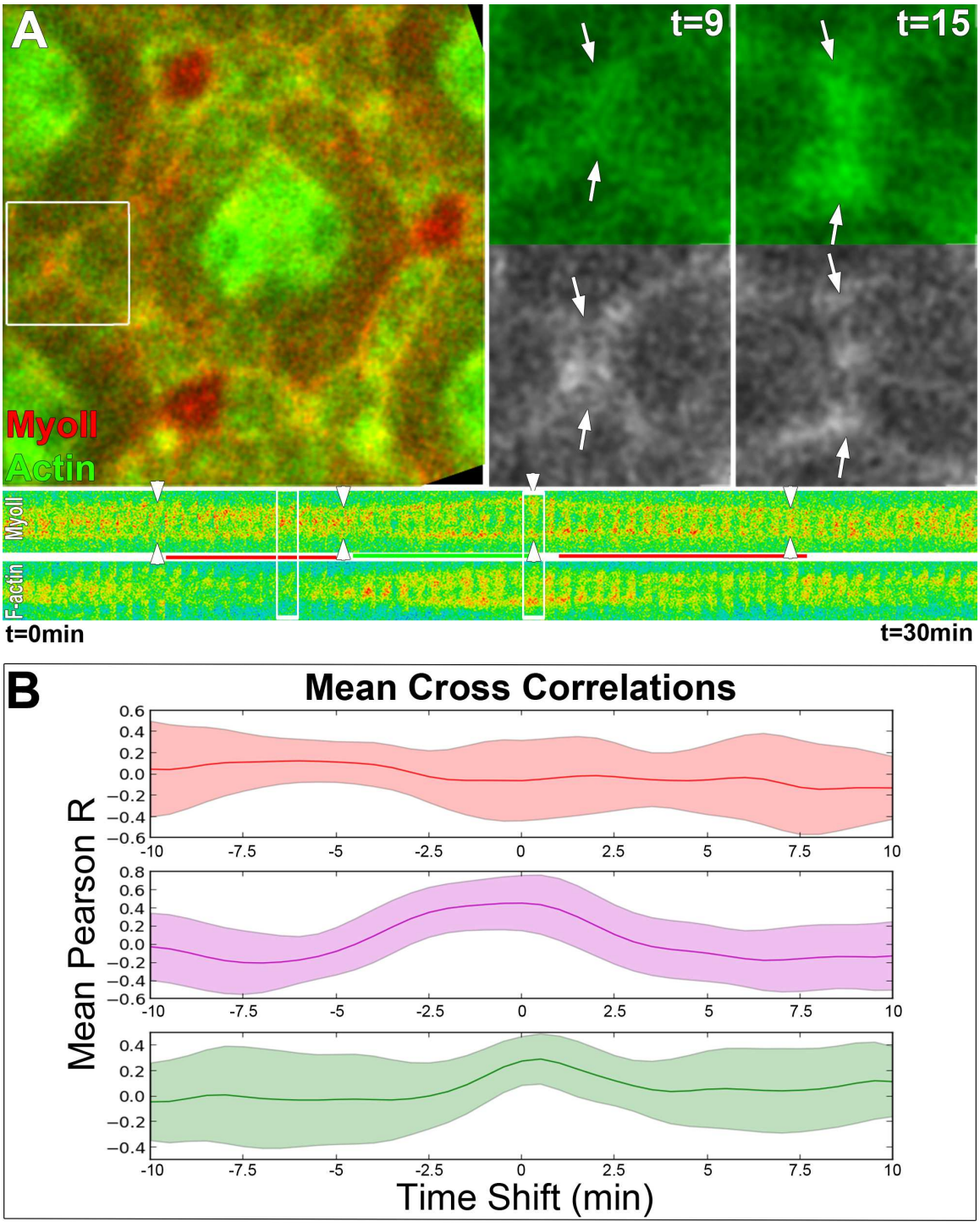

Figure 3.3: F-actin pulses correlate with contact expansion. (A) 32hr APF pupal eye expressing Sqh::GFP (MyoII, red) and lifeact::ruby (Actin, green). MyoII and F-actin localized to cell contacts and to the apical membrane domain. F-actin transiently enriched at 2°-3° cell contacts (insets) in

pulses that correlated with contact length expansion (contact length demarcated by arrows; see cross correlations in B). By contrast, MyoII did not correlate with fluctuations in contact length.

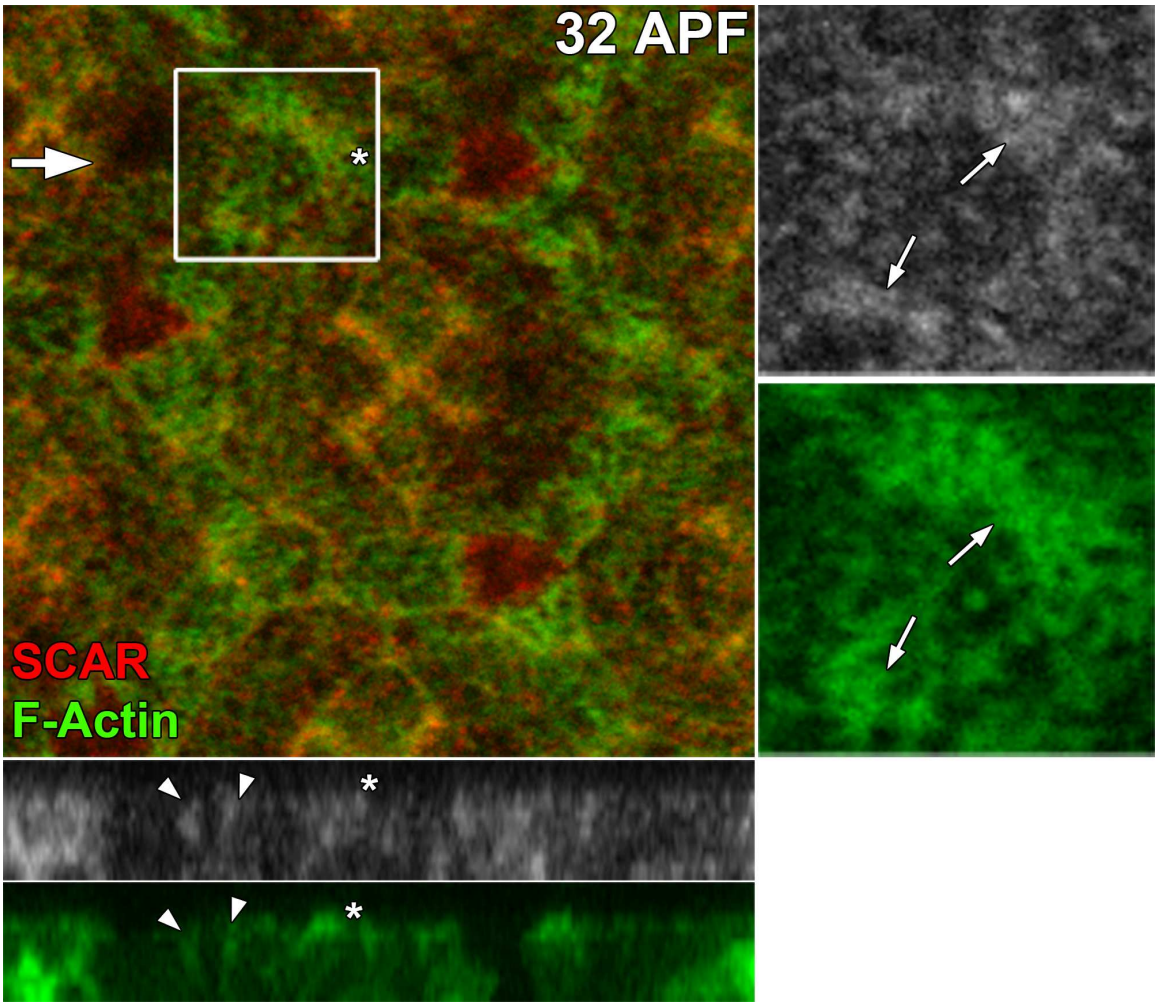

Figure 3.4: SCAR colocalizes with F-actin at the apico-lateral surface of cell contacts. Fixed 32hr pupal eye expressing lifeact::Ruby (green) and stained for SCAR (red). SCAR and F-actin co-localized at cell contacts (arrows, inset). In particular, SCAR enriched in the apico-lateral region, marked by F-actin (see Z sections, plane marked by arrow in main panel). Foci of SCAR are particularly obvious at cone-cone, cone-1°, and 1°-2° contacts (arrowheads), by contrast, accumulation at 2°-3° contacts is more diffuse (asterisk in Z, arrows inset).

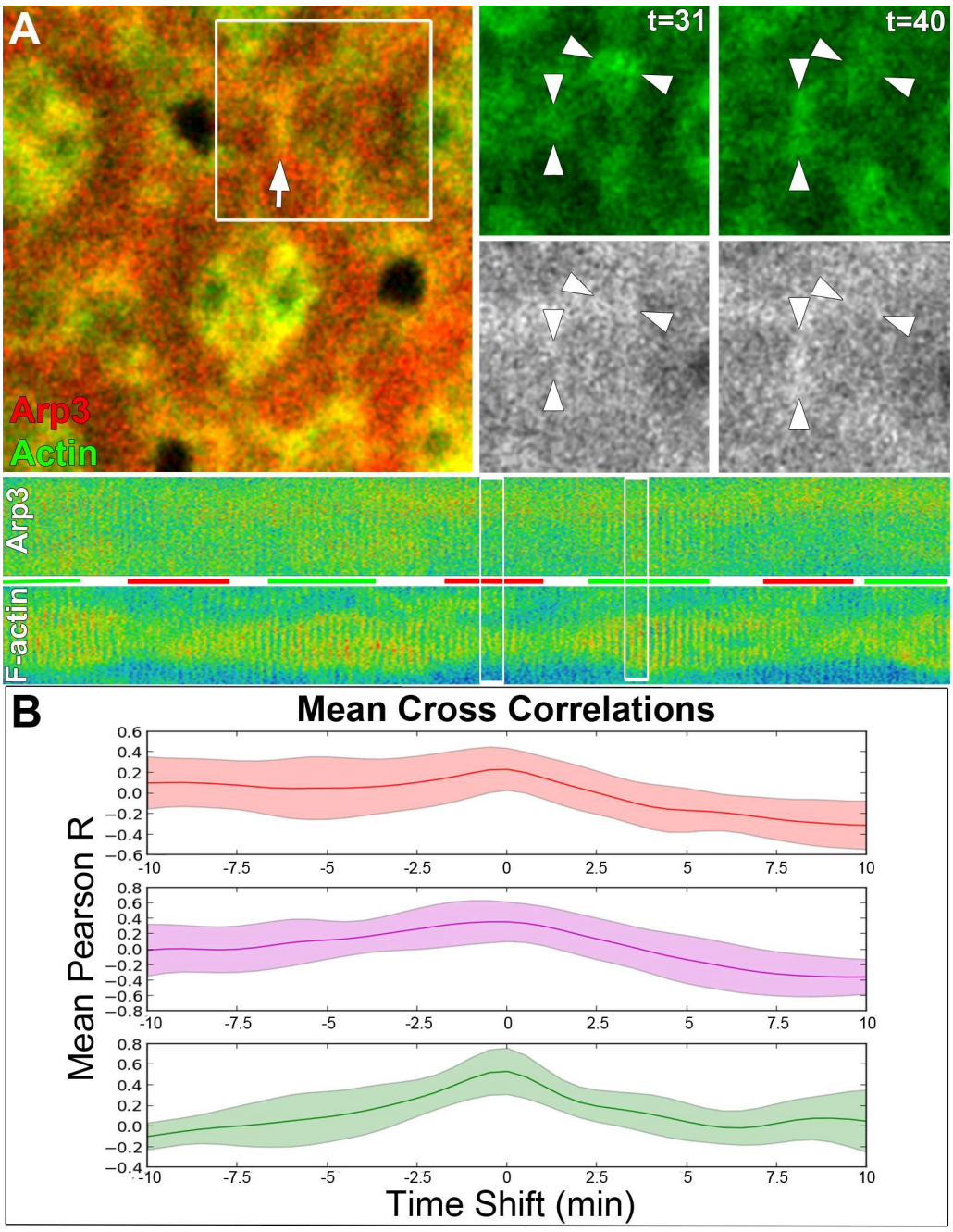

Figure 3.5: Arp3 and F-actin are dynamically enriched at expanding 2°-3° contacts. (A) Still image taken from a 1 hour time series of a 32hr pupal eye expressing lifeact::Ruby and Arp3::GFP. F-actin (green) and Arp3 (red, white inset) localize to expanded 2°-3° cell contacts. Insets show contacts marked by box in A at frame 31 and 40. In particular, the left contact is

constricted at t=31, and expanded at t=40. (A, lower panel) Kymograph of 2°-3° cell contact marked by arrow in A. Arp3 (top) and F-actin (bottom) levels correlate with contact expansion (green bars) (B) Pearson cross correlations between contact length, F-actin levels, and Arp3 levels. Both Arp3 and F-actin positively correlate with contact length, and strongly correlate with one another.

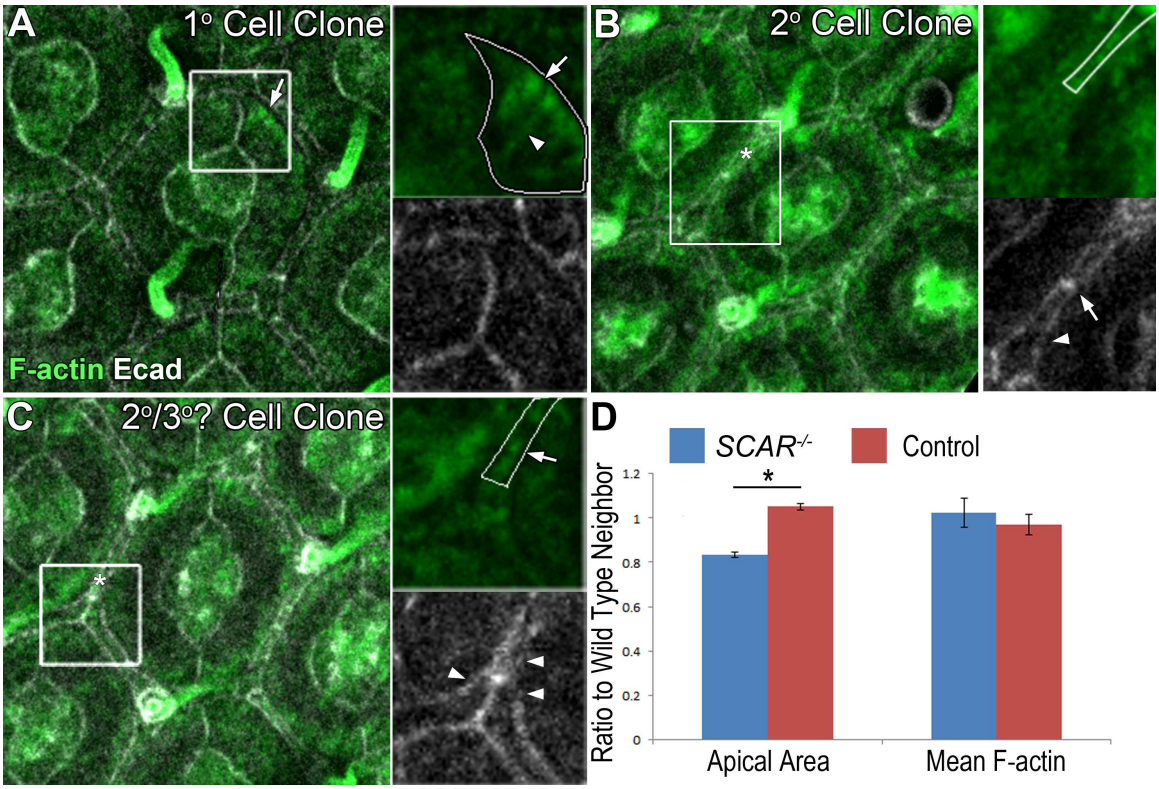

Figure 3.6: The Arp3 regulator SCAR is required for normal apical morphogenesis. (A-C) 40hr APF pupal eyes bearing *SCAR* mutant clones, marked positively (red, white outlined cells inset). SCAR mutant 1° cells (A) constrict apically, as observed by the reduced apical area, and the shift of 1°-1° contacts away from the midline of the ommatidium toward the mutant clone (see quantification in D). In addition, F-actin accumulated in more intense punctae (arrow, inset) and occasional transverse fibrils (arrowhead, inset), though overall levels of F-actin did not appear different (see D). (B) Cell clone forms aberrant cell contacts at the 3° cell niche. As there is one cell missing, it is not possible to determine whether the mutant cell is a 2° filling the 3° niche or vice versa. Similarly, it is also possible that the missing cell was *SCAR*$^{-/-}$(C) 2° cell clone, which constricts along the long axis of the cell, displacing the 2°-3° cell contact (asterisk, approximate normal location marked with arrowhead). (D) Quantification of 1° cell apical area (left) and F-actin intensity (right). *SCAR* mutant clones have significantly smaller apical surfaces ($p<.001$).

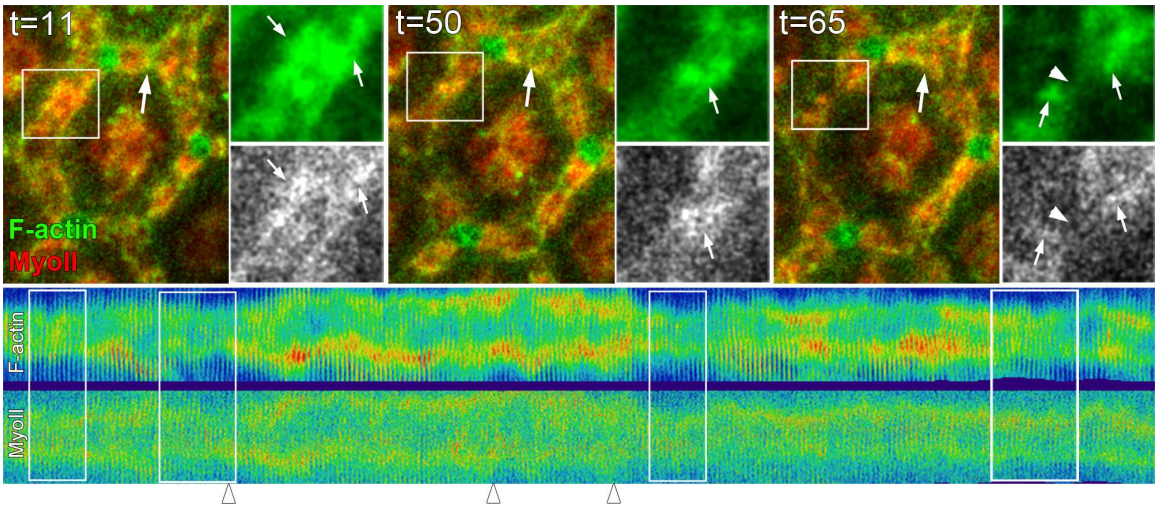

Figure 3.7 Dominant negative Rac (RacN17) leads to a disorganized hyper contractile actomyosin network. Top panels-Selected frames from a time lapse of a Rac^{N17} eye imaged from 32 hours APF at 30 sec intervals. Insets show selected contact which is inappropriately eliminated by t=130. This contact shows a band of intense F-actin and MyoII (frame 23, small inset arrows), which ultimately resolves to a tight focus (frame 100, small arrows). This contact is eventually eliminated (frame 130), resulting in the inappropriate contact of adjacent 1° cells (arrowhead, inset). This inappropriate contact is flanked by remnant foci of F-actin and MyoII (small arrowheads, inset). Even contacts that were preserved showed abnormal patterns of actomyosin and contact dynamics. Kymograph shown at bottom depicts dynamic behavior of junction indicated by larger arrow in upper frame. This junction shows striking enrichment of actomyosin flanking the 2°-3° cell contact, though this enrichment does not appear to correlate with contact constriction. Rather, constriction occurs when lower flanking levels are accompanied by higher levels of actomyosin throughout the contact (see boxed regions) Black arrowheads indicate times of upper panels.

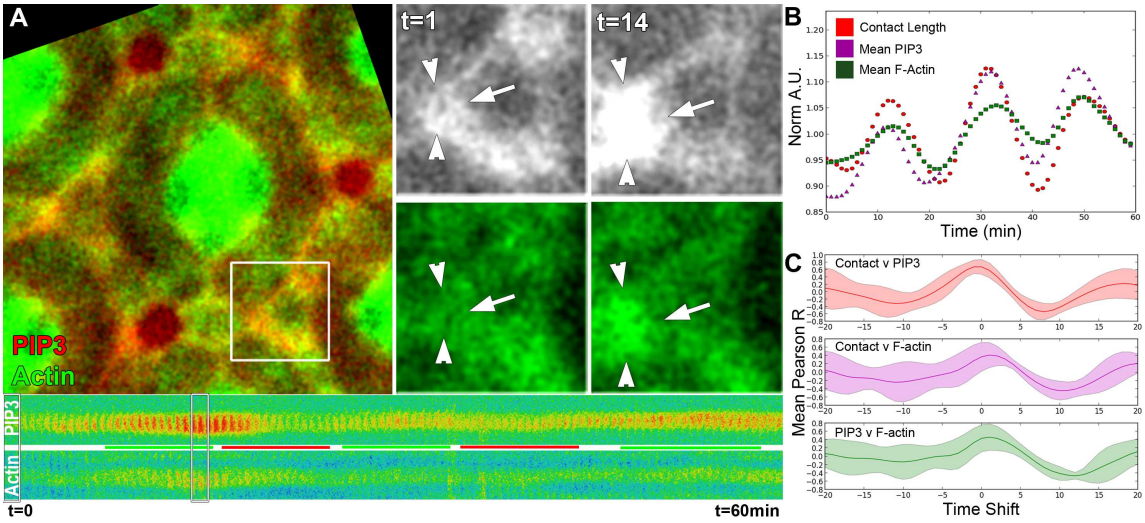

Figure 3.8 PIP3 correlates with contact length. (A) 32hr pupal eye expressing lifeact::ruby (Actin, green) and Grp1^{PH}::GFP (PIP3, red, white inset). PIP3 accumulated dynamically at 2°-3° cell contacts. Transient pulses of PIP3 correlated with similar pulses of F-actin during phases of contact expansion (compare inset t=14 to t=1). (B-C) Contact length correlates strongly with levels of PIP3 and F-actin. (B) Trace of contact length, PIP3 intensity, and F-actin intensity over time for the contact marked with arrowheads in A inset. (C) Pearson cross correlations for contact length, PIP3, and F-actin.

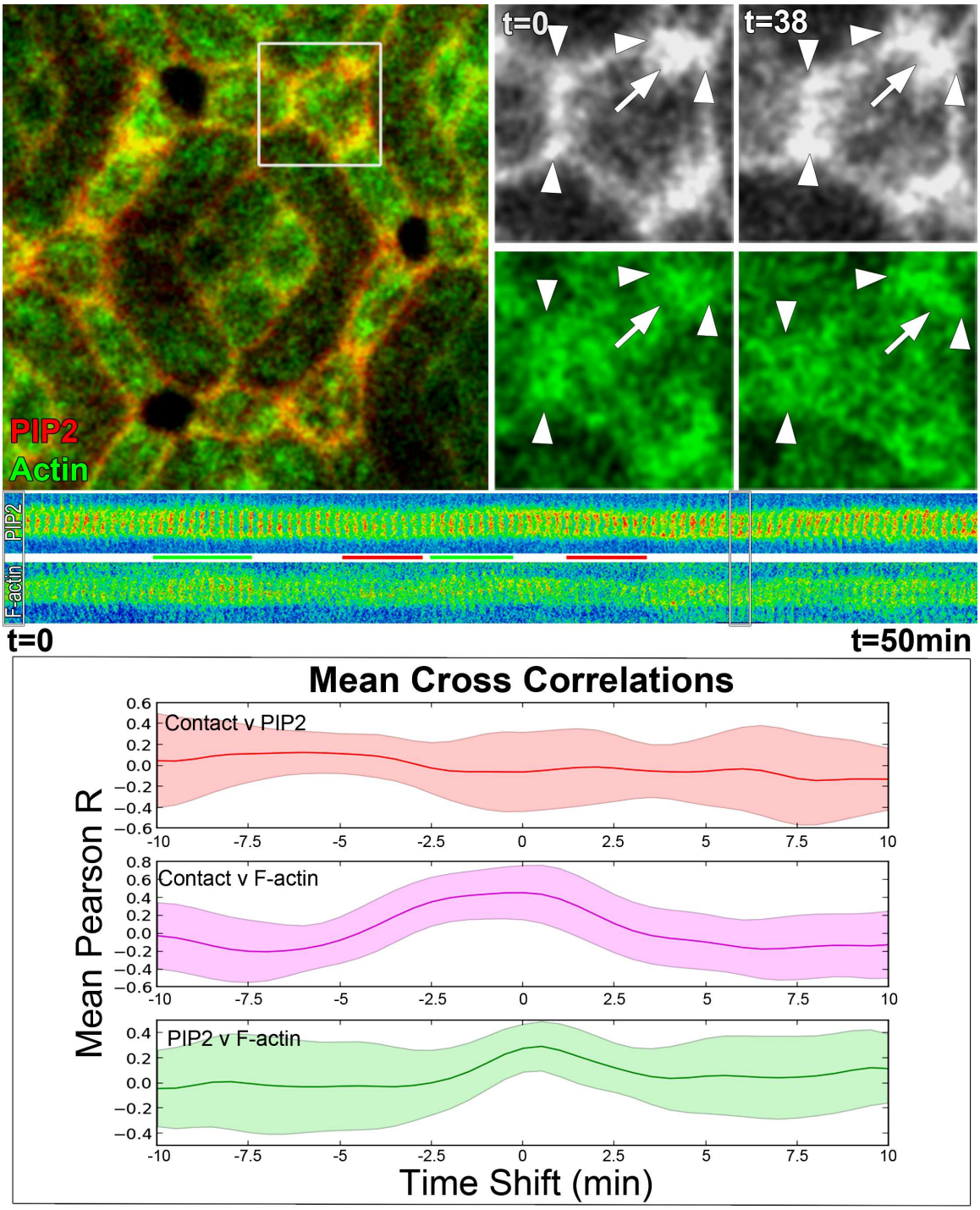

Figure 3.9: PIP2 does not correlate with contact length. (A) 32hr pupal eye disc expressing lifeact::ruby (Actin, green) and PLCy::GFP (PIP2, red). PIP2 appeared enriched at 2°-3° cell

contacts (arrows, inset), though levels did not change noticeably over time (see kymograph) and did not correlate with contact dynamics (see cross correlations, B).

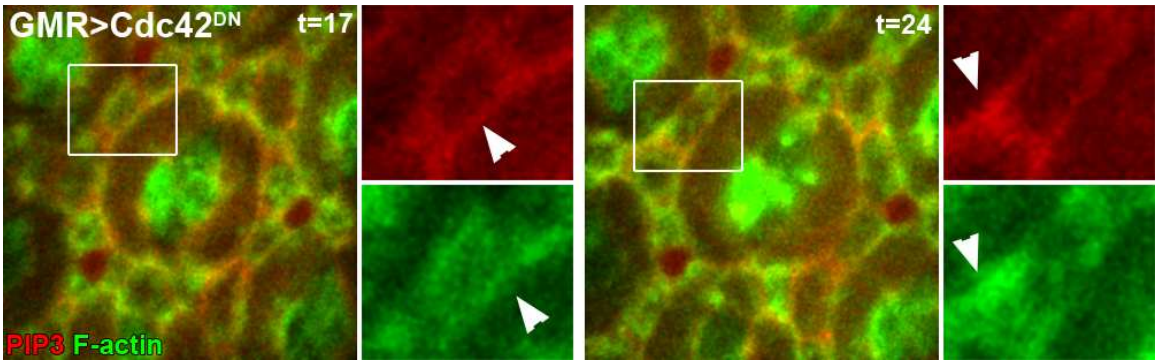

Fig 3.10 Expression of Cdc42^{DN} causes expanded PIP3 dynamics. Broad expression of Cdc42^{DN} caused cells to acquire a more isometric shape, and resulted in broader induction of PIP3 and F-actin pulses relative to controls. Note in particular enriched PIP3 and F-actin along 1°-2° contacts (arrowhead inset, t=17). Pulses of PIP3 and F-actin were also observed at 2°-3° contacts, as in controls (arrowhead inset, t=24)

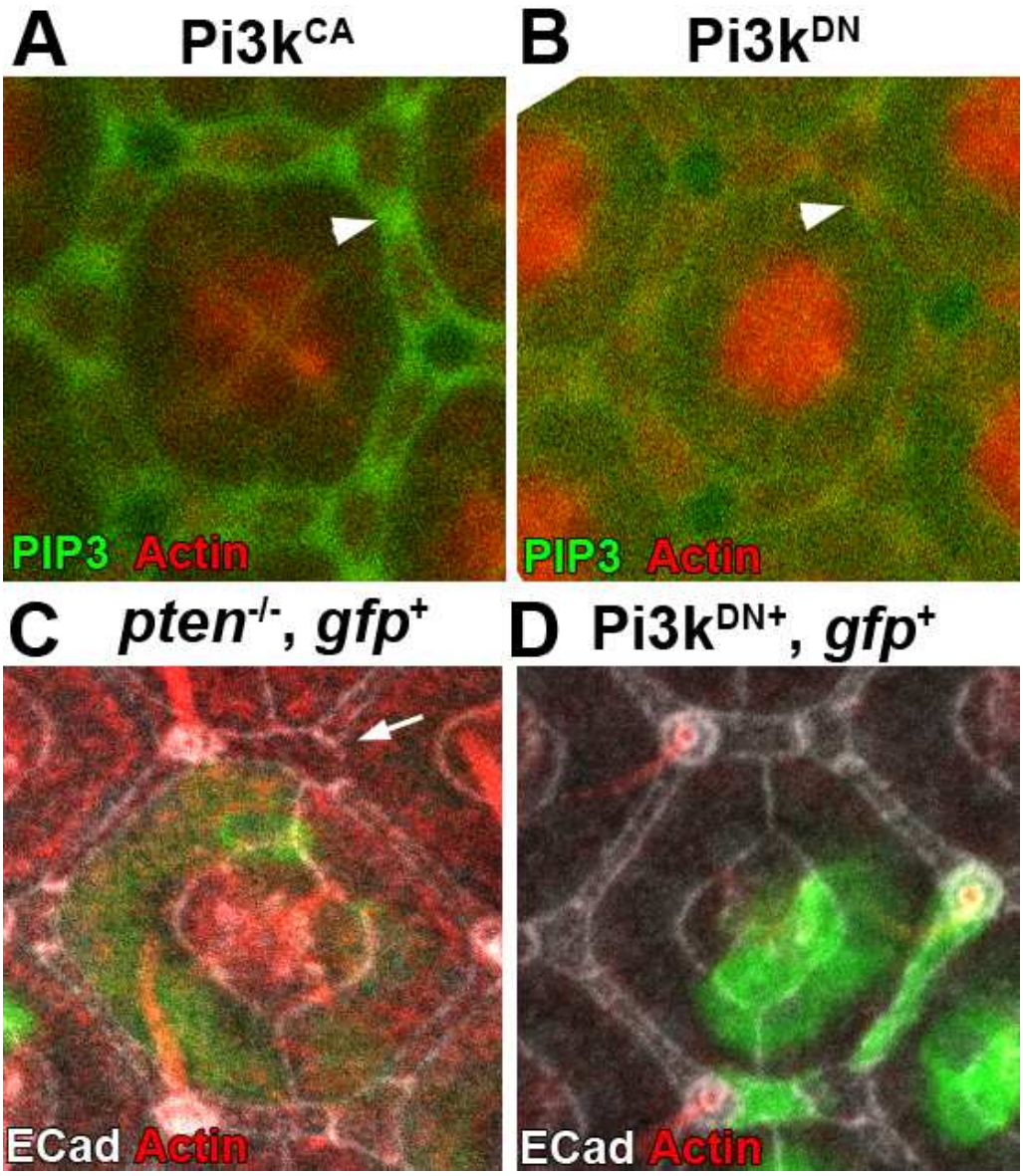

Figure 3.11: Manipulation of Pi3k fails to completely abolish PIP3 polarization or cause cell shape defects. (A-B) Still images taken from time lapse data of live 32 hr pupal eyes expressing PH::GFP (PIP3, green) and lifeact::ruby (Actin, red). (A) $Pi3k^{CA}$ increases association of PH::GFP with the membrane, though PIP3 accumulation remains polarized. (B) $Pi3k^{DN}$ decreases, but does not eliminate, polarized association of PH::GFP with the membrane (arrowhead). (C) 40 hr APF pupal eye bearing *pten* mutant clones (green). Instance of inappropriate 2°-2° contact

(arrow) adjacent to *pten* clone. The vast majority of isolated clones had a normal morphology. (D) 40hr APF eye disk bearing $Pi3k^{DN}$ clones (green). Clones had normal morphology. Apparent constriction of lower 2° cell is within normal variation.

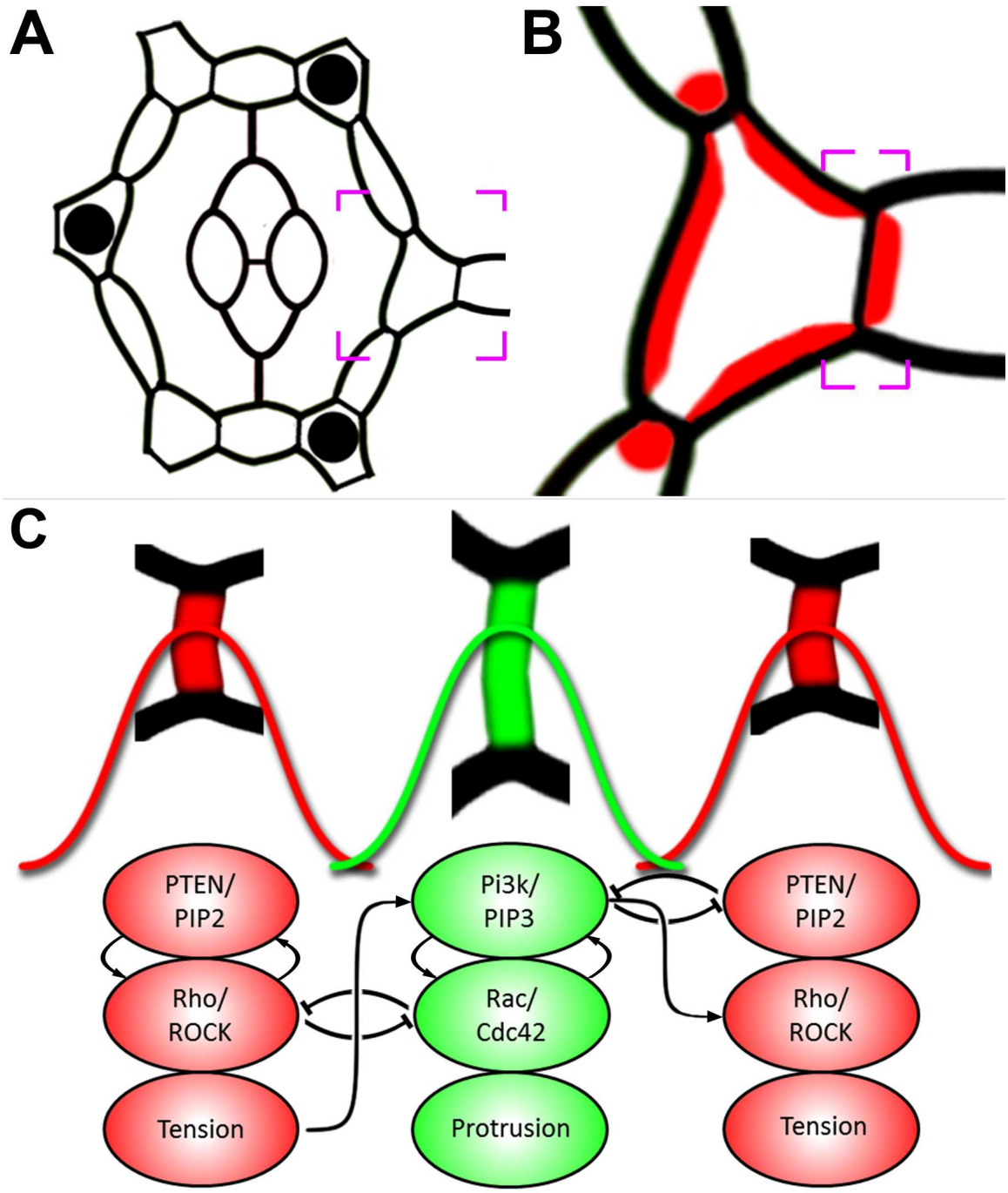

Figure 3.12 Model of pulsed contractile and protrusive dynamics at 2°-3° contacts. (A) Ommatidium at 32 hours. (B) Zoom of boxed region in A. Red highlights zones of increased tension at contractile cell contacts. (C) Oscillations of tensile and branched F-actin and myosin pathways balance constractile forces at 2°-3° contacts, highlighted in boxed region in (B).

Positive feedback between PTEN and Rok could contribute to robust activation of contractile forces, while similar positive feedback between Pi3k and Rac could robustly promote protrusive forces. Pathway activities could be linked, for example, by delayed or high threshold positive regulatory interactions between tension and Pi3k, and/or between PIP3 and Rok.

	Gene	Notes
Rac	Cdep	GEF
	CG30440	GEF
	GEFmeso	GEF
	CG33275	GEF
	Akt1	
Rho	chico/IRS	insReceptor binding
	Btk29A	
Rac/Rho	Rok	
	sl	PLCy
Cdc42/Rac	Ziz	GEF
	gek/dMRCK	DS kinase,DAG binding
Cdc/Rac/Rho	CG42674	GEF
	Exn	GEF
	Vav	GEF
	CG10188	GEF
	RhoGAP15B	
	Graf	GAP
	RhoGAP1A	GAP
	trio	GEF
	RhoGEF2	
	RtGEF	
	Sos	RasGEF
	PLD	PX domain

Table 4.1: List of phosphoinositide binding Rho family interactors. Of 20 Rho family GEFs encoded in the *Drosophila* genome, 60% contain phosphoinositide binding PH domains. Of these, four are predicted to interact specifically with Rac, one with both Rac and Cdc42, while the remaining genes are predicted to interact with Rac, Cdc42, and Rho. Three RhoGAPs also contain PH domains, and each of these is predicted to interact with all three small Rho family GTPases. Also of note, both PLCy (sl) and PLD interact with multiple Rho family GTPases. Not shown are DHR-1 containing GEFs Mbc and DOCK4, which are specific to Rac.

Chapter 4

Summary & Future Directions

My work generally has focused on the investigation of basic mechanisms that mediate normal development. *Drosophila* provides an incredibly tractable model to investigate a wide range of biological questions by a wide range of methods. Indeed, my own work has shifted from the study of genetic patterning of the notum to the control of cell shape in the eye. While these are quite different questions, many of the answers at which I have arrived are strikingly similar. In each case, I have identified a pathway that confers a measure robustness to the developmental process at hand. In the notum, *odd-skipped* genes establish an anterior organizer that coordinates with the better known posterior organizer to promote the molecular patterning of the tissue. In the eye, PIP3 and F-actin pulses appear to act antagonistically to MyoII based tension at the 2°-3° cell contact, and this may be required for contact maintenance during shape change. Champions of parsimony would likely lament both sets of findings, given that one dimensional control, either of patterning by Dpp, or of contact length by MyoII, could in principle be sufficient for normal development. One possible explanation for the evolution of this level of control is that it confers robustness to these developmental processes. These are hardly unique findings; robust regulation is present at every level of development, from the control of intercellular signaling, to the transduction of these signals into programs of gene expression, to the control of cell behavior. The goal of this work has been to understand two specific mechanisms by which these robust programs of patterning and morphogenesis generate morphological and functional diversity in development.

odd-skipped genes pattern the notum AP axis

Summary

In my first project, I investigated whether the *odd-skipped* genes were required for normal AP patterning of the *Drosophila* notum. Despite a well characterized checkerboard pattern of gene expression [59], the mechanisms of notum AP were unclear. Thus far, the sole organizer of notum AP patterning was thought to be Dpp, secreted from the posterior margin. The expression of *odd-skipped* genes at the anterior margin of the notum, combined with previously described roles in cell fate specification, suggested that these genes may be good candidates establish a complementary anterior organizer.

The molecular regulation of Bowl reinforces this idea. Bowl is ubiquitously expressed, but rapidly degraded by the protein Lines. Expression of one or more *odd-skipped* genes can titrate Lines from Bowl and promote Bowl accumulation (Fig. 2.6). Thus, *odd-skipped* genes and Lines can act as a binary switch between adjacent tissue domains[70]. In the notum, we found that *odd-skipped* genes are expressed in the anterior prescutum (Fig. 2.1), where they are required for early specification of the notum field (Figs. 2.3-2.4), and for the subsequent organization of notum anterior patterning. Specifically, Bowl was required to promote expression of the prescutum specific gene Bar, and to repress Dl expression (Fig. 2.11). We extended these findings to the eye, where *odd-skipped* genes were similarly required for normal pattering of the eye margin through the expression of Wg (Fig. 2.18). These data are consistent with work in the leg, where the complementary accumulation of Bowl and Lines participates in a feedback loop with Notch signaling to maintain a stable signaling interface at the leg segment border [71]. Together this work suggests conserved roles for *odd-skipped* genes and Lines in the control of gene expression at tissue boundaries.

Surprisingly, however, we detected several non-autonomous effects of *odd*-skipped family activity. Perhaps most surprising was the finding that Drm resulted in the non-autonomous stabilization of Bowl. We detected subtle graded accumulation of Bowl beyond the endogenous Drm domain (Fig 2.6, 2.9). This pattern was recapitulated by Drm overexpressing clones, and was particularly striking in Drm expressing clones mutant for Bowl (Fig. 2.9). This confirms that Drm expression is able to mediate the stabilization of Bowl produced by neighboring cells. It is not clear yet by what mechanism this Drm mediates this effect, not whether it is required for normal physiology (see future directions). Of note, only Drm expressing clones induced non-autonomous Bowl accumulation, and only these clones remained intact in the disc epithelium, in contrast to *lines*$^{-}$, Odd^{+}, or Sob^{+} clones (Fig. 2.6). In addition to the non-autonomous Bowl stabilization, Drm overexpression was sufficient to induce Eyg accumulation broadly across the notum field (Fig. 2.7). Importantly, this induction required Bowl expression (Fig. 2.8).

The coordinate regulation of tissue patterning by multiple organizers is a common theme in animal development, exemplified by the coordinate regulation of *Drosophila* embryonic AP patterning by Bicoid and Nanos [306]. These studies uncovered a novel regulator of notum AP patterning, and suggest that Dpp from the posterior coordinates with some positive signal induced by Drm at the anterior notum. At the same time, this work raises fundamentally novel questions about the core functions and mechanisms of the Lines-Drm-Bowl cassette in the control of tissue patterning.

Future Directions

Perhaps the most pressing question raised by this work regards the mechanism by which Drm mediates the non-autonomous induction of Bowl and/or Eyg. It is possible that Drm

regulates the activity of a secondary signal which patterns broadly. One signal could be Fat-Ds juxtacrine signaling. Ds accumulates in a graded pattern across the notum AP axis (not shown). In addition to published roles for this pathway in the control of wing growth [357], Ft-Ds signaling mediates expansion of the wing field by a feed forward mechanism that promotes induction of the wing specification gene *vestigial* (*vg*) in non *vg* cells that abut the wing field [310,311]. Ft-Ds long range signaling is further supported by the finding that localized ectopic Ft-Ds signaling could propagate long range changes in the polarity of the atypical myosin Dachs. This polarity is a primary readout for Ft-Ds signaling. In this way, Drm expression could induce a local change in Ft-Ds that would propagate through Dachs. A first step in testing this model would be to determine whether Ft-Ds signaling itself can regulate Eyg expression. This could be addressed by the overexpression of Dachs or the transcriptional regulator Yorkie, or by reduction of pathway components Warts or Expanded [311]. Alternatively, the finding that Drm is able to induce Eyg and Bowl provides a useful assay to analyze downstream effects on Ft-Ds signaling, which could be assayed by the Dachs polarization or by the induction of Four-jointed. Any changes could then be compared ectopic Eyg expression.

It is not obvious what might link *odd-skipped* gene activity to Ft-Ds signaling, if a relationship to Eyg were to be detected, nor is it clear what might link Drm and Bowl to the non-autonomous induction of Eyg. Thus far, two genes have been described to promote Eyg expression in the notum. However, these genes cover only a small portion of the Eyg domain, suggesting that other factors may be required for normal Eyg expression [358]. Interestingly, N signaling regulates Eyg in the eye [359], and the pattern of N activity corresponds well with Four-jointed expression. Similarly, in the notum Dl accumulates complementary to Ds. Together these data suggest it is possible that these pathways could interact in the regulation of Eyg.

Though Ft-Ds could hypothetically mediate the non-autonomous Bowl stabilization, the very short range of Bowl induction renders this less likely. More likely perhaps is the hypothesis that N signaling might mediate this activity. N signals by juxtacrine signaling, which matches the range of the Bowl induction. Additionally, *odd-skipped* genes act both downstream and upstream of N signaling[71,291,292]. Perhaps this represents a subtle elaboration in the regulatory relationship between these pathways. If this is the case, the more interesting question would be to understand if and how this graded accumulation of Bowl affects N signaling. We found that clones that induced Bowl autonomously, but not surrounding the clone, segregated from the epithelium. As these clones were all different manipulations than Drm expression, it is equally possible that the clone segregation is due to some other factor, or that the lack of non-autonomous Bowl is secondary to clone segregation. However, given roles for N signaling at tissue interfaces and at regions of epithelial buckling [71,75,76], it is also possible that graded Bowl modulates N output. There are no characterized N patterning targets in the notum, so these studies may be more fruitfully pursued in the embryo or the leg, where N targets are better known.

Alternatively, Drm could directly mediate Bowl stabilization in neighboring cells by intercellular diffusion. Drm could diffuse through ring canals, which have recently been shown to mediate direct cell-cell communication in *Drosophila* follicle and imaginal epithelia, in addition to their well characterized role in nurse cells[312]. Consistent with this hypothesis, these somatic ring canals were proposed to promote buffering of signals by allowing the free diffusion and equilibration of proteins among clonal patches of cells. In this way, diffusion of Drm might not serve to equilibrate, but rather to grade Bowl discontinuities. The requirement for intercellular diffusion may be testable by blocking ring canal formation, for instance by downregulation of ring canal proteins such as Kelch [360]. These studies would be particularly

interesting, not simply to determine if Bowl is stabilized in this manner, but because they would provide a pathway independent means to manipulate the non-autonomous induction of Bowl. This would allow more rigorous testing of the hypotheses that graded Bowl is required for epithelial integrity at the Bowl-Dl interface, and that this gradation modulates N signaling.

From a more general perspective, this interface could serve as an interesting model to understand subtleties of boundary formation. In the notum, epithelial folding only occurs along the lateral ~20%. Interestingly, Odd accumulates very highly in this region, and at very low levels along the remainder of the prescutum. Hence, this arrangement could be used to study the mechanisms that regulate strictly genetic vs morphological boundary formation. This could also provide further insight into mechanisms of *odd-skipped* gene activities. Odd and Bowl both interact with the co-repressor Groucho, and varying levels or ratios of Odd-skipped proteins could mediate a range of transcriptional outcomes [292,314].

Pulses of PIP3 and F-actin mediate shape change in the eye

Summary

Cortical tension and Cadherin based adhesion are the primary determinants of cell shape during morphogenesis. Despite significant progress in understanding mechanisms of contact constriction during shape changes such as apical constriction [188,252] and cell intercalation [142], comparatively little is known about mechanisms that promote contact expansion during morphogenesis, or that attenuate tension to produce stable shape changes. In chapter three, I presented my efforts to investigate this latter question in the elongation of 2° cells in the *Drosophila* pigment cell epithelium.

Here I showed that, based on Rok and MyoII enrichment and MyoII loss of function clones, constricting 2°-3° cell contacts appear to be under more tension than elongating 2°-1°

cell contacts (Fig. 3.2, 3.3). However, contacts were not completely eliminated, despite a lack of core AJ components at 2°-3° contacts during elongation. Instead, dynamic pulses of PIP3 and F-actin correlated with transient phases of contact expansion. This F-actin correlated with the branched F-actin regulator Arp3 (Fig. 3.5), and the Arp3 regulator SCAR was required for normal apical area and contact maintenance (Fig. 3.6). Additionally, normal Rho family GTPase signaling was required for normal contact dynamics and epithelial integrity. In particular, expression of Rac^{DN} resulted in the preferential elimination of 2°-3° contacts as a result of constitutive actomyosin localization (Fig. 3.12).

Many morphogenetic processes proceed by pulsed or oscillatory constrictions of an actomyosin network. In most contexts, these pulses have been described as being strictly products of actomyosin constriction and relaxation. Here, I describe for the first time a process whereby antagonistic branched F-actin networks mediate pulsatile contact expansion, in an overall contractile context. It is unclear how general a mechanism this may be; the 2°-3° cell contact is fairly unique in its remarkable degree of AJ polarization. This could be quite interesting, however, from a physiological standpoint. Loss of E-Cadherin, dysregulated phosphoinositide signaling, and dynamic protrusive behaviors are hallmarks of metastatic cells. As both phosphoinositide[361] and RhoGTPase[362] signaling are dysregulated in many cancers, this system could provide valuable insight into how these pathways are modulated to produce cytoskeletal dynamics within a physiologically tenable range.

The Longmore lab has published two sets of studies that specifically address the balance of tension in the pigment epithelium. This work clearly establishes that a balance of Cdc42 and Rho activity is required for normal morphogenesis[339,363]. These studies raise many questions as to the nature of this balance. While this work described this balance in isotropic terms, my data suggest that the balance of adhesion and tension is not homogenous at the apical cortex.

Indeed, it necessarily must not be, to allow the dramatic shape changes that occur. Key questions are how balance is achieved between these two mutually inhibitory pathways, and how this balance is controlled spatially to promote shape change.

Future Directions

Spatial control of PIP3/F-actin dynamics

Understanding the mechanisms that control the spatial restriction of these pathways is critical. I propose several hypotheses as to how polarity is achieved. The Longmore lab showed that Cdc42 recruits a *Par-6*/aPKC complex AJs to inhibit Rho pathway activity[363]. As AJs are strongly enriched at 1°-2° contacts, this represents one form of polarization. However, our observations of 2°-3° F-actin dynamics suggest the possibility that Cdc42 could act there to promote contact expansion by mechanisms other than the inhibition of Rho. To test this hypothesis, one could compare Cdc42 mutant cells to *Par-6* or aPKC mutant cells. I hypothesize that Cdc42 clones will constrict relatively isometrically, due to increased tension at both 2°-3° and 1°-2° contacts. By contrast, I hypothesize that apical *Par-6* or aPKC clones will constrict preferentially along the long axis of the cell, under the working hypothesis that this complex inhibits Rho only at the AJ.

Another mechanism for pigment cell polarization likely arises from the differential expression of the Neph1/Nephrin proteins Hbs and Rst, which are expressed in 1° cells and IOCs[268], respectively. While early work suggested that these proteins mediate preferential adhesion, the mechanism by which this might occur is unknown. More recent work has demonstrated interactions between Rst and the CIN85 homolog Cindr[270], which in turn can bind to the Arf6 GAPs dASAP and ArfGAP1[265]. Genetically, Cindr interacts with a host of cytoskeleton regulators in the morphogenesis of the eye. Perhaps most relevant to my studies, however, are

potential roles for Arf6. Preferential recruitment of Arf GAPs to 1°-2° contacts by Rst could polarize Arf6 activity toward 2°-3° contacts. Arf6 is a key regulator of PIP5K [274], which promotes formation of PIP2. Hence, polarized Arf6 activity at 2°-3° contacts could explain the enrichment of PIP2 at 2°-3° cell junction (Fig. 3.9). In turn, PIP2 enrichment could recruit or activate a host of downstream cytoskeletal regulators [335]. This mechanism could occur upstream or downstream of changes in AJ levels.

Functional roles of phosphoinositide and Rho GTPase signaling

One significant issue with these studies is that I have as yet been unable to establish a functional role for PIP3 signaling, based on *pten* mutant clones and overexpression of $Pi3k^{CA}$ or $Pi3k^{DN}$ constructs. It is possible that my analyses have not been sensitive enough to detect subtle changes in cell shape, or that transient differences are eliminated by the time of analysis (40hr APF). During cell migration and embryonic dorsal closure, PIP3 signaling correlates highly with polarized F-actin dynamics, but is not strictly required for either process. PIP3 could play a similar modulatory role in this system as well. Another possibility is that PIP3 pulses provide a measure of robustness, and that under normal developmental conditions these dynamics are not required. This hypothesis could be tested by altering environmental parameters such as temperature of nutrient availability, or by a standard genetic enhancer screen to identify whether, for example, loss of PTEN sensitizes the system to alterations in other components. Alternatively, the experimental manipulations performed may not have been sufficiently strong to elicit phenotypes. The relatively normal distribution of PIP3 and F-actin in $Pi3k^{CA}$ and $Pi3k^{DN}$ discs suggests this is a possibility (Fig. 3.10). There are a number of alternative methods to employ, such as the use of PTEN or PH domain overexpression to titrate levels of PIP3. These methods could also be used in combination to more thoroughly alter PIP3 levels. Importantly,

such studies must also be done live to assess whether these manipulations alter contact or cell dynamics, if not final cell shape.

It will also be of interest to determine what mechanisms regulate Pi3k to promote PIP3 pulse formation. Given the mechanosensitive nature of the AJ, and the association of Pi3k and AJ, one possibility is that increased AJ recruits a Pi3k regulator to enhance PIP3 production. To test the more conservative hypothesis that PIP3 pulses require actomyosin tension in some way, I propose to image PIP3 and/or F-actin dynamics in cells in which MyoII activity is either diminished (by MyoII RNAi) or enhanced (by overexpression of Rok). Alternatively, MyoII tension could be attenuated with spatial and temporal specificity by CALI[78], allowing a more direct examination the response of PIP3 or F-actin to changes in tension. I hypothesize that increased tension will enhance PIP3 pulse frequency or amplitude, and that decreased tension will decrease PIP3 pulse frequency or amplitude.

Additionally, PIP3 dynamics or localization could require a pre-existing polarized PIP2 domain, such as might be generated by Arf6. It will also be important to characterize whether Arf6 indeed activates PIP5K to generate a polarized PIP2 domain, and subsequently whether PIP3 dynamics depend on this lipid domain. High levels of PIP2 could promote PIP3 synthesis simply by increased availability of precursor, or by the recruitment of cytoskeletal regulators that could potentiate Rac and/or Pi3k through positive feedback.

To better characterize the requirements for Rho GTPase signaling, additional studies will be required to examine genetic loss of function alleles for GTPase family members, as the dominant negative alleles utilized exhibit more serious defects than result from genetic loss of function [363], possibly due to the non-specific sequestration of GEFs. These data could suggest redundant functions for Cdc42 and Rac1 to promote expansion of the 2°-3° contact. Indeed, broad knockdown of both Rac1 and Cdc42 did lead to more severe defects than loss of either

one alone [363]. Of particular interest would be the identification of particular GAPs or GEFs that might mediate localized pathway activity or cross-talk.

Characterization of contact dynamics

It is unclear as yet how contact fluctuations contribute to cell shape change. One initial approach to investigate this question would be to perform a developmental time course of contact dynamics. If PIP3, F-actin, or contact fluctuations are important in driving morphogenesis of the eye, then these dynamics should correlate with rates of shape change. Quantification of the frequency and amplitude of fluctuations before, during, and following shape changes should begin to address this question, and serve as a resource for future studies that manipulate pathway activities.

More interesting would be to analyze PIP3, F-actin, and contact dynamics on a tissue scale. One hypothetical role for these dynamics could be to allow cells to dynamically sense the mechanical state of neighboring cells, and coordinate levels of tension and/or adhesion. This would coordinate the detection and adoption of a global interfacial energy minimum, as has been proposed to predict eye morphology. Another member of the lab is developing tissue tracking and analysis software, which could be used to perform this type of analysis. If PIP3 dynamics do indeed mediate coordination, then patterns of activity should be systematic, and behave in the context of a cellular network.

Appendix 1

From “The Once and Future King” by TH White. Two knights, Sirs Grummore and Palomides, attempt to disguise themselves as the four-legged Questing Beast, with tragic results:

“Look out for the spots, Palomides. There, you've smudged them.”
“A thousand pardons!”
“You ought to look where you are goin'.”
“Well, who put his foot through the ribs?”

On the second day there was trouble with the back end.
“These haunches are too tight.”
“Don't bend over.”
“I have to bend over, if I am the back end.”
“They won't split.”
“Yes, they will.”
“No, they won't.”
“Well, they have.”

“Look out for my tail,” said Sir Grummore on the third day. “You are treadin' on it.”
“Don't hold so tight, Grummore. My neck is twisted.”
“Can't you see?”
“No, I can't, my neck is twisted.”
“There goes my tail.”
There was a pause while they sorted themselves out.
“Now, carefully this time. We must walk in step.”
“I think my haunches are comin' down.”
“If you let go of yours truly's waist, we shall come in half.”
“Well, I can't hold up my haunches unless I do.”
“There go the buttons.”

References

1. Lawrence, P. A. & Struhl, G. Morphogens, compartments, and pattern: lessons from drosophila? *Cell* **85,** 951–961 (1996).
2. Davy, A., Bush, J. O. & Soriano, P. Inhibition of Gap Junction Communication at Ectopic Eph/ephrin Boundaries Underlies Craniofrontonasal Syndrome. *PLoS Biol* **4,** e315 (2006).
3. Pérez-Pomares, J. M. & Foty, R. A. Tissue fusion and cell sorting in embryonic development and disease: biomedical implications. *BioEssays News Rev. Mol. Cell. Dev. Biol.* **28,** 809–821 (2006).
4. Twigg, S. R. F. *et al.* Mutations of ephrin-B1 (EFNB1), a marker of tissue boundary formation, cause craniofrontonasal syndrome. *Proc. Natl. Acad. Sci. U. S. A.* **101,** 8652–8657 (2004).
5. Gierer, A. & Meinhardt, H. A theory of biological pattern formation. *Kybernetik* **12,** 30–39 (1972).
6. Meinhardt, H. & Gierer, A. Pattern formation by local self-activation and lateral inhibition. *BioEssays* **22,** 753–760 (2000).
7. Turing, A. M. The Chemical Basis of Morphogenesis. *Philos. Trans. R. Soc. Lond. B. Biol. Sci.* **237,** 37–72 (1952).
8. Wolpert, L. Positional information and the spatial pattern of cellular differentiation. *J. Theor. Biol.* **25,** 1–47 (1969).
9. Driever, W. & Nüsslein-Volhard, C. The bicoid protein determines position in the Drosophila embryo in a concentration-dependent manner. *Cell* **54,** 95–104 (1988).
10. Ferguson, E. L. & Anderson, K. V. decapentaplegic acts as a morphogen to organize dorsal-ventral pattern in the Drosophila embryo. *Cell* **71,** 451–461 (1992).
11. Nellen, D., Burke, R., Struhl, G. & Basler, K. Direct and Long-Range Action of a DPP Morphogen Gradient. *Cell* **85,** 357–368 (1996).
12. Neumann, C. J. & Cohen, S. M. Long-range action of Wingless organizes the dorsal-ventral axis of the Drosophila wing. *Dev. Camb. Engl.* **124,** 871–880 (1997).
13. Lander, A. D. Morpheus Unbound: Reimagining the Morphogen Gradient. *Cell* **128,** 245–256 (2007).
14. Kay, R. R. & Thompson, C. R. L. Forming Patterns in Development without Morphogen Gradients: Scattered Differentiation and Sorting Out. *Cold Spring Harb. Perspect. Biol.* **1,** a001503 (2009).
15. Paulsson, J. Summing up the noise in gene networks. *Nature* **427,** 415–418 (2004).
16. Goentoro, L. A. *et al.* Quantifying the Gurken Morphogen Gradient in Drosophila Oogenesis. *Dev. Cell* **11,** 263–272 (2006).
17. Ahn, S. & Joyner, A. L. Dynamic Changes in the Response of Cells to Positive Hedgehog Signaling during Mouse Limb Patterning. *Cell* **118,** 505–516 (2004).
18. Dessaud, E. *et al.* Interpretation of the sonic hedgehog morphogen gradient by a temporal adaptation mechanism. *Nature* **450,** 717–720 (2007).
19. Harfe, B. D. *et al.* Evidence for an Expansion-Based Temporal Shh Gradient in Specifying Vertebrate Digit Identities. *Cell* **118,** 517–528 (2004).
20. Galli, L. M., Barnes, T. L., Secrest, S. S., Kadowaki, T. & Burrus, L. W. Porcupine-mediated lipid-modification regulates the activity and distribution of Wnt proteins in the chick neural tube. *Development* **134,** 3339–3348 (2007).
21. Taylor, F. R. *et al.* Enhanced potency of human Sonic hedgehog by hydrophobic modification. *Biochemistry (Mosc.)* **40,** 4359–4371 (2001).
22. Eugster, C., Panáková, D., Mahmoud, A. & Eaton, S. Lipoprotein-Heparan Sulfate Interactions in the Hh Pathway. *Dev. Cell* **13,** 57–71 (2007).
23. Gallet, A., Ruel, L., Staccini-Lavenant, L. & Thérond, P. P. Cholesterol modification is necessary for controlled planar long-range activity of Hedgehog in Drosophila epithelia. *Dev. Camb. Engl.* **133,** 407–418 (2006).

24. Panáková, D., Sprong, H., Marois, E., Thiele, C. & Eaton, S. Lipoprotein particles are required for Hedgehog and Wingless signalling. *Nature* **435,** 58–65 (2005).
25. Burke, R. *et al.* Dispatched, a novel sterol-sensing domain protein dedicated to the release of cholesterol-modified hedgehog from signaling cells. *Cell* **99,** 803–815 (1999).
26. Callejo, A., Torroja, C., Quijada, L. & Guerrero, I. Hedgehog lipid modifications are required for Hedgehog stabilization in the extracellular matrix. *Development* **133,** 471–483 (2006).
27. Porter, J. A. *et al.* Hedgehog Patterning Activity: Role of a Lipophilic Modification Mediated by the Carboxy-Terminal Autoprocessing Domain. *Cell* **86,** 21–34 (1996).
28. Su, V. F., Jones, K. A., Brodsky, M. & The, I. Quantitative analysis of Hedgehog gradient formation using an inducible expression system. *BMC Dev. Biol.* **7,** 43 (2007).
29. Ducuing, A., Mollereau, B., Axelrod, J. D. & Vincent, S. Absolute requirement of cholesterol binding for Hedgehog gradient formation in Drosophila. *Biol. Open* **2,** 596–604 (2013).
30. Callejo, A. *et al.* Dispatched mediates Hedgehog basolateral release to form the long-range morphogenetic gradient in the Drosophila wing disk epithelium. *Proc. Natl. Acad. Sci. U. S. A.* **108,** 12591–12598 (2011).
31. Yan, D. & Lin, X. Shaping Morphogen Gradients by Proteoglycans. *Cold Spring Harb. Perspect. Biol.* **1,** a002493 (2009).
32. Bellaiche, Y., The, I. & Perrimon, N. Tout-velu is a Drosophila homologue of the putative tumour suppressor EXT-1 and is needed for Hh diffusion. *Nature* **394,** 85–88 (1998).
33. Hacker, U., Lin, X. & Perrimon, N. The Drosophila sugarless gene modulates Wingless signaling and encodes an enzyme involved in polysaccharide biosynthesis. *Development* **124,** 3565–3573 (1997).
34. Han, C., Yan, D., Belenkaya, T. Y. & Lin, X. Drosophila glypicans Dally and Dally-like shape the extracellular Wingless morphogen gradient in the wing disc. *Development* **132,** 667–679 (2005).
35. Eldar, A., Rosin, D., Shilo, B.-Z. & Barkai, N. Self-enhanced ligand degradation underlies robustness of morphogen gradients. *Dev. Cell* **5,** 635–646 (2003).
36. Cadigan, K. M., Fish, M. P., Rulifson, E. J. & Nusse, R. Wingless Repression of Drosophila frizzled 2 Expression Shapes the Wingless Morphogen Gradient in the Wing. *Cell* **93,** 767–777 (1998).
37. Chen, Y. & Struhl, G. Dual Roles for Patched in Sequestering and Transducing Hedgehog. *Cell* **87,** 553–563 (1996).
38. Wilson, C. W. & Chuang, P.-T. Mechanism and evolution of cytosolic Hedgehog signal transduction. *Development* **137,** 2079–2094 (2010).
39. Lee, J. R., Urban, S., Garvey, C. F. & Freeman, M. Regulated Intracellular Ligand Transport and Proteolysis Control EGF Signal Activation in Drosophila. *Cell* **107,** 161–171 (2001).
40. Tsruya, R. *et al.* Intracellular trafficking by Star regulates cleavage of the Drosophila EGF receptor ligand Spitz. *Genes Dev.* **16,** 222–234 (2002).
41. Urban, S., Lee, J. R. & Freeman, M. Drosophila rhomboid-1 defines a family of putative intramembrane serine proteases. *Cell* **107,** 173–182 (2001).
42. Tsruya, R. *et al.* Rhomboid cleaves Star to regulate the levels of secreted Spitz. *EMBO J.* **26,** 1211–1220 (2007).
43. Yogev, S., Schejter, E. D. & Shilo, B.-Z. Drosophila EGFR signalling is modulated by differential compartmentalization of Rhomboid intramembrane proteases. *EMBO J.* **27,** 1219–1230 (2008).
44. Etheridge, L. A., Crawford, T. Q., Zhang, S. & Roelink, H. Evidence for a role of vertebrate Disp1 in long-range Shh signaling. *Development* **137,** 133–140 (2010).
45. Parks, A. L. *et al.* Structure-function analysis of delta trafficking, receptor binding and signaling in Drosophila. *Genetics* **174,** 1947–1961 (2006).
46. Gradilla, A.-C. & Guerrero, I. Cytoneme-mediated cell-to-cell signaling during development. *Cell Tissue Res.* **352,** 59–66 (2013).
47. Kornberg, T. B. & Guha, A. Understanding morphogen gradients: a problem of dispersion and containment. *Curr. Opin. Genet. Dev.* **17,** 264–271 (2007).
48. Ramírez-Weber, F.-A. & Kornberg, T. B. Cytonemes: Cellular Processes that Project to the Principal Signaling Center in Drosophila Imaginal Discs. *Cell* **97,** 599–607 (1999).

49. Hsiung, F., Ramirez-Weber, F.-A., Iwaki, D. D. & Kornberg, T. B. Dependence of Drosophila wing imaginal disc cytonemes on Decapentaplegic. *Nature* **437,** 560–563 (2005).
50. Roy, S., Hsiung, F. & Kornberg, T. B. Specificity of Drosophila cytonemes for distinct signaling pathways. *Science* **332,** 354–358 (2011).
51. Sato, M. & Kornberg, T. B. FGF is an essential mitogen and chemoattractant for the air sacs of the drosophila tracheal system. *Dev. Cell* **3,** 195–207 (2002).
52. Feinberg, E. H. *et al.* GFP Reconstitution Across Synaptic Partners (GRASP) defines cell contacts and synapses in living nervous systems. *Neuron* **57,** 353–363 (2008).
53. Roy, S., Huang, H., Liu, S. & Kornberg, T. B. Cytoneme-Mediated Contact-Dependent Transport of the Drosophila Decapentaplegic Signaling Protein. *Science* (2014). doi:10.1126/science.1244624
54. Bischoff, M. *et al.* Cytonemes are required for the establishment of a normal Hedgehog morphogen gradient in Drosophila epithelia. *Nat. Cell Biol.* **15,** 1269–1281 (2013).
55. Peng, Y., Han, C. & Axelrod, J. D. Planar Polarized Protrusions Break the Symmetry of EGFR Signaling during Drosophila Bract Cell Fate Induction. *Dev. Cell* **23,** 507–518 (2012).
56. Davis, D. M. & Sowinski, S. Membrane nanotubes: dynamic long-distance connections between animal cells. *Nat. Rev. Mol. Cell Biol.* **9,** 431–436 (2008).
57. Rustom, A., Saffrich, R., Markovic, I., Walther, P. & Gerdes, H.-H. Nanotubular highways for intercellular organelle transport. *Science* **303,** 1007–1010 (2004).
58. Salas-Vidal, E. & Lomelí, H. Imaging filopodia dynamics in the mouse blastocyst. *Dev. Biol.* **265,** 75–89 (2004).
59. Calleja, M. *et al.* How to pattern an epithelium: lessons from achaete-scute regulation on the notum of Drosophila. *Gene* **292,** 1–12 (2002).
60. Sato, M., Kojima, T., Michiue, T. & Saigo, K. Bar homeobox genes are latitudinal prepattern genes in the developing Drosophila notum whose expression is regulated by the concerted functions of decapentaplegic and wingless. *Dev. Camb. Engl.* **126,** 1457–1466 (1999).
61. Pistillo, D., Skaer, N. & Simpson, P. scute expression in Calliphora vicina reveals an ancestral pattern of longitudinal stripes on the thorax of higher diptera. *Development* **129,** 563–572 (2002).
62. Tomoyasu, Y., Ueno, N. & Nakamura, M. The decapentaplegic morphogen gradient regulates the notal wingless expression through induction of pannier and u-shaped in Drosophila. *Mech. Dev.* **96,** 37–49 (2000).
63. Haenlin, M. *et al.* Transcriptional activity of Pannier is regulated negatively by heterodimerization of the GATA DNA-binding domain with a cofactor encoded by the u-shaped gene of Drosophila. *Genes Dev.* **11,** 3096–3108 (1997).
64. Cubadda, Y. *et al.* u-shaped encodes a zinc finger protein that regulates the proneural genes achaete and scute during the formation of bristles in Drosophila. *Genes Dev.* **11,** 3083–3095 (1997).
65. Green, R. B., Hatini, V., Johansen, K. A., Liu, X.-J. & Lengyel, J. A. Drumstick is a zinc finger protein that antagonizes Lines to control patterning and morphogenesis of the Drosophila hindgut. *Dev. Camb. Engl.* **129,** 3645–3656 (2002).
66. Hatini, V., Green, R. B., Lengyel, J. A., Bray, S. J. & Dinardo, S. The Drumstick/Lines/Bowl regulatory pathway links antagonistic Hedgehog and Wingless signaling inputs to epidermal cell differentiation. *Genes Dev.* **19,** 709–718 (2005).
67. Iwaki, D. D., Johansen, K. A., Singer, J. B. & Lengyel, J. A. drumstick, bowl, and lines are required for patterning and cell rearrangement in the Drosophila embryonic hindgut. *Dev. Biol.* **240,** 611–626 (2001).
68. Johansen, K. A., Green, R. B., Iwaki, D. D., Hernandez, J. B. & Lengyel, J. A. The Drm-Bowl-Lin relief-of-repression hierarchy controls fore- and hindgut patterning and morphogenesis. *Mech. Dev.* **120,** 1139–1151 (2003).
69. Dinardo, S., Okegbe, T., Wingert, L., Freilich, S. & Terry, N. lines and bowl affect the specification of cyst stem cells and niche cells in the Drosophila testis. *Dev. Camb. Engl.* **138,** 1687–1696 (2011).
70. Nusinow, D., Greenberg, L. & Hatini, V. Reciprocal roles for bowl and lines in specifying the peripodial epithelium and the disc proper of the Drosophila wing primordium. *Dev. Camb. Engl.* **135,** 3031–3041 (2008).

71. Greenberg, L. & Hatini, V. Essential roles for lines in mediating leg and antennal proximodistal patterning and generating a stable Notch signaling interface at segment borders. *Dev. Biol.* **330,** 93–104 (2009).
72. Hao, I., Green, R. B., Dunaevsky, O., Lengyel, J. A. & Rauskolb, C. The odd-skipped family of zinc finger genes promotes Drosophila leg segmentation. *Dev. Biol.* **263,** 282–295 (2003).
73. Micchelli, C. A. & Blair, S. S. Dorsoventral lineage restriction in wing imaginal discs requires Notch. *Nature* **401,** 473–476 (1999).
74. Rauskolb, C., Correia, T. & Irvine, K. D. Fringe-dependent separation of dorsal and ventral cells in the Drosophila wing. *Nature* **401,** 476–480 (1999).
75. Major, R. J. & Irvine, K. D. Influence of Notch on dorsoventral compartmentalization and actin organization in the Drosophila wing. *Dev. Camb. Engl.* **132,** 3823–3833 (2005).
76. Major, R. J. & Irvine, K. D. Localization and requirement for Myosin II at the dorsal-ventral compartment boundary of the Drosophila wing. *Dev. Dyn. Off. Publ. Am. Assoc. Anat.* **235,** 3051–3058 (2006).
77. Landsberg, K. P. *et al.* Increased Cell Bond Tension Governs Cell Sorting at the Drosophila Anteroposterior Compartment Boundary. *Curr. Biol.* **19,** 1950–1955 (2009).
78. Monier, B., Pélissier-Monier, A., Brand, A. H. & Sanson, B. An actomyosin-based barrier inhibits cell mixing at compartmental boundaries in Drosophila embryos. *Nat. Cell Biol.* **12,** 60–65 (2010).
79. Simone, R. P. & DiNardo, S. Actomyosin contractility and Discs large contribute to junctional conversion in guiding cell alignment within the Drosophila embryonic epithelium. *Dev. Camb. Engl.* **137,** 1385–1394 (2010).
80. Townes, P. L. & Holtfreter, J. Directed movements and selective adhesion of embryonic amphibian cells. *J. Exp. Zool.* **128,** 53–120 (1955).
81. STEINBERG, M. S. Reconstruction of tissues by dissociated cells. Some morphogenetic tissue movements and the sorting out of embryonic cells may have a common explanation. *Science* **141,** 401–408 (1963).
82. Redies, C. Cadherins in the central nervous system. *Prog. Neurobiol.* **61,** 611–648 (2000).
83. Fishell, G., Mason, C. A. & Hatten, M. E. Dispersion of neural progenitors within the germinal zones of the forebrain. *Nature* **362,** 636–638 (1993).
84. Inoue, T. *et al.* Role of cadherins in maintaining the compartment boundary between the cortex and striatum during development. *Dev. Camb. Engl.* **128,** 561–569 (2001).
85. Inoue, T., Chisaka, O., Matsunami, H. & Takeichi, M. Cadherin-6 expression transiently delineates specific rhombomeres, other neural tube subdivisions, and neural crest subpopulations in mouse embryos. *Dev. Biol.* **183,** 183–194 (1997).
86. Fraser, S., Keynes, R. & Lumsden, A. Segmentation in the chick embryo hindbrain is defined by cell lineage restrictions. *Nature* **344,** 431–435 (1990).
87. Guthrie, S., Prince, V. & Lumsden, A. Selective dispersal of avian rhombomere cells in orthotopic and heterotopic grafts. *Dev. Camb. Engl.* **118,** 527–538 (1993).
88. Wizenmann, A. & Lumsden, A. Segregation of rhombomeres by differential chemoaffinity. *Mol. Cell. Neurosci.* **9,** 448–459 (1997).
89. Lumsden, A. & Krumlauf, R. Patterning the vertebrate neuraxis. *Science* **274,** 1109–1115 (1996).
90. Holland, S. J. *et al.* Bidirectional signalling through the EPH-family receptor Nuk and its transmembrane ligands. *Nature* **383,** 722–725 (1996).
91. Pasquale, E. B. Eph receptor signalling casts a wide net on cell behaviour. *Nat. Rev. Mol. Cell Biol.* **6,** 462–475 (2005).
92. Mellitzer, G., Xu, Q. & Wilkinson, D. G. Control of cell behaviour by signalling through Eph receptors and ephrins. *Curr. Opin. Neurobiol.* **10,** 400–408 (2000).
93. Xu, Q., Mellitzer, G., Robinson, V. & Wilkinson, D. G. In vivo cell sorting in complementary segmental domains mediated by Eph receptors and ephrins. *Nature* **399,** 267–271 (1999).
94. Flanagan, J. G. & Vanderhaeghen, P. The ephrins and Eph receptors in neural development. *Annu. Rev. Neurosci.* **21,** 309–345 (1998).

95. Cortina, C. *et al.* EphB-ephrin-B interactions suppress colorectal cancer progression by compartmentalizing tumor cells. *Nat. Genet.* **39,** 1376–1383 (2007).
96. Poliakov, A., Cotrina, M. L., Pasini, A. & Wilkinson, D. G. Regulation of EphB2 activation and cell repulsion by feedback control of the MAPK pathway. *J. Cell Biol.* **183,** 933–947 (2008).
97. Tanaka, M., Kamo, T., Ota, S. & Sugimura, H. Association of Dishevelled with Eph tyrosine kinase receptor and ephrin mediates cell repulsion. *EMBO J.* **22,** 847–858 (2003).
98. Dickinson, D. J., Nelson, W. J. & Weis, W. I. A polarized epithelium organized by β- and α-catenin predates cadherin and metazoan origins. *Science* **331,** 1336–1339 (2011).
99. Kim, N.-G., Koh, E., Chen, X. & Gumbiner, B. M. E-cadherin mediates contact inhibition of proliferation through Hippo signaling-pathway components. *Proc. Natl. Acad. Sci.* **108,** 11930–11935 (2011).
100. Schlegelmilch, K. *et al.* Yap1 Acts Downstream of α-Catenin to Control Epidermal Proliferation. *Cell* **144,** 782–795 (2011).
101. Cavey, M. & Lecuit, T. Molecular Bases of Cell–Cell Junctions Stability and Dynamics. *Cold Spring Harb. Perspect. Biol.* **1,** (2009).
102. Budnar, S. & Yap, A. S. A mechanobiological perspective on cadherins and the actin-myosin cytoskeleton. *F1000Prime Rep.* **5,** (2013).
103. Levayer, R. & Lecuit, T. Biomechanical regulation of contractility: spatial control and dynamics. *Trends Cell Biol.* **22,** 61–81 (2012).
104. Lecuit, T. & Lenne, P.-F. Cell surface mechanics and the control of cell shape, tissue patterns and morphogenesis. *Nat. Rev. Mol. Cell Biol.* **8,** 633–644 (2007).
105. Foty, R. A. & Steinberg, M. S. Differential adhesion in model systems. *Wiley Interdiscip. Rev. Dev. Biol.* **2,** 631–645 (2013).
106. Dahmann, C. & Basler, K. Opposing transcriptional outputs of Hedgehog signaling and engrailed control compartmental cell sorting at the Drosophila A/P boundary. *Cell* **100,** 411–422 (2000).
107. Hackett-Jones, E. J., Landman, K. A., Newgreen, D. F. & Zhang, D. On the role of differential adhesion in gangliogenesis in the enteric nervous system. *J. Theor. Biol.* **287,** 148–159 (2011).
108. Bao, S. & Cagan, R. Preferential Adhesion Mediated by Hibris and Roughest Regulates Morphogenesis and Patterning in the Drosophila Eye. *Dev. Cell* **8,** 925–935 (2005).
109. Hayashi, T. & Carthew, R. W. Surface mechanics mediate pattern formation in the developing retina. *Nature* **431,** 647–652 (2004).
110. Käfer, J., Hayashi, T., Marée, A. F. M., Carthew, R. W. & Graner, F. Cell adhesion and cortex contractility determine cell patterning in the Drosophila retina. *Proc. Natl. Acad. Sci. U. S. A.* **104,** 18549–18554 (2007).
111. Beysens, D. A., Forgacs, G. & Glazier, J. A. Cell sorting is analogous to phase ordering in fluids. *Proc. Natl. Acad. Sci. U. S. A.* **97,** 9467–9471 (2000).
112. Nose, A., Nagafuchi, A. & Takeichi, M. Expressed recombinant cadherins mediate cell sorting in model systems. *Cell* **54,** 993–1001 (1988).
113. Detrick, R. J., Dickey, D. & Kintner, C. R. The effects of N-cadherin misexpression on morphogenesis in Xenopus embryos. *Neuron* **4,** 493–506 (1990).
114. Fujimori, T., Miyatani, S. & Takeichi, M. Ectopic expression of N-cadherin perturbs histogenesis in Xenopus embryos. *Dev. Camb. Engl.* **110,** 97–104 (1990).
115. Niessen, C. M. & Gumbiner, B. M. Cadherin-mediated cell sorting not determined by binding or adhesion specificity. *J. Cell Biol.* **156,** 389–400 (2002).
116. Prakasam, A. K., Maruthamuthu, V. & Leckband, D. E. Similarities between heterophilic and homophilic cadherin adhesion. *Proc. Natl. Acad. Sci. U. S. A.* **103,** 15434–15439 (2006).
117. Foty, R. A. & Steinberg, M. S. The differential adhesion hypothesis: a direct evaluation. *Dev. Biol.* **278,** 255–263 (2005).
118. Youssef, J., Nurse, A. K., Freund, L. B. & Morgan, J. R. Quantification of the forces driving self-assembly of three-dimensional microtissues. *Proc. Natl. Acad. Sci. U. S. A.* **108,** 6993–6998 (2011).
119. Maître, J.-L. *et al.* Adhesion Functions in Cell Sorting by Mechanically Coupling the Cortices of Adhering Cells. *Science* **338,** 253–256 (2012).

120. Maruthamuthu, V., Sabass, B., Schwarz, U. S. & Gardel, M. L. Cell-ECM traction force modulates endogenous tension at cell-cell contacts. *Proc. Natl. Acad. Sci. U. S. A.* **108,** 4708–4713 (2011).
121. Mertz, A. F. *et al.* Scaling of traction forces with the size of cohesive cell colonies. *Phys. Rev. Lett.* **108,** 198101 (2012).
122. Harris, A. K. Is Cell sorting caused by differences in the work of intercellular adhesion? A critique of the Steinberg hypothesis. *J. Theor. Biol.* **61,** 267–285 (1976).
123. Brodland, G. W. The Differential Interfacial Tension Hypothesis (DITH): a comprehensive theory for the self-rearrangement of embryonic cells and tissues. *J. Biomech. Eng.* **124,** 188–197 (2002).
124. Wayne Brodland, G. & Chen, H. H. The mechanics of cell sorting and envelopment. *J. Biomech.* **33,** 845–851 (2000).
125. Amack, J. D. & Manning, M. L. Knowing the boundaries: Extending the differential adhesion hypothesis in embryonic cell sorting. *Science* **338,** 212–215 (2012).
126. Krieg, M. *et al.* Tensile forces govern germ-layer organization in zebrafish. *Nat. Cell Biol.* **10,** 429–436 (2008).
127. Krens, S. F. G., Möllmert, S. & Heisenberg, C.-P. Enveloping cell-layer differentiation at the surface of zebrafish germ-layer tissue explants. *Proc. Natl. Acad. Sci. U. S. A.* **108,** E9–10; author reply E11 (2011).
128. Laplante, C. & Nilson, L. A. Differential expression of the adhesion molecule Echinoid drives epithelial morphogenesis in Drosophila. *Dev. Camb. Engl.* **133,** 3255–3264 (2006).
129. Manning, M. L., Foty, R. A., Steinberg, M. S. & Schoetz, E.-M. Coaction of intercellular adhesion and cortical tension specifies tissue surface tension. *Proc. Natl. Acad. Sci. U. S. A.* **107,** 12517–12522 (2010).
130. Ivanov, A. I., McCall, I. C., Parkos, C. A. & Nusrat, A. Role for Actin Filament Turnover and a Myosin II Motor in Cytoskeleton-driven Disassembly of the Epithelial Apical Junctional Complex. *Mol. Biol. Cell* **15,** 2639–2651 (2004).
131. Ivanov, A. I., Hunt, D., Utech, M., Nusrat, A. & Parkos, C. A. Differential roles for actin polymerization and a myosin II motor in assembly of the epithelial apical junctional complex. *Mol. Biol. Cell* **16,** 2636–2650 (2005).
132. Krendel, M. F. & Bonder, E. M. Analysis of actin filament bundle dynamics during contact formation in live epithelial cells. *Cell Motil. Cytoskeleton* **43,** 296–309 (1999).
133. Shewan, A. M. *et al.* Myosin 2 Is a Key Rho Kinase Target Necessary for the Local Concentration of E-Cadherin at Cell–Cell Contacts. *Mol. Biol. Cell* **16,** 4531–4542 (2005).
134. Yamada, S. & Nelson, W. J. Localized zones of Rho and Rac activities drive initiation and expansion of epithelial cell-cell adhesion. *J. Cell Biol.* **178,** 517–527 (2007).
135. Larson, D. E. *et al.* Computer simulation of cellular patterning within the Drosophila pupal eye. *PLoS Comput. Biol.* **6,** e1000841 (2010).
136. Aigouy, B. *et al.* Cell Flow Reorients the Axis of Planar Polarity in the Wing Epithelium of Drosophila. *Cell* **142,** 773–786 (2010).
137. Bardet, P.-L. *et al.* PTEN controls junction lengthening and stability during cell rearrangement in epithelial tissue. *Dev. Cell* **25,** 534–546 (2013).
138. Bosveld, F. *et al.* Mechanical control of morphogenesis by fat/dachsous/four-jointed planar cell polarity pathway. *Science* **336,** 724–727 (2012).
139. Bertet, C., Sulak, L. & Lecuit, T. Myosin-dependent junction remodelling controls planar cell intercalation and axis elongation. *Nature* **429,** 667–671 (2004).
140. Levayer, R. & Lecuit, T. Oscillation and polarity of E-cadherin asymmetries control actomyosin flow patterns during morphogenesis. *Dev. Cell* **26,** 162–175 (2013).
141. Levayer, R., Pelissier-Monier, A. & Lecuit, T. Spatial regulation of Dia and Myosin-II by RhoGEF2 controls initiation of E-cadherin endocytosis during epithelial morphogenesis. *Nat. Cell Biol.* **13,** 529–540 (2011).
142. Rauzi, M., Lenne, P.-F. & Lecuit, T. Planar polarized actomyosin contractile flows control epithelial junction remodelling. *Nature* **468,** 1110–1114 (2010).

143. Vaezi, A., Bauer, C., Vasioukhin, V. & Fuchs, E. Actin cable dynamics and Rho/Rock orchestrate a polarized cytoskeletal architecture in the early steps of assembling a stratified epithelium. *Dev. Cell* **3,** 367–381 (2002).
144. Bershadsky, A. Magic touch: how does cell-cell adhesion trigger actin assembly? *Trends Cell Biol.* **14,** 589–593 (2004).
145. Vasioukhin, V., Bauer, C., Yin, M. & Fuchs, E. Directed Actin Polymerization Is the Driving Force for Epithelial Cell–Cell Adhesion. *Cell* **100,** 209–219 (2000).
146. Kobielak, A., Pasolli, H. A. & Fuchs, E. Mammalian formin-1 participates in adherens junctions and polymerization of linear actin cables. *Nat. Cell Biol.* **6,** 21–30 (2004).
147. Kovacs, E. M., Goodwin, M., Ali, R. G., Paterson, A. D. & Yap, A. S. Cadherin-Directed Actin Assembly: E-Cadherin Physically Associates with the Arp2/3 Complex to Direct Actin Assembly in Nascent Adhesive Contacts. *Curr. Biol.* **12,** 379–382 (2002).
148. Daly, R. J. Cortactin signalling and dynamic actin networks. *Biochem. J.* **382,** 13–25 (2004).
149. Verma, S. *et al.* Arp2/3 Activity Is Necessary for Efficient Formation of E-cadherin Adhesive Contacts. *J. Biol. Chem.* **279,** 34062–34070 (2004).
150. Helwani, F. M. *et al.* Cortactin is necessary for E-cadherin–mediated contact formation and actin reorganization. *J. Cell Biol.* **164,** 899–910 (2004).
151. Ehrlich, J. S., Hansen, M. D. H. & Nelson, W. J. Spatio-temporal regulation of Rac1 localization and lamellipodia dynamics during epithelial cell-cell adhesion. *Dev. Cell* **3,** 259–270 (2002).
152. Herszterg, S., Leibfried, A., Bosveld, F., Martin, C. & Bellaiche, Y. Interplay between the Dividing Cell and Its Neighbors Regulates Adherens Junction Formation during Cytokinesis in Epithelial Tissue. *Dev. Cell* **24,** 256–270 (2013).
153. Krendel, M. *et al.* Myosin-dependent contractile activity of the actin cytoskeleton modulates the spatial organization of cell–cell contacts in cultured epitheliocytes. *Proc. Natl. Acad. Sci.* **96,** 9666–9670 (1999).
154. Gloushankova, N. A. *et al.* Cell–cell contact changes the dynamics of lamellar activity in nontransformed epitheliocytes but not in their ras-transformed descendants. *Proc. Natl. Acad. Sci.* **94,** 879–883 (1997).
155. Adams, C. L., Chen, Y.-T., Smith, S. J. & Nelson, W. J. Mechanisms of Epithelial Cell–Cell Adhesion and Cell Compaction Revealed by High-resolution Tracking of E-Cadherin– Green Fluorescent Protein. *J. Cell Biol.* **142,** 1105–1119 (1998).
156. Kametani, Y. & Takeichi, M. Basal-to-apical cadherin flow at cell junctions. *Nat. Cell Biol.* **9,** 92–98 (2007).
157. Angres, B., Barth, A. & Nelson, W. J. Mechanism for transition from initial to stable cell-cell adhesion: kinetic analysis of E-cadherin-mediated adhesion using a quantitative adhesion assay. *J. Cell Biol.* **134,** 549–557 (1996).
158. Yap, A. S., Brieher, W. M., Pruschy, M. & Gumbiner, B. M. Lateral clustering of the adhesive ectodomain: a fundamental determinant of cadherin function. *Curr. Biol. CB* **7,** 308–315 (1997).
159. Hong, S., Troyanovsky, R. B. & Troyanovsky, S. M. Binding to F-actin guides cadherin cluster assembly, stability, and movement. *J. Cell Biol.* **201,** 131–143 (2013).
160. Gowrishankar, K. *et al.* Active remodeling of cortical actin regulates spatiotemporal organization of cell surface molecules. *Cell* **149,** 1353–1367 (2012).
161. Cavey, M., Rauzi, M., Lenne, P.-F. & Lecuit, T. A two-tiered mechanism for stabilization and immobilization of E-cadherin. *Nature* **453,** 751–756 (2008).
162. Martin, A. C., Gelbart, M., Fernandez-Gonzalez, R., Kaschube, M. & Wieschaus, E. F. Integration of contractile forces during tissue invagination. *J. Cell Biol.* **188,** 735–749 (2010).
163. Tabdanov, E., Borghi, N., Brochard-Wyart, F., Dufour, S. & Thiery, J.-P. Role of E-Cadherin in Membrane-Cortex Interaction Probed by Nanotube Extrusion. *Biophys. J.* **96,** 2457–2465 (2009).
164. Maître, J.-L. & Heisenberg, C.-P. The role of adhesion energy in controlling cell-cell contacts. *Curr. Opin. Cell Biol.* **23,** 508–514 (2011).
165. Twiss, F. & De Rooij, J. Cadherin mechanotransduction in tissue remodeling. *Cell. Mol. Life Sci.* **70,** 4101–4116 (2013).

166. Bray, D. & White, J. G. Cortical flow in animal cells. *Science* **239,** 883–888 (1988).
167. Werner, M., Munro, E. & Glotzer, M. Astral Signals Spatially Bias Cortical Myosin Recruitment to Break Symmetry and Promote Cytokinesis. *Curr. Biol.* **17,** 1286–1297 (2007).
168. Mayer, M., Depken, M., Bois, J. S., Jülicher, F. & Grill, S. W. Anisotropies in cortical tension reveal the physical basis of polarizing cortical flows. *Nature* **467,** 617–621 (2010).
169. Munro, E., Nance, J. & Priess, J. R. Cortical Flows Powered by Asymmetrical Contraction Transport PAR Proteins to Establish and Maintain Anterior-Posterior Polarity in the Early C. elegans Embryo. *Dev. Cell* **7,** 413–424 (2004).
170. Irvine, K. D. & Wieschaus, E. Cell intercalation during Drosophila germband extension and its regulation by pair-rule segmentation genes. *Development* **120,** 827–841 (1994).
171. Bertet, C., Sulak, L. & Lecuit, T. Myosin-dependent junction remodelling controls planar cell intercalation and axis elongation. *Nature* **429,** 667–671 (2004).
172. Zallen, J. A. & Zallen, R. Cell-pattern disordering during convergent extension in Drosophila. *J. Phys. Condens. Matter* **16,** S5073 (2004).
173. Blankenship, J. T., Backovic, S. T., Sanny, J. S. P., Weitz, O. & Zallen, J. A. Multicellular Rosette Formation Links Planar Cell Polarity to Tissue Morphogenesis. *Dev. Cell* **11,** 459–470 (2006).
174. Fernandez-Gonzalez, R. & Zallen, J. A. Oscillatory behaviors and hierarchical assembly of contractile structures in intercalating cells. *Phys. Biol.* **8,** 045005 (2011).
175. Zallen, J. A. & Wieschaus, E. Patterned Gene Expression Directs Bipolar Planar Polarity in Drosophila. *Dev. Cell* **6,** 343–355 (2004).
176. Tamada, M., Farrell, D. L. & Zallen, J. A. Abl Regulates Planar Polarized Junctional Dynamics through β-Catenin Tyrosine Phosphorylation. *Dev. Cell* **22,** 309–319 (2012).
177. Simões, S. de M. *et al.* Rho-Kinase Directs Bazooka/Par-3 Planar Polarity during Drosophila Axis Elongation. *Dev. Cell* **19,** 377–388 (2010).
178. Mori, M. *et al.* Intracellular Transport by an Anchored Homogeneously Contracting F-Actin Meshwork. *Curr. Biol.* **21,** 606–611 (2011).
179. Huang, Y. E. *et al.* Receptor-mediated Regulation of PI3Ks Confines PI(3,4,5)P3 to the Leading Edge of Chemotaxing Cells. *Mol. Biol. Cell* **14,** 1913–1922 (2003).
180. Paluch, E., Piel, M., Prost, J., Bornens, M. & Sykes, C. Cortical Actomyosin Breakage Triggers Shape Oscillations in Cells and Cell Fragments. *Biophys. J.* **89,** 724–733 (2005).
181. Murthy, K. & Wadsworth, P. Myosin-II-Dependent Localization and Dynamics of F-Actin during Cytokinesis. *Curr. Biol.* **15,** 724–731 (2005).
182. Duc, Q. le *et al.* Vinculin potentiates E-cadherin mechanosensing and is recruited to actin-anchored sites within adherens junctions in a myosin II–dependent manner. *J. Cell Biol.* **189,** 1107–1115 (2010).
183. Liu, Z. *et al.* Mechanical tugging force regulates the size of cell–cell junctions. *Proc. Natl. Acad. Sci.* **107,** 9944–9949 (2010).
184. Yonemura, S., Wada, Y., Watanabe, T., Nagafuchi, A. & Shibata, M. α-Catenin as a tension transducer that induces adherens junction development. *Nat. Cell Biol.* **12,** 533–542 (2010).
185. Cremo, C. R. & Geeves, M. A. Interaction of Actin and ADP with the Head Domain of Smooth Muscle Myosin: Implications for Strain-Dependent ADP Release in Smooth Muscle†. *Biochemistry (Mosc.)* **37,** 1969–1978 (1998).
186. Kee, Y.-S. & Robinson, D. N. Motor Proteins: Myosin Mechanosensors. *Curr. Biol.* **18,** R860–R862 (2008).
187. Kovács, M., Thirumurugan, K., Knight, P. J. & Sellers, J. R. Load-dependent mechanism of nonmuscle myosin 2. *Proc. Natl. Acad. Sci.* **104,** 9994–9999 (2007).
188. Martin, A. C., Kaschube, M. & Wieschaus, E. F. Pulsed contractions of an actin–myosin network drive apical constriction. *Nature* **457,** 495–499 (2009).
189. Costa, M., Wilson, E. T. & Wieschaus, E. A putative cell signal encoded by the folded gastrulation gene coordinates cell shape changes during Drosophila gastrulation. *Cell* **76,** 1075–1089 (1994).

190. Kölsch, V., Seher, T., Fernandez-Ballester, G. J., Serrano, L. & Leptin, M. Control of Drosophila Gastrulation by Apical Localization of Adherens Junctions and RhoGEF2. *Science* **315,** 384–386 (2007).
191. Mason, F. M., Tworoger, M. & Martin, A. C. Apical domain polarization localizes actin-myosin activity to drive ratchet-like apical constriction. *Nat. Cell Biol.* **15,** 926–936 (2013).
192. Greenberg, L. & Hatini, V. Systematic expression and loss-of-function analysis defines spatially restricted requirements for Drosophila RhoGEFs and RhoGAPs in leg morphogenesis. *Mech. Dev.* **128,** 5–17 (January).
193. Manjon, C., Sanchez-Herrero, E. & Suzanne, M. Sharp boundaries of Dpp signalling trigger local cell death required for Drosophila leg morphogenesis. *Nat Cell Biol* **9,** 57–63 (2007).
194. Mirth, C. & Akam, M. Joint Development in the Drosophila Leg: Cell Movements and Cell Populations. *Dev. Biol.* **246,** 391–406 (2002).
195. Tajiri, R., Misaki, K., Yonemura, S. & Hayashi, S. Dynamic shape changes of ECM-producing cells drive morphogenesis of ball-and-socket joints in the fly leg. *Development* **137,** 2055 –2063 (2010).
196. Wang, Y.-C., Khan, Z., Kaschube, M. & Wieschaus, E. F. Differential positioning of adherens junctions is associated with initiation of epithelial folding. *Nature* **484,** 390–393 (2012).
197. Wang, Y.-C., Khan, Z. & Wieschaus, E. F. Distinct Rap1 activity states control the extent of epithelial invagination via α-catenin. *Dev. Cell* **25,** 299–309 (2013).
198. Haigo, S. L., Hildebrand, J. D., Harland, R. M. & Wallingford, J. B. Shroom Induces Apical Constriction and Is Required for Hingepoint Formation during Neural Tube Closure. *Curr. Biol.* **13,** 2125–2137 (2003).
199. Roh-Johnson, M. *et al.* Triggering a Cell Shape Change by Exploiting Preexisting Actomyosin Contractions. *Science* **335,** 1232–1235 (2012).
200. Sawyer, J. K. *et al.* A contractile actomyosin network linked to adherens junctions by Canoe/afadin helps drive convergent extension. *Mol. Biol. Cell* **22,** 2491–2508 (2011).
201. Balaban, N. Q. *et al.* Force and focal adhesion assembly: a close relationship studied using elastic micropatterned substrates. *Nat. Cell Biol.* **3,** 466–472 (2001).
202. Del Rio, A. *et al.* Stretching single talin rod molecules activates vinculin binding. *Science* **323,** 638–641 (2009).
203. Riveline, D. *et al.* Focal contacts as mechanosensors: externally applied local mechanical force induces growth of focal contacts by an mDia1-dependent and ROCK-independent mechanism. *J. Cell Biol.* **153,** 1175–1186 (2001).
204. Borghi, N. *et al.* E-cadherin is under constitutive actomyosin-generated tension that is increased at cell–cell contacts upon externally applied stretch. *Proc. Natl. Acad. Sci.* **109,** 12568–12573 (2012).
205. Conway, D. E. *et al.* Fluid shear stress on endothelial cells modulates mechanical tension across VE-cadherin and PECAM-1. *Curr. Biol. CB* **23,** 1024–1030 (2013).
206. Huveneers, S. *et al.* Vinculin associates with endothelial VE-cadherin junctions to control force-dependent remodeling. *J. Cell Biol.* **196,** 641–652 (2012).
207. Liu, Z. *et al.* Mechanical tugging force regulates the size of cell-cell junctions. *Proc. Natl. Acad. Sci. U. S. A.* **107,** 9944–9949 (2010).
208. Fernandez-Gonzalez, R., Simoes, S. de M., Röper, J.-C., Eaton, S. & Zallen, J. A. Myosin II Dynamics Are Regulated by Tension in Intercalating Cells. *Dev. Cell* **17,** 736–743 (2009).
209. Di Paolo, G. & De Camilli, P. Phosphoinositides in cell regulation and membrane dynamics. *Nature* **443,** 651–657 (2006).
210. Bernards, A. GAPs galore! A survey of putative Ras superfamily GTPase activating proteins in man and Drosophila. *Biochim. Biophys. Acta BBA - Rev. Cancer* **1603,** 47–82 (2003).
211. Bos, J. L., Rehmann, H. & Wittinghofer, A. GEFs and GAPs: Critical Elements in the Control of Small G Proteins. *Cell* **129,** 865–877 (2007).
212. Guilluy, C., Garcia-Mata, R. & Burridge, K. Rho protein crosstalk: another social network? *Trends Cell Biol.* **21,** 718–726 (2011).
213. Rossman, K. L., Der, C. J. & Sondek, J. GEF means go: turning on RHO GTPases with guanine nucleotide-exchange factors. *Nat. Rev. Mol. Cell Biol.* **6,** 167–180 (2005).

214. Xu, J. *et al.* Divergent Signals and Cytoskeletal Assemblies Regulate Self-Organizing Polarity in Neutrophils. *Cell* **114,** 201–214 (2003).
215. Iglesias, P. A. Spatial regulation of PI3K signaling during chemotaxis. *Wiley Interdiscip. Rev. Syst. Biol. Med.* **1,** 247–253 (2009).
216. Funamoto, S., Meili, R., Lee, S., Parry, L. & Firtel, R. A. Spatial and Temporal Regulation of 3-Phosphoinositides by PI 3-Kinase and PTEN Mediates Chemotaxis. *Cell* **109,** 611–623 (2002).
217. Niggli, V. A membrane-permeant ester of phosphatidylinositol 3,4,5-trisphosphate (PIP3) is an activator of human neutrophil migration. *FEBS Lett.* **473,** 217–221 (2000).
218. Iijima, M. & Devreotes, P. Tumor Suppressor PTEN Mediates Sensing of Chemoattractant Gradients. *Cell* **109,** 599–610 (2002).
219. Nishio, M. *et al.* Control of cell polarity and motility by the PtdIns(3,4,5)P3 phosphatase SHIP1. *Nat. Cell Biol.* **9,** 36–44 (2007).
220. Côté, J.-F., Motoyama, A. B., Bush, J. A. & Vuori, K. A novel and evolutionarily conserved PtdIns(3,4,5)P3-binding domain is necessary for DOCK180 signalling. *Nat. Cell Biol.* **7,** 797–807 (2005).
221. Kunisaki, Y. *et al.* DOCK2 is a Rac activator that regulates motility and polarity during neutrophil chemotaxis. *J. Cell Biol.* **174,** 647–652 (2006).
222. Weiner, O. D. *et al.* A PtdInsP3- and Rho GTPase-mediated positive feedback loop regulates neutrophil polarity. *Nat. Cell Biol.* **4,** 509–513 (2002).
223. Benard, V., Bohl, B. P. & Bokoch, G. M. Characterization of Rac and Cdc42 Activation in Chemoattractant-stimulated Human Neutrophils Using a Novel Assay for Active GTPases. *J. Biol. Chem.* **274,** 13198–13204 (1999).
224. Hawkins, P. T. *et al.* PDGF stimulates an increase in GTP–Rac via activation of phosphoinositide 3-kinase. *Curr. Biol.* **5,** 393–403 (1995).
225. Genot, E. M. *et al.* The T-Cell Receptor Regulates Akt (Protein Kinase B) via a Pathway Involving Rac1 and Phosphatidylinositide 3-Kinase. *Mol. Cell. Biol.* **20,** 5469–5478 (2000).
226. Yoo, S. K. *et al.* Differential Regulation of Protrusion and Polarity by PI(3)K during Neutrophil Motility in Live Zebrafish. *Dev. Cell* **18,** 226–236 (2010).
227. Loovers, H. M. *et al.* Distinct roles of PI(3,4,5)P3 during chemoattractant signaling in Dictyostelium: a quantitative in vivo analysis by inhibition of PI3-kinase. *Mol. Biol. Cell* **17,** 1503–1513 (2006).
228. Bosgraaf, L., Keizer-Gunnink, I. & Haastert, P. J. M. V. PI3-kinase signaling contributes to orientation in shallow gradients and enhances speed in steep chemoattractant gradients. *J. Cell Sci.* **121,** 3589–3597 (2008).
229. Ferguson, G. J. *et al.* PI(3)Kγ has an important context-dependent role in neutrophil chemokinesis. *Nat. Cell Biol.* **9,** 86–91 (2007).
230. Gruver, J. S., Wikswo, J. P. & Chung, C. Y. 3'-phosphoinositides regulate the coordination of speed and accuracy during chemotaxis. *Biophys. J.* **95,** 4057–4067 (2008).
231. Wang, F. *et al.* Lipid products of PI(3)Ks maintain persistent cell polarity and directed motility in neutrophils. *Nat. Cell Biol.* **4,** 513–518 (2002).
232. Pestonjamasp, K. N. *et al.* Rac1 links leading edge and uropod events through Rho and myosin activation during chemotaxis. *Blood* **108,** 2814–2820 (2006).
233. Van Keymeulen, A. *et al.* To stabilize neutrophil polarity, PIP3 and Cdc42 augment RhoA activity at the back as well as signals at the front. *J. Cell Biol.* **174,** 437–445 (2006).
234. Xiong, Y., Huang, C.-H., Iglesias, P. A. & Devreotes, P. N. Cells navigate with a local-excitation, global-inhibition-biased excitable network. *Proc. Natl. Acad. Sci. U. S. A.* **107,** 17079–17086 (2010).
235. Pramanik, M. K., Iijima, M., Iwadate, Y. & Yumura, S. PTEN is a mechanosensing signal transducer for myosin II localization in Dictyostelium cells. *Genes Cells Devoted Mol. Cell. Mech.* **14,** 821–834 (2009).
236. Subauste, M. C., Nalbant, P., Adamson, E. D. & Hahn, K. M. Vinculin Controls PTEN Protein Level by Maintaining the Interaction of the Adherens Junction Protein β-Catenin with the Scaffolding Protein MAGI-2. *J. Biol. Chem.* **280,** 5676–5681 (2005).
237. White, T. H. *The once and future king*. (Ace Books, 1987).

238. Kurokawa, K. & Matsuda, M. Localized RhoA Activation as a Requirement for the Induction of Membrane Ruffling. *Mol. Biol. Cell* **16,** 4294–4303 (2005).
239. Pertz, O., Hodgson, L., Klemke, R. L. & Hahn, K. M. Spatiotemporal dynamics of RhoA activity in migrating cells. *Nature* **440,** 1069–1072 (2006).
240. Machacek, M. *et al.* Coordination of Rho GTPase activities during cell protrusion. *Nature* **461,** 99–103 (2009).
241. Benink, H. A. & Bement, W. M. Concentric zones of active RhoA and Cdc42 around single cell wounds. *J. Cell Biol.* **168,** 429–439 (2005).
242. Mandato, C. A. & Bement, W. M. Contraction and polymerization cooperate to assemble and close actomyosin rings around Xenopus oocyte wounds. *J. Cell Biol.* **154,** 785–797 (2001).
243. Bement, W. M., Benink, H. A. & Dassow, G. von. A microtubule-dependent zone of active RhoA during cleavage plane specification. *J. Cell Biol.* **170,** 91–101 (2005).
244. Shewan, A., Eastburn, D. J. & Mostov, K. Phosphoinositides in cell architecture. *Cold Spring Harb. Perspect. Biol.* **3,** a004796 (2011).
245. Gassama-Diagne, A. *et al.* Phosphatidylinositol-3,4,5-trisphosphate regulates the formation of the basolateral plasma membrane in epithelial cells. *Nat. Cell Biol.* **8,** 963–970 (2006).
246. Jeanes, A., Smutny, M., Leerberg, J. M. & Yap, A. S. Phosphatidylinositol 3'-kinase signalling supports cell height in established epithelial monolayers. *J. Mol. Histol.* **40,** 395–405 (2009).
247. Martin-Belmonte, F. *et al.* PTEN-Mediated Apical Segregation of Phosphoinositides Controls Epithelial Morphogenesis through Cdc42. *Cell* **128,** 383–397 (2007).
248. Von Stein, W., Ramrath, A., Grimm, A., Müller-Borg, M. & Wodarz, A. Direct association of Bazooka/PAR-3 with the lipid phosphatase PTEN reveals a link between the PAR/aPKC complex and phosphoinositide signaling. *Development* **132,** 1675 –1686 (2005).
249. Yu, W. *et al.* β1-Integrin Orients Epithelial Polarity via Rac1 and Laminin. *Mol. Biol. Cell* **16,** 433–445 (2005).
250. Pinal, N. *et al.* Regulated and Polarized PtdIns(3,4,5)P3 Accumulation Is Essential for Apical Membrane Morphogenesis in Photoreceptor Epithelial Cells. *Curr. Biol.* **16,** 140–149 (2006).
251. Cain, R. J. & Ridley, A. J. Phosphoinositide 3-kinases in cell migration. *Biol. Cell Auspices Eur. Cell Biol. Organ.* **101,** 13–29 (2009).
252. David, D. J. V., Tishkina, A. & Harris, T. J. C. The PAR complex regulates pulsed actomyosin contractions during amnioserosa apical constriction in Drosophila. *Development* **137,** 1645–1655 (2010).
253. Gorfinkiel, N., Blanchard, G. B., Adams, R. J. & Arias, A. M. Mechanical control of global cell behaviour during dorsal closure in Drosophila. *Development* **136,** 1889–1898 (2009).
254. Solon, J., Kaya-Çopur, A., Colombelli, J. & Brunner, D. Pulsed Forces Timed by a Ratchet-like Mechanism Drive Directed Tissue Movement during Dorsal Closure. *Cell* **137,** 1331–1342 (2009).
255. Kiehart, D. P., Galbraith, C. G., Edwards, K. A., Rickoll, W. L. & Montague, R. A. Multiple Forces Contribute to Cell Sheet Morphogenesis for Dorsal Closure in Drosophila. *J. Cell Biol.* **149,** 471–490 (2000).
256. Woolner, S., Jacinto, A. & Martin, P. The small GTPase Rac plays multiple roles in epithelial sheet fusion--dynamic studies of Drosophila dorsal closure. *Dev. Biol.* **282,** 163–173 (2005).
257. Pickering, K., Alves-Silva, J., Goberdhan, D. & Millard, T. H. Par3/Bazooka and phosphoinositides regulate actin protrusion formation during Drosophila dorsal closure and wound healing. *Dev. Camb. Engl.* **140,** 800–809 (2013).
258. Green, P., Hartenstein, A. Y. & Hartenstein, V. The embryonic development of the Drosophila visual system. *Cell Tissue Res.* **273,** 583–598 (1993).
259. Cagan, R. L. & Ready, D. F. The emergence of order in the Drosophila pupal retina. *Dev. Biol.* **136,** 346–362 (1989).
260. Kumar, J. P. Retinal determination the beginning of eye development. *Curr. Top. Dev. Biol.* **93,** 1–28 (2010).
261. Kumar, J. P. My what big eyes you have: How the Drosophila retina grows. *Dev. Neurobiol.* **71,** 1133–1152 (2011).

262. Kumar, J. P. Building an ommatidium one cell at a time. *Dev. Dyn.* **241,** 136–149 (2012).
263. Charlton-Perkins, M., Brown, N. L. & Cook, T. A. The lens in focus: a comparison of lens development in Drosophila and vertebrates. *Mol. Genet. Genomics MGG* **286,** 189–213 (2011).
264. Charlton-Perkins, M. & Cook, T. A. Building a fly eye: terminal differentiation events of the retina, corneal lens, and pigmented epithelia. *Curr. Top. Dev. Biol.* **93,** 129–173 (2010).
265. Johnson, R. I., Sedgwick, A., D'Souza-Schorey, C. & Cagan, R. L. Role for a Cindr-Arf6 axis in patterning emerging epithelia. *Mol. Biol. Cell* **22,** 4513–4526 (2011).
266. Nagaraj, R. & Banerjee, U. Combinatorial signaling in the specification of primary pigment cells in the Drosophila eye. *Dev. Camb. Engl.* **134,** 825–831 (2007).
267. Carthew, R. W. Pattern formation in the Drosophila eye. *Curr. Opin. Genet. Dev.* **17,** 309–313 (2007).
268. Bao, S., Fischbach, K.-F., Corbin, V. & Cagan, R. L. Preferential adhesion maintains separation of ommatidia in the Drosophila eye. *Dev. Biol.* **344,** 948–956 (2010).
269. Reiter, C., Schimansky, T., Nie, Z. & Fischbach, K.-F. Reorganization of membrane contacts prior to apoptosis in the Drosophila retina: The role of the IrreC-rst protein. *Development* **122,** 1931–1940 (1996).
270. Johnson, R. I., Seppa, M. J. & Cagan, R. L. The Drosophila CD2AP/CIN85 orthologue Cindr regulates junctions and cytoskeleton dynamics during tissue patterning. *J. Cell Biol.* **180,** 1191–1204 (2008).
271. Santy, L. C., Ravichandran, K. S. & Casanova, J. E. The DOCK180/Elmo Complex Couples ARNO-Mediated Arf6 Activation to the Downstream Activation of Rac1. *Curr. Biol.* **15,** 1749–1754 (2005).
272. Myers, K. R. & Casanova, J. E. Regulation of actin cytoskeleton dynamics by Arf-family GTPases. *Trends Cell Biol.* **18,** 184–192 (2008).
273. Brown, H. A., Gutowski, S., Moomaw, C. R., Slaughter, C. & Sternweis, P. C. ADP-ribosylation factor, a small GTP-dependent regulatory protein, stimulates phospholipase D activity. *Cell* **75,** 1137–1144 (1993).
274. Honda, A. *et al.* Phosphatidylinositol 4-phosphate 5-kinase alpha is a downstream effector of the small G protein ARF6 in membrane ruffle formation. *Cell* **99,** 521–532 (1999).
275. Perrimon, N., Pitsouli, C. & Shilo, B.-Z. Signaling Mechanisms Controlling Cell Fate and Embryonic Patterning. *Cold Spring Harb. Perspect. Biol.* **4,** a005975 (2012).
276. Grieder, N. C., Morata, G., Affolter, M. & Gehring, W. J. Spalt major controls the development of the notum and of wing hinge primordia of the Drosophila melanogaster wing imaginal disc. *Dev. Biol.* **329,** 315–326 (2009).
277. Baonza, A., Roch, F. & Martin-Blanco, E. DER signaling restricts the boundaries of the wing field during Drosophila development. *Proc. Natl. Acad. Sci. U. S. A.* **97,** 7331–7335 (2000).
278. Diez del Corral, R., Aroca, P., G mez-Skarmeta, J. L., Cavodeassi, F. & Modolell, J. The Iroquois homeodomain proteins are required to specify body wall identity in Drosophila. *Genes Dev.* **13,** 1754–1761 (1999).
279. Simcox, A. A. *et al.* Molecular, phenotypic, and expression analysis of vein, a gene required for growth of the Drosophila wing disc. *Dev. Biol.* **177,** 475–489 (1996).
280. Wang, S. H., Simcox, A. & Campbell, G. Dual role for Drosophila epidermal growth factor receptor signaling in early wing disc development. *Genes Dev.* **14,** 2271–2276 (2000).
281. Zecca, M. & Struhl, G. Control of growth and patterning of the Drosophila wing imaginal disc by EGFR-mediated signaling. *Dev. Camb. Engl.* **129,** 1369–1376 (2002).
282. Cavodeassi, F., Rodríguez, I. & Modolell, J. Dpp signalling is a key effector of the wing-body wall subdivision of the Drosophila mesothorax. *Dev. Camb. Engl.* **129,** 3815–3823 (2002).
283. De Navascués, J. & Modolell, J. tailup, a LIM-HD gene, and Iro-C cooperate in Drosophila dorsal mesothorax specification. *Dev. Camb. Engl.* **134,** 1779–1788 (2007).
284. De Navascués, J. & Modolell, J. The pronotum LIM-HD gene tailup is both a positive and a negative regulator of the proneural genes achaete and scute of Drosophila. *Mech. Dev.* **127,** 393–406 (2010).
285. Fromental-Ramain, C., Vanolst, L., Delaporte, C. & Ramain, P. pannier encodes two structurally related isoforms that are differentially expressed during Drosophila development and display distinct functions during thorax patterning. *Mech. Dev.* **125,** 43–57 (2008).

286. García-García, M. J., Ramain, P., Simpson, P. & Modolell, J. Different contributions of pannier and wingless to the patterning of the dorsal mesothorax of Drosophila. *Dev. Camb. Engl.* **126,** 3523–3532 (1999).
287. Letizia, A., Barrio, R. & Campuzano, S. Antagonistic and cooperative actions of the EGFR and Dpp pathways on the iroquois genes regulate Drosophila mesothorax specification and patterning. *Dev. Camb. Engl.* **134,** 1337–1346 (2007).
288. Sato, M. & Saigo, K. Involvement of pannier and u-shaped in regulation of decapentaplegic-dependent wingless expression in developing Drosophila notum. *Mech. Dev.* **93,** 127–138 (2000).
289. Aldaz, S., Morata, G. & Azpiazu, N. The Pax-homeobox gene eyegone is involved in the subdivision of the thorax of Drosophila. *Development* **130,** 4473 –4482 (2003).
290. Bras-Pereira, C., Bessa, J. & Casares, F. Odd-skipped genes specify the signaling center that triggers retinogenesis in Drosophila. *Dev. Camb. Engl.* **133,** 4145–4149 (2006).
291. De Celis Ibeas, J. M. & Bray, S. J. Bowl is required downstream of Notch for elaboration of distal limb patterning. *Dev. Camb. Engl.* **130,** 5943–5952 (2003).
292. Benítez, E., Bray, S. J., Rodriguez, I. & Guerrero, I. Lines is required for normal operation of Wingless, Hedgehog and Notch pathways during wing development. *Dev. Camb. Engl.* **136,** 1211–1221 (2009).
293. Golic, K. G. Site-specific recombination between homologous chromosomes in Drosophila. *Science* **252,** 958–961 (1991).
294. Xu, T. & Rubin, G. M. Analysis of genetic mosaics in developing and adult Drosophila tissues. *Dev. Camb. Engl.* **117,** 1223–1237 (1993).
295. Lee, T. & Luo, L. Mosaic analysis with a repressible cell marker (MARCM) for Drosophila neural development. *Trends Neurosci.* **24,** 251–254 (2001).
296. Kassis, J. A., Noll, E., VanSickle, E. P., Odenwald, W. F. & Perrimon, N. Altering the insertional specificity of a Drosophila transposable element. *Proc. Natl. Acad. Sci. U. S. A.* **89,** 1919–1923 (1992).
297. Pignoni, F. *et al.* The eye-specification proteins So and Eya form a complex and regulate multiple steps in Drosophila eye development. *Cell* **91,** 881–891 (1997).
298. Rhiner, C. *et al.* Flower forms an extracellular code that reveals the fitness of a cell to its neighbors in Drosophila. *Dev. Cell* **18,** 985–998 (2010).
299. Agnès, F., Suzanne, M. & Noselli, S. The Drosophila JNK pathway controls the morphogenesis of imaginal discs during metamorphosis. *Dev. Camb. Engl.* **126,** 5453–5462 (1999).
300. Shen, J. & Dahmann, C. Extrusion of cells with inappropriate Dpp signaling from Drosophila wing disc epithelia. *Science* **307,** 1789–1790 (2005).
301. Villa-Cuesta, E., González-Pérez, E. & Modolell, J. Apposition of iroquois expressing and non-expressing cells leads to cell sorting and fold formation in the Drosophila imaginal wing disc. *BMC Dev. Biol.* **7,** 106 (2007).
302. Legent, K. & Treisman, J. E. Wingless signaling in Drosophila eye development. *Methods Mol. Biol. Clifton NJ* **469,** 141–161 (2008).
303. Pichaud, F. & Casares, F. homothorax and iroquois-C genes are required for the establishment of territories within the developing eye disc. *Mech. Dev.* **96,** 15–25 (2000).
304. Singh, A. *et al.* Opposing interactions between homothorax and Lobe define the ventral eye margin of Drosophila eye. *Dev. Biol.* **359,** 199–208 (2011).
305. Stultz, B. G., Park, S. Y., Mortin, M. A., Kennison, J. A. & Hursh, D. A. Hox proteins coordinate peripodial decapentaplegic expression to direct adult head morphogenesis in Drosophila. *Dev. Biol.* **369,** 362–376 (2012).
306. Hoch, M. & Jäckle, H. Transcriptional regulation and spatial patterning in Drosophila. *Curr. Opin. Genet. Dev.* **3,** 566–573 (1993).
307. Hatini, V. & DiNardo, S. Divide and conquer: pattern formation in Drosophila embryonic epidermis. *Trends Genet. TIG* **17,** 574–579 (2001).
308. Gomez-Skarmeta, J. L., Campuzano, S. & Modolell, J. Half a century of neural prepatterning: the story of a few bristles and many genes. *Nat Rev Neurosci* **4,** 587–598 (2003).

309. Wilson, L. & Maden, M. The mechanisms of dorsoventral patterning in the vertebrate neural tube. *Dev. Biol.* **282,** 1–13 (2005).
310. Zecca, M. & Struhl, G. Recruitment of cells into the Drosophila wing primordium by a feed-forward circuit of vestigial autoregulation. *Dev. Camb. Engl.* **134,** 3001–3010 (2007).
311. Zecca, M. & Struhl, G. A feed-forward circuit linking wingless, fat-dachsous signaling, and the warts-hippo pathway to Drosophila wing growth. *PLoS Biol.* **8,** e1000386 (2010).
312. McLean, P. F. & Cooley, L. Protein equilibration through somatic ring canals in Drosophila. *Science* **340,** 1445–1447 (2013).
313. De Joussineau, C. *et al.* Delta-promoted filopodia mediate long-range lateral inhibition in Drosophila. *Nature* **426,** 555–559 (2003).
314. Goldstein, R. E. *et al.* An eh1-like motif in odd-skipped mediates recruitment of Groucho and repression in vivo. *Mol. Cell. Biol.* **25,** 10711–10720 (2005).
315. Lengyel, J. A. & Iwaki, D. D. It takes guts: the Drosophila hindgut as a model system for organogenesis. *Dev. Biol.* **243,** 1–19 (2002).
316. Wang, L. & Coulter, D. E. bowel, an odd-skipped homolog, functions in the terminal pathway during Drosophila embryogenesis. *EMBO J.* **15,** 3182–3196 (1996).
317. Coulter, D. E. & Wieschaus, E. Gene activities and segmental patterning in Drosophila: analysis of odd-skipped and pair-rule double mutants. *Genes Dev.* **2,** 1812–1823 (1988).
318. Coulter, D. E. *et al.* Molecular analysis of odd-skipped, a zinc finger encoding segmentation gene with a novel pair-rule expression pattern. *EMBO J.* **9,** 3795–3804 (1990).
319. Brás-Pereira, C. & Casares, F. An antennal-specific role for bowl in repressing supernumerary appendage development in Drosophila. *Mech. Dev.* **125,** 809–821 (2008).
320. Postlethwait, J. H. Development of the temperature-sensitive homoeotic mutant ophthalmoptera of Drosophila melanogaster. *Dev. Biol.* **36,** 212–217 (1974).
321. Schmid, H. Transdetermination in the homeotic eye--antenna imaginal disc of Drosophila melanogaster. *Dev. Biol.* **107,** 28–37 (1985).
322. Guillot, C. & Lecuit, T. Mechanics of epithelial tissue homeostasis and morphogenesis. *Science* **340,** 1185–1189 (2013).
323. Heisenberg, C.-P. & Bellaïche, Y. Forces in Tissue Morphogenesis and Patterning. *Cell* **153,** 948–962 (2013).
324. Spiering, D. & Hodgson, L. Dynamics of the Rho-family small GTPases in actin regulation and motility. *Cell Adhes. Migr.* **5,** 170–180 (2011).
325. Vicente-Manzanares, M., Ma, X., Adelstein, R. S. & Horwitz, A. R. Non-muscle myosin II takes centre stage in cell adhesion and migration. *Nat. Rev. Mol. Cell Biol.* **10,** 778–790 (2009).
326. Evangelista, M., Zigmond, S. & Boone, C. Formins: signaling effectors for assembly and polarization of actin filaments. *J. Cell Sci.* **116,** 2603–2611 (2003).
327. Derivery, E. & Gautreau, A. Generation of branched actin networks: assembly and regulation of the N-WASP and WAVE molecular machines. *BioEssays News Rev. Mol. Cell. Dev. Biol.* **32,** 119–131 (2010).
328. Eden, S., Rohatgi, R., Podtelejnikov, A. V., Mann, M. & Kirschner, M. W. Mechanism of regulation of WAVE1-induced actin nucleation by Rac1 and Nck. *Nature* **418,** 790–793 (2002).
329. Leibfried, A., Fricke, R., Morgan, M. J., Bogdan, S. & Bellaiche, Y. Drosophila Cip4 and WASp Define a Branch of the Cdc42-Par6-aPKC Pathway Regulating E-Cadherin Endocytosis. *Curr. Biol.* **18,** 1639–1648 (2008).
330. Rohatgi, R., Ho, H. Y. & Kirschner, M. W. Mechanism of N-WASP activation by CDC42 and phosphatidylinositol 4, 5-bisphosphate. *J. Cell Biol.* **150,** 1299–1310 (2000).
331. Tseng, Y. & Wirtz, D. Dendritic Branching and Homogenization of Actin Networks Mediated by Arp2/3 Complex. *Phys. Rev. Lett.* **93,** 258104 (2004).
332. Yamamoto, M. *et al.* Phosphatidylinositol 4,5-Bisphosphate Induces Actin Stress-Fiber Formation and Inhibits Membrane Ruffling in Cv1 Cells. *J. Cell Biol.* **152,** 867–876 (2001).
333. Cain, R. J., Vanhaesebroeck, B. & Ridley, A. J. The PI3K p110alpha isoform regulates endothelial adherens junctions via Pyk2 and Rac1. *J. Cell Biol.* **188,** 863–876 (2010).

334. Viaud, J., Gaits-Iacovoni, F. & Payrastre, B. Regulation of the DH-PH tandem of guanine nucleotide exchange factor for Rho GTPases by phosphoinositides. *Adv. Biol. Regul.* **52,** 303–314 (2012).
335. Janmey, P. A. & Lindberg, U. Cytoskeletal regulation: rich in lipids. *Nat. Rev. Mol. Cell Biol.* **5,** 658–666 (2004).
336. Li, Z. *et al.* Roles of PLC-β2 and -β3 and PI3Kγ in Chemoattractant-Mediated Signal Transduction. *Science* **287,** 1046–1049 (2000).
337. Levental, I., Grzybek, M. & Simons, K. Greasing their way: lipid modifications determine protein association with membrane rafts. *Biochemistry (Mosc.)* **49,** 6305–6316 (2010).
338. Meiri, K. F. Lipid rafts and regulation of the cytoskeleton during T cell activation. *Philos. Trans. R. Soc. Lond. B. Biol. Sci.* **360,** 1663–1672 (2005).
339. Warner, S. J. & Longmore, G. D. Distinct functions for Rho1 in maintaining adherens junctions and apical tension in remodeling epithelia. *J. Cell Biol.* **185,** 1111–1125 (2009).
340. Warner, S. J. & Longmore, G. D. Cdc42 antagonizes Rho1 activity at adherens junctions to limit epithelial cell apical tension. *J. Cell Biol.* **187,** 119–133 (2009).
341. Sander, E. E., Klooster, J. P. ten, Delft, S. van, Kammen, R. A. van der & Collard, J. G. Rac Downregulates Rho Activity Reciprocal Balance between Both Gtpases Determines Cellular Morphology and Migratory Behavior. *J. Cell Biol.* **147,** 1009–1022 (1999).
342. Wu, Y. I. *et al.* A genetically encoded photoactivatable Rac controls the motility of living cells. *Nature* **461,** 104–108 (2009).
343. Larson, D. E., Liberman, Z. & Cagan, R. L. Cellular behavior in the developing Drosophila pupal retina. *Mech. Dev.* **125,** 223–232 (March).
344. Weaver, A. M., Young, M. E., Lee, W.-L. & Cooper, J. A. Integration of signals to the Arp2/3 complex. *Curr. Opin. Cell Biol.* **15,** 23–30 (2003).
345. Suetsugu, S. *et al.* Optimization of WAVE2 complex-induced actin polymerization by membrane-bound IRSp53, PIP(3), and Rac. *J. Cell Biol.* **173,** 571–585 (2006).
346. Haviv, L., Gillo, D., Backouche, F. & Bernheim-Groswasser, A. A Cytoskeletal Demolition Worker: Myosin II Acts as an Actin Depolymerization Agent. *J. Mol. Biol.* **375,** 325–330 (2008).
347. Hilgenfeldt, S., Erisken, S. & Carthew, R. W. Physical modeling of cell geometric order in an epithelial tissue. *Proc. Natl. Acad. Sci. U. S. A.* **105,** 907–911 (2008).
348. Li, Z. *et al.* Regulation of PTEN by Rho small GTPases. *Nat. Cell Biol.* **7,** 399–404 (2005).
349. Germena, G. & Hirsch, E. PI3Ks and small GTPases in neutrophil migration: two sides of the same coin. *Mol. Immunol.* **55,** 83–86 (2013).
350. Dufour, S., Mège, R.-M. & Thiery, J. P. α-catenin, vinculin, and F-actin in strengthening E-cadherin cell-cell adhesions and mechanosensing. *Cell Adhes. Migr.* **7,** 345–350 (2013).
351. Weber, G. F., Bjerke, M. A. & DeSimone, D. W. A Mechanoresponsive Cadherin-Keratin Complex Directs Polarized Protrusive Behavior and Collective Cell Migration. *Dev. Cell* **22,** 104–115 (2012).
352. Clark, K., Langeslag, M., Figdor, C. G. & van Leeuwen, F. N. Myosin II and mechanotransduction: a balancing act. *Trends Cell Biol.* **17,** 178–186 (2007).
353. Wilson, C. A. *et al.* Myosin II contributes to cell-scale actin network treadmilling through network disassembly. *Nature* **465,** 373–377 (2010).
354. Mondal, S., Subramanian, K., Sakai, J., Bajrami, B. & Luo, H. R. Phosphoinositide lipid phosphatase SHIP1 and PTEN coordinate to regulate cell migration and adhesion. *Mol. Biol. Cell* mbc.E11–10–0889 (2012). doi:10.1091/mbc.E11-10-0889
355. Koh, T.-W., Verstreken, P. & Bellen, H. J. Dap160/intersectin acts as a stabilizing scaffold required for synaptic development and vesicle endocytosis. *Neuron* **43,** 193–205 (2004).
356. Verstreken, P. *et al.* Synaptojanin is recruited by endophilin to promote synaptic vesicle uncoating. *Neuron* **40,** 733–748 (2003).
357. Rogulja, D., Rauskolb, C. & Irvine, K. D. Morphogen control of wing growth through the Fat signaling pathway. *Dev. Cell* **15,** 309–321 (2008).
358. Aldaz, S., Morata, G. & Azpiazu, N. The Pax-homeobox gene eyegone is involved in the subdivision of the thorax of Drosophila. *Dev. Camb. Engl.* **130,** 4473–4482 (2003).

359. Dominguez, M., Ferres-Marco, D., Gutierrez-Aviño, F. J., Speicher, S. A. & Beneyto, M. Growth and specification of the eye are controlled independently by Eyegone and Eyeless in Drosophila melanogaster. *Nat. Genet.* **36,** 31–39 (2004).
360. Hudson, A. M. & Cooley, L. Drosophila Kelch functions with Cullin-3 to organize the ring canal actin cytoskeleton. *J. Cell Biol.* **188,** 29–37 (2010).
361. Riehle, R. D., Cornea, S. & Degterev, A. Role of phosphatidylinositol 3,4,5-trisphosphate in cell signaling. *Adv. Exp. Med. Biol.* **991,** 105–139 (2013).
362. Alan, J. K. & Lundquist, E. A. Mutationally activated Rho GTPases in cancer. *Small GTPases* **4,** (2013).
363. Warner, S. J., Yashiro, H. & Longmore, G. D. The Cdc42/Par6/aPKC polarity complex regulates apoptosis-induced compensatory proliferation in epithelia. *Curr. Biol. CB* **20,** 677–686 (2010).